PÉCSI TUDOMÁNYEGYETEM
UNIVERSITY OF PÉCS
Doctoral School of Chemistry

DOCTORAL DISSERTATION

Chemical characteristics and source apportionment on ionic composition of rainwater in the Romanian Carpathians, Europe, and Conterminous United States

PhD Candidate:
Keresztesi Ágnes Zsuzsa

Supervisor:
Dr. Szép Róbert
Senior Researcher

Pécs
2022

Contents

1. Introduction 8
   1.1. Context and scientific interest of the work 8
   1.2. Research objectives 9
2. State-of-the-art 10
3. Materials and methods 12
   3.1. Sampling sites description 12
   3.2. Sampling and data analysis 14
      3.2.1. Sampling and analytical procedures 14
      3.2.2. Quality control 15
      3.2.3. Meteorological data and classification methods of atmospheric circulation types 16
      3.2.4. Zonal circulations and zonal index construction 18
      3.2.5. Air mass trajectory and cluster analysis 18
      3.2.6. Multivariate statistical analysis 19
   3.3. Methods used in the assessment of chemical composition of rainwater 19
      3.3.1. The acidic and neutralization potential 19
      3.3.2. Neutralization factor (NF) 19
      3.3.3. Fractional acidity (FA) 19
      3.3.4. Ammonium Availability Index (AAI) 20
      3.3.5. Wet deposition flux 20
      3.3.6. Marine and crustal enrichment factors 20
      3.3.7. Sea salt and non-sea salt fractions 21
4. Results and discussion 22
   4.1. Atmospheric circulation and effects of the Eastern Carpathians on precipitation 22
   4.2. General variability and chemical composition of precipitation 27
   4.3. Variation of pH 34
   4.4. Acid neutralization 38
   4.5. Spatial and temporal variability of Wet Deposition fluxes 46
   4.6. Origins of major ions in rainwater 52
      4.6.1. Ionic correlation using Spearman's Rank Correlation Analysis 52
      4.6.2. Marine and crustal enrichment factors 58
      4.6.3. Marine and non-marine salt contributions 62
      4.6.4. Principal Component Analysis (PCA) 69
   4.7. Zonal circulations, zonal index, and chemical composition of air masses 75
   4.8. Cluster analysis. General air flow transport patterns 78
5. Conclusions 80
6. References 82
7. Aknowledgements 90
8. Publications 91

Abstract

The thesis is a complex study of precipitation chemistry using methods and models of environmental chemistry and geochemistry. Its elaboration started from the validation of some mathematical models, and by analyzing the dispersion behavior of some chemical species in atmospheric precipitation samples collected in closed intramountain basins. These closed basins are characterized by the specific microclimate conditions, which helps to develop the models mentioned above. In the intramountain depressions studied in the Eastern and Southwestern Carpathians, the influence of the Carpathian arc can be observed on the continental and/or oceanic air masses, and on the specific local characteristics, respectively. By analyzing the chemical composition of precipitation corroborated with the air masses circulation, significant modifications can be observed due to climate change that is present both at local level (by the appearance of local anticyclonic systems) and at continental level, by changing the trajectory of continental air masses. These changes are visible by the long-range transport of some chemical species present in different regions. The concentration of sea salts, respectively the significant specific correlation between chloride and sodium or its loss in certain regions are indicators of the changes occurred in the air masses. The Foehn effect of the Dinaric Alps on the chemical composition of atmospheric precipitation has been highlighted. By extrapolating the results obtained in intramountain depressions to the European level, corroborating them with the climate policies assumed in the last two decades by the European Union member states indicates a homogenization and an accentuated decrease of acid ions, in comparison to non-EU countries, where higher levels of acidic pollutants were observed. The calculation techniques used at European level were extrapolated to the contiguous United States, which in comparison to the European continent, has a much greater climate variability, and the applied environmental policies are not unitary, hence there is a clear trend of less visible decrease of different pollutants compared to EU countries.

List of abbreviations

AAI – Ammonium Availability Index
AF – anthropogenic source fraction
AGL – above ground level
AP – Acidic Potential
BH – Baile Herculane
BM – Baia Mare
BZ – Bozinta
CB – Ciuc Basin
CF – crust fraction
COT – Cloud Optical Thickness
CT – circulation types
DON – Degree of neutralisation
DTP – Deda-Toplita Pass
EEA – European Environmental Agency
EF – Enrichment Factor
EF_{crust} – Crustal Enrichment Factor
EF_{sea} – Marine Enrichment Factor
FA – Fractional Acidity
GAW – Global Atmosphere Watch
GAW – Global Atmosphere Watch
GB – Giurgeu Basin
GDAS – Global Data Assimilation System
GIS – Geographical Information System
GWT – Grosswetter-Types
HYSPLIT - Hybrid Single-Particle Lagrangian Integrated Trajectory model
ICP-AES – Inductively coupled plasma-atomic emission spectroscopy
LWP – Liquid Water Path
MN – Moldova Noua
MSLP – Mean sea level pressure
NAAQS – National Ambient Air Quality Standards
NADP – National Atmospheric Deposition Program
NF – Neutralisation Factor
NP – Neutralisation Potential
NSS – Non-sea salt
NSSF – Non-sea salt factor
NTN – National Trends Network
OSB – Odorheiu Secuiesc Basin
PCA – Principal Component Analysis
RS – Resita
SAG-PC – Scientific Advisory Group for Precipitation Chemistry
SM – Somcuta
SN – Seini
SPVAR – cluster spatial variance
SS – sea salt
SSF – Sea salt factor
TP – Toxicity potential
TSV – total spatial variance
VWM – Volume weighted mean
WD – Wet Deposition
WDCPC – World Data Centre for Precipitation Chemistry
WMO – World Meteorological Organization

List of figures

1. **Fig. 1.** Sampling site locations from the Central- and Northern- group of the Eastern Carpathians, and Southern Carpathians.
2. **Fig. 2.** The classification domain for cost733class.
3. **Fig. 3.** Multiannual mean precipitation (1981-2016) in Romania.
4. **Fig. 4.** Spatial domain for applying linear regression between precipitation and elevation (a); prediction model for observed and predicted precipitation (b).
5. **Fig. 5.** Longitudinal profile of precipitation amount and elevation.
6. **Fig. 6.** Conditional probabilities (%) for GWT, K-means, Kruizinga and Lund classification.
7. **Fig. 7.** MSLP centroids for GWT and LUND types leading most frequently to high precipitation.
8. **Fig. 8.** Mean sea level pressure for 11 July 2004: typical east cyclonic circulation type over the classification domain. Source: metoffice.gov.co.uk.
9. **Fig. 9.** Mean cloud optical thickness (μm) for CT (GWT) 4 and 9 (LND) for the 2005-2014 period.
10. **Fig. 10.** Mean all sky liquid water path values (kg/m^2) for CT 4 (GWT) and 9 (LND) for the 2005-2014 period.
11. **Fig. 11.** Mean cloud top height difference against the multiannual mean (m) for CT 4 (GWT) and 9 (LND) for the 2004-2015 period.
12. **Fig. 12.** Chemical composition percentages of precipitation from Baia Mare (BM), Bozinta (BZ), Somcuta (SM) and Seini (SE).
13. **Fig. 13.** Volume weighted means of major ions in rainwater samples collected in Europe.
14. **Fig. 14.** The spatial variability of volume weighted means (μeq L^{-1}) of major ions in precipitation over the U.S. during 1978-2017.
15. **Fig. 15.** Distribution of rainwater pH at the sampling sites.
16. **Fig. 16.** Frequency distribution of rainwater pH at Baia Mare (BM), Bozinta (BZ), Somcuta (SM) and Seini (SE).
17. **Fig. 17.** Distribution of rainwater pH at Resita (RS), Moldova Noua (MN) and Baile Herculane (BH).
18. **Fig. 18.** Frequency distribution of pH for all studied countries during 2000-2017.
19. **Fig. 19.** Distribution of rainwater volume weighted mean (VWM) pH (a) and the 30-year annual precipitation amounts (1981-2010) at the sampling sites.
20. **Fig. 20.** Linear regressions of (NO_3^- + SO_4^{2-}) vs. the sum of cations.
21. **Fig. 21.** Neutralization factors of major alkaline ions in precipitation samples collected in Europe.
22. **Fig. 22.** The mean AP/NP ratios and the neutralization factors of major cations in precipitation for each sampling site over the conterminous US.
23. **Fig. 23.** Average FA values for each sampling site across the conterminous US.
24. **Fig. 24.** Average AAI values during the sampling period over the conterminous US.
25. **Fig. 25.** The average multi annual wet flux depositions (kg ha^{-1}yr^{-1}) of major ions at the studied sampling sites from the central group of the Eastern Carpathians.
26. **Fig. 26.** The average multi annual wet flux depositions (kg ha^{-1}yr^{-1}) of major ions at the studied sampling sites from the northern group of the Eastern Carpathians.
27. **Fig. 27.** The average multi annual wet flux depositions (kg ha^{-1}yr^{-1}) of major ions at the studied sampling sites.
28. **Fig. 28.** Average multiannual wet deposition rates (kg ha^{-1}yr^{-1}) of major ions at the studied regions.
29. **Fig. 29.** Multiannual mean wet deposition fluxes of major ions during 2000-2017 over the conterminous US.
30. **Fig. 30.** Spearman correlation coefficients of ionic constituents in precipitation.
31. **Fig. 31.** Spearman correlation coefficients for ionic constituents in precipitation for all studied countries in Europe.

32. **Fig. 32.** Spearman's rank correlation analysis performed on major ionic constituents and pH in precipitation samples harvested across the conterminous US.
33. **Fig. 33**. Marine and crustal enrichment factors with reference to sodium and calcium across the conterminous US.
34. **Fig. 34.** Multiannual means of precipitation sums according to each cyclonic weather type.
35. **Fig. 35.** GWT circulation types resembling to Mediterranean lows upon Balkan peninsula.
36. **Fig. 36.** Monthly frequency of cyclonic weather types in southern Europe.
37. **Fig. 37.** Source contributions of different components in precipitation over Europe with reference to Cl^-.
38. **Fig. 38.** Sea salt contributions (expressed in %) of different components in precipitation with reference to Cl^- in the contiguous US.
39. **Fig. 39.** Monthly multiannual percentages of precipitation recorded on days with different advections.
40. **Fig. 40.** Multiannual seasonal wind direction frequency.
41. **Fig. 41.** Averaged monthly number of days with strong westerly component (>8 hPa difference between the minimum and maximum latitude) according to the MSLP method (left) and the JC scheme (right).
42. **Fig. 42.** Rainfall quantities recorded during strong ZI (percent from seasonal mean).
43. **Fig. 43.** Backward trajectory distribution obtained with HYSPLIT for the three locations for the 2014-2017 period in the Southern Carpathians.

List of tables

1. **Table 1.** Weather stations and their location
2. **Table 2.** Classification methods and their inputs.
3. **Table 3.** Volume-weighted mean concentration of major ion (in μeql^{-1}) and pH along with statistical results in rainwater samples in the central group of the Eastern Carpathians.
4. **Table 4.** Volume-weighted mean concentration of major ion (in μeql^{-1}) and pH along with statistical results in rainwater samples in northern group of the Eastern Carpathians.
5. **Table 5.** Volume-weighted mean (VWM) concentration of major ions (in μeql^{-1}) and pH along with statistical results in rainwater samples from the Southern Carpathians.
6. **Table 6.** Neutralization factors and acidic/neutralization potential ratio at all sampling sites and their seasonal variations in the central group of the Eastern Carpathians.
7. **Table 7.** Ionic ratios of the measured ions over the studied regions from the Central Group of the Eastern Carpathians.
8. **Table 8.** Neutralization factors of the major ions and AP/NP ratio in rainwater samples from the Northern Group of the Eastern Carpathians.
9. **Table 9**. Ionic ratios among measured major ions.
10. **Table 10.** Neutralization factors of the major ions and AP/NP ratio in rainwater samples from the Southern Carpathians.
11. **Table 11.** Ionic ratios among measured ions in rainwater collected in the Southern Carpathians.
12. **Table 12.** Spearman correlation coefficients among ionic constituents in precipitation collected in the central group of the Eastern Carpathians
13. **Table 13.** Spearman correlation coefficients for ionic constituents in precipitation at the sampling sites from the Southern Carpathians.
14. **Table 14.** Enrichment factors for soil and sea salt components relative to rainwater.
15. **Table 15.** Enrichment factors for sea salt and soil components relative to rainwater in the Northern Group of the Eastern Carpathians.
16. **Table 16.** EFs for sea salt and soil components relative to rainwater in the Southern Carpathians.
17. **Table 17.** Enrichment factors for sea salt and soil components relative to rainwater in Europe.
18. **Table 18.** Source contributions (in %) for different ions in rainwater from the four sampling sites in the central group of the Eastern Carpathians.
19. **Table 19.** Equivalent ratios of different components with reference to Na^+ in rainwater in the Northern group of the Eastern Carpathians.
20. **Table 20.** Equivalent ratios of different components with reference to Na^+ in rainwater in the Southern Carpathians.
21. **Table 21.** Varimax rotated factor loadings, total variance, and ionic sources at the studied sampling sites.
22. **Table 22.** Varimax rotated factor loadings, total variance, and ionic sources for the Northern Group of the Eastern Carpathians.
23. **Table 23.** Varimax rotated factor loadings, total variance, and ionic sources at the Southern Carpathians.
24. **Table 24.** Varimax rotated factor loadings, total variance, and possible sources over Europe.
25. **Table 25.** Varimax rotated component matrix, total variance, and possible major ion sources over the contiguous US.

1. Introduction

1.1. Context and scientific interest of the work

The impacts of climate change are being felt in all geospheres. The effects are visible and inevitable due to the inertia of the climate system, regardless of the result of short- and medium-term emission reduction actions. The quantity and composition of emissions are found not only in air quality but also in atmospheric precipitation. This is a sensitive indicator of changes in the natural and anthropogenic environment. Intramountain depressions are no different from this phenomenon either. They have a specific microclimate where certain mathematical models can be developed, and which will be extrapolated to the regional and even continental scale in the present thesis. The specificity of closed intramountain basins consists in the specific microclimate character, which is distinguished by very cold periods in winter, and conditions of accentuated static stability of the atmosphere in winter-summer period, which appear due to the presence of local, very persistent anticyclonic systems. The specificity of intramountain basins from the Romanian Carpathians consists in the distinct microclimate conditions, characterized by periods of accentuated static stability, and the installation of persistent local anticyclonic systems (Szép et al., 2018, 2017). The basins concave shapes favor the thermal stratification of the air (Whiteman et al., 2001).

Thus, the cold air descends and accumulates on the bottom of these depressions causing thermal inversions, extremely common in the cold season (Panday et al., 2009; Wekker and Kossmann, 2015). Moreover, due to the sheltering character of the mountains, the wind frequency decreases inside the basins, while the relative humidity of the air is higher, increasing fog frequency (Kossmann et al., 2002). The above-mentioned phenomena are also characteristic to the basins of the Romanian Carpathians, such as the Ciuc basin, Giurgeu basin and Maramures basin. These basins are characterized by unevolved and organic soils, with acidophilic vegetation and ascending mineral springs, developed on tectonic fault lines, their chemistry being imposed by the host rocks (volcanic and magmatic on the eastern frame and sedimentation on the western one) (Szép et al., 2017).

The agricultural policies applied between the years of 1960-1980 led to drastic changes in land use. Thus, the transition to extensive agriculture caused the drainage of these basins, followed by significant evapotranspiration losses. This phenomenon accelerated the decomposition of organic matter, releasing large amounts of CO_2 and intensifying climate change. In the case of a warmer climate, carbon deposits preserved by cold and humid climatic conditions will release significant amounts of CO_2, CH_4, and NH_3 into the atmosphere. This occurs when wetlands are drained or when peat is mined (Szép et al., 2018). The loss of evapotranspiration, the decrease of the relative humidity and of the precipitations favors the development of heavy drought phenomena and the accumulation of the pollutants and the particles derived from them (Szép and Mátyás, 2014). Lately, the occurrence of heavy drought led to the ignition of the natural peat deposits, either through auto combustion, or through stubble burnout in the Ciuc and Giurgeu basins (Szép et al., 2017).

Air pollution affects everyone, being a permanent risk factor for all regions, and to fight against its negative and harmful effects environmental policies must be adapted to local specificities. The relationship between air pollution and atmospheric precipitation is one of interest, especially in terms of wet deposition and the impact on the pedosphere, biosphere and built heritage values. The chemical composition of atmospheric precipitation has been intensely studied during the last decades, hence the major ion concentrations in rainwater can indicate air quality, showing the relative sources that contributed to polluting the atmosphere.

1.2. Research objectives

The main aims of this thesis are:

- to identify the sources of natural and/or anthropogenic contamination/pollution of atmospheric precipitations and the contribution of various sources to their chemical composition.

- to present the relationship of interdependence between geology, geomorphology, climate specificities of the studied areas and precipitation chemistry.

- to examine the atmospheric circulations and the microclimate influences on the rainwater chemistry in the studied areas

- to assess the variation of sea salt concentration depending on the dominant air masses and the specific influences of high relief on the chemical composition of precipitation (Foehn winds in the Southern Carpathians)

- to decipher the pH variation, the neutralizing capacity of different chemical species, the wet deposition, the contribution of marine and non-marine salts and the influence of different pollutant sources on the chemical composition of rainwater, taking under account the spatial-temporal evolution of the European continent to establish the dependent relationship with the environmental policies of the European Union.

- to extrapolate and validate the results obtained at the level of the European continent to the level of the contiguous US during the last four decades, including the major ion concentrations, the variation of pH values, the acidifying and neutralizing capacity of rainwater, the wet deposition, the influence of sea-salts and of different pollutant sources, in order to characterize the spatiotemporal differences and interrelationships between different regions in terms of geographical location, climate and economic development, which may present a significant contribution to environmental specialists and political decision makers, offering a benchmark in order to highlight the effects on the chemical composition of rainwater of the implementation of environmental regulations.

2. State-of-the-art

One of the most discussed subjects over the past 30 years and nowadays is the chemical composition of rainwater and the study of atmospheric precipitation, hence it provides important insights on the atmospheric chemistry, raising awareness to the negative effects of air pollution on the environment and human health. As mentioned in the studies of Aiuppa et al., 2003; Celle-Jeanton et al., 2009; Das et al., 2005; Tiwari et al., 2012; Vet et al., 2014; Wu et al., 2016, the investigation of major ion and trace elements concentration in atmospheric precipitations can provide information on the chemical species, gaseous and particulate pollutants, on the type and distribution of pollutant sources, as well as on long-range transported air pollutants and air mass origins. Another important aspect is the understanding of scavenging and deposition mechanisms, hence they can offer a broader view on the influencing sources and the potential effects of local and regional pollutant dispersion processes (Mouli et al., 2005).

Precipitation is the most effective process in removing and transporting different ionic compounds, pollutants, and soluble gases from the atmosphere to the earth's surface. Precipitation chemistry differs from region to region due to the dissimilarities of the local emission sources (Pu et al., 2017), reflecting all the local traits of air pollutants (Sakihama et al., 2008). Other important aspects when discussing precipitation chemistry are the complex relationship between cloud dynamics and microphysical processes, as well as the chemical reactions that take place in-cloud and below-cloud (Herrera et al., 2009). According to Greaver et al., (2012) the removal of air pollutants from the atmosphere can occur either by wet deposition through precipitation, or by dry deposition of particulate matter. Rainwater plays a key part in scavenging suspended aerosol particles from the atmosphere, sustaining the equilibrium between the sinks and sources of atmospheric pollutants (Chate et al., 2003), reflecting the atmosphere's quality during the time of the rainfall (Mahato et al., 2016). The composition of rainwater can have a significant influence on the environment and all ecosystems, and its chemical characteristics can be altered by rainfall amount and rate, airmass trajectories and cloud base height (Báez et al., 1997; Tang et al., 2005; Xu et al., 2015). The chemical composition of atmospheric precipitation and wet deposition can harm vulnerable ecosystems, leading to acidification and altering the nutrient balances (Greaver et al., 2012; Lehmann et al., 2005), therefore its analysis can offer valuable information to environmental scientist. Through nitrogen deposition the nutrient balance can be altered, contributing to acidification, whilst NH_4 can have a positive effect, such as the stimulation of crop development, or a negative effect by modifying native plant community diversity and structure (Krupa, 2003). Sulphur as a primary acidifying agent, has a significant influence on ecosystems that are vulnerable to acidic compounds, contributing to the methylation of mercury, simplifying its entrance in the food chain and favoring its bioaccumulation (Greaver et al., 2012). Anthropogenic activities are the main acidifying factors, hence the emissions of SO_2 and NO_x and other acidic gases cand change the nature of precipitation, favoring its acidification. By the dissolution of the above-mentioned pollutants in clouds, the formation of nitric and sulfuric acids occurs (Kulshrestha et al., 2003). In urban areas, acidic rainfall is more common, caused by industrial activities and traffic. Terrestrial elements, such as calcium, magnesium and potassium can neutralize a part of the acidifying components, due to their buffering ability, hence reducing the negative effects of acidic deposition on soils and waters (Lynch and Grimmf, 1995).

Starting with the year of 1995, three important studies were published, assessing the global rainwater chemistry, mostly highlighting the wet and dry deposition (Vet et al.,

2014). The report released by the World Meteorological Organization in 1996, and published as an article later in 1997, presented a global analysis on acidic deposition, stating that the areas with the most elevated sulfate and nitrate deposition fluxes are the ones where the highest SO_2 and NO_x emissions were observed (Whelpdale et al., 1997; Whelpdale and Kaiser, 1996). Later, Dentener et al., (2006) evaluated the deposition fluxes of N and S on a regional and global scale, simulating chemical fate and transport in the atmosphere with ensemble-mean modelling, using 21 Eulerian (fixed grid) global models. In 2014, a global analysis of chemical composition of rainwater and deposition was released under the direction of the World Meteorological Organization (WMO), Global Atmosphere Watch (GAW), and Scientific Advisory Group for Precipitation Chemistry (SAG-PC), in order to assess the major ion concentrations in rainwater, wet and dry deposition for S, N, acidic potential, marine salts and organic acids, respectively, during 200-2002 and 2005-2007 (Vet et al., 2014). According to Vet et al., (2014), considerable reductions of sulfur and nitrogen concentration and deposition have been observed in Europe, the U.S. and Canada, due to the implemented emission reduction policies and programs. In the study published by the European Environmental Agency it is shown that the decrease in SO_x emissions led to improvement regarding the effects of acidification, with various ecosystems showing signs of recovery (European Environmental Agency (EEA), 2018; Maas and Grennfelt, 2016). In 2017, Fagerli et al., (2017) in the European Monitoring and Evaluation Programme (EMEP) report stated that in Europe acidity exceedances can be observed in 5.3% of the ecosystems, projecting that if current environmental policies will be implemented, by 2020 only 4% of the European ecosystems will present critical values of acidification. According to the projection made by Vet et al., (2014), increases of N emissions from agricultural activities, such as use of synthetic fertilizers and the biomass burning in case of wildfires imply the need for long-term examinations of precipitation chemistry, as well as wet and dry deposition to assess future effects. However, global estimates for changes in marine salt, organic acids and total phosphorus are impossible to made since the precipitation-weighted means of the above present a great temporal and spatial variation across the globe.

Unfortunately, the current challenges are much more complex than those stated above. Today not only acidic precipitation causes global damage, but also basic precipitation. These are identified in some urban agglomerations with specific industry, respectively in closed depression areas. Both acidic and basic precipitation contribute to the loss of biodiversity and degradation of the built environment, increasing the contribution of wet deposition on the biosphere and pedosphere.

By analyzing numerous studies published on chemical composition of rainwater and deposition, one can see that this subject is of great interest in understanding atmospheric processes. Air mass transport models associated with precipitation chemistry can offer information about major ion cycling in the atmosphere, while wet deposition estimates, that are a function of atmospheric precipitation amount and major ion concentration can offer insights on the effects of precipitation regarding chemical composition and deposition on a local and regional scale. As it appears, to thoroughly assess the negative effects of pollutants from the atmosphere on the environment and human health, a multitude of processes need to be taken into account, including the long-term monitoring of precipitation chemistry and deposition, based on a unitary and comprehensive international methodology.

3. Materials and methods

3.1. Sampling sites description

To conduct the studies on which the present thesis is based, several basins were selected from the Romanian Carpathians, which can be classified into intra-mountain and extra-mountain areas. Later, the results obtained on a local and regional scale were extrapolated to a continental scale, applying the used mathematical models and estimates to the European continent and to the contiguous United States.

Fig. 1 shows the sampling sites selected at the level of the Romanian Carpathians, analyzing rainwater samples from four different locations in the Northern group of the Eastern Carpathians (Baia Mare - BM, Bozinta - BZ, Seini - SE, Somcuta Mare – SM), three intramountain- and one extramountain basin from the Central group of the Eastern Carpathians (Ciuc basin – CB, Giurgeu basin – GB, Deda-Toplita Pass (DTP) and Odorheiu Secuiesc extramountain basin (OSB). From the Southern Carpathians three sampling locations were chosen: Resita (RS), Baile Herculane (BH) and Moldova Noua (MN).

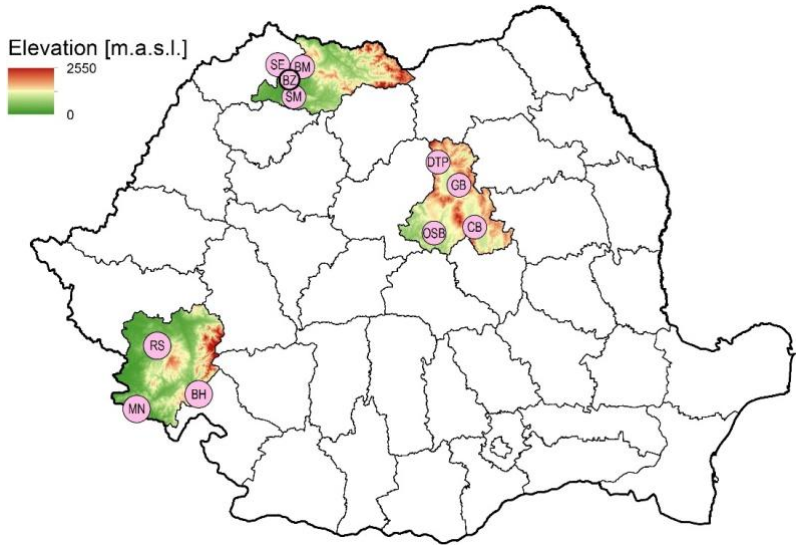

Fig. 1. Sampling site locations from the Central- and Northern- group of the Eastern Carpathians, and Southern Carpathians.

The studied basins in the Eastern Carpathians are flanked on the western side by the Neogene eruption which manifested itself in three main eruption cycles, Badenian, Sarmatian, Lower Pliocene and Upper Pliocene - Lower Quaternary. In the perimeter of Calimani, Ghurgiu-Harghita, typical stratovolcano structures were formed, closing the actual volcanic chain. This was differentiated in the second eruptive stage. In this cycle, the most representative structural elements of the current relief were formed (chimneys, calderas, craters, plateaus). The third cycle, Upper Pliocene-Quaternary, volcanic manifestations of a more restricted character resume in the perimeters of the previous cycles. Explosive demonstrations became smaller in number and area in the Calimani, Ghurghiu-Harghita, Oas-Gutai groups. The Neogene eruption is also present in the Apuseni Mountains (Metaliferous Mountains) being andesitic, dacitic and in places rhyolitic in nature, and acid pyroclastic projections. The central frame of the Eastern Carpathians is defined by the Mesozoic crystalline, formed in the distensive-compressive

cycles of the Carpathian geosyncline basin opened in the Triassic. This basin worked until the late tectogenesis of the Alpine orogeny. Following the evolution of this geosyncline, the morpho structures of the Carpathian orogen were formed. The eastern and southern edge over which the Subcarpathian area currently overlaps is part of the Carpathian Orogen.

The climate in the basins of the central group of the Eastern Carpathians is characterized by a moderate degree of continentalism, in which the winters are long and rich in snow, the summers are cool and relatively humid; the average annual temperatures show low values, and the atmospheric precipitations are frequent. Throughout a year the strongest influences are given by the circulation of western air masses, determining an accentuated instability of the weather and precipitation in the form of rain during the summer period, while during winter temperatures are mostly below the limit of frost, accentuated nebulosity and solid precipitations can be observed. The polar circulation is specific to the cold season, manifesting itself by temperature decrease, the increase of the nebulosity and precipitation in the form of snow. Tropical, southeastern, and eastern continental influences are less common, due to the position of these basins in the Eastern Carpathians. The greatest stability of the weather is registered at the end of summer and autumn, between August and October, the period with many clear days, leading to numerous thermal inversion phenomena. The pronounced instability manifests itself in the spring months, but it can continue at the beginning of summer, on the background of a western circulation. The studied extra mountain basin, OSB, presents a quite different climate, with wet and warm summers and colder winters, where blizzards are also frequent. In the studied basins, annual mean temperatures range between 4-6 ºC in the intra-mountain areas and volcanic plateau, and between 6-8 ºC in the hills area, respectively. The mean annual rainfall in the central group is strongly determined by the volcanic chain of the Eastern Carpathians, creating a barrier in front of the air masses, explaining the larger amounts of rainfall in the northwestern part of the Eastern Carpathians, in comparison to the amounts recorded in the central part of intramountain basins.

The studied areas from the northern group of the Eastern Carpathians are similar to the ones from the central group, being influenced by a temperate-continental climate, characterized by subpolar air masses in the eastern area, while in the western area are dominated by a moderate continental climate with oceanic contributions. Due to similar climate conditions as presented for the central group, the phenomenon of high atmospheric stability often appears, followed by thermal inversion, which has a negative outcome to the dispersion of atmospheric pollutants, causing their accumulation.

The sampling sites chosen from the Southern Carpathians are known for their great relief diversity, and their geographical position, being close to the Adriatic Sea. This greatly influence the climate in the studied areas, showing the dominance of Atlantic and Mediterranean air masses, providing a moderate thermal regime, characterized by frequent warm periods during wintertime and early spring, receiving high amounts of precipitation throughout the year.

A more detailed description of the sampling sites discussed in the present thesis can be found in previously published articles (Keresztesi et al., 2020c, 2020a; Szép et al., 2018).

3.2. Sampling and data analysis

3.2.1. Sampling and analytical procedures

During the sampling period, 2006–2017, in the Romanian Carpathians, 2095 rainwater samples were analyzed. Precipitation was collected in all three Carpathian regions by placing rainwater samplers 1.5-2m above ground, from the onset until the end of the rainfall event. A thorough rinse was made before and after each sample collection to avoid any possible contamination. The pH values of the samples were immediately measured with digital pH meters standardized with 4.0 and 9.2 pH buffer solutions. Conductivity meters were used to measure the conductivity of each sample. To prevent biological degradation of the sample, thymol was used, followed by the removal of insoluble particles, by filtering the samples through membrane filters. Then, all samples were refrigerated at 4 ºC until further analysis. At all sampling sites from the Romanian Carpathians, anions were measured with Ion Chromatograph (Dionex 2000i/SP) using a CO_3^{2-}/HCO_3^- buffer as eluent (1.7 mM Na_2CO_3/1.8 mM $NaHCO_3$), used in isocratic analysis, and 25 mM H_2SO_4 as regenerant, preparing 100 ppm stock solutions of sodium salts of each of the ions, calculating the concentrations based on the peak area of the above-mentioned standards (Keresztesi et al., 2020c, 2020a; Szép et al., 2018). Cations collected in the central and northern groups of the Eastern Carpathians were analyzed by atomic absorption (AAS, Perkin Emler, model 2380, Air/C_2H_2, 422.7 nm), while in the case of samples gathered in the Southern Carpathians Inductively Coupled Plasma-Atomic Emission Spectroscopy (ICP-AES, iCAP 6300 Duo View ICP-AES Spectrometer) was used (Keresztesi et al., 2020a, 2020c). The Cl^- and NH_4^+ were measured by U-VIS spectrometer method (Nicolet Evolution 100, 463 and 440 nm) (Nollet, 2007; Szép et al., 2017).

For a more detailed description of the sampling procedures please check the previously published articles (Keresztesi et al., 2020c, 2020a; Szép et al., 2018).

In the central group of the Eastern Carpathians a total of 362 samples were collected at CB, 114 at GB, 118 samples at DTP and 114 samples at OSB from January 2006 to 2016 November, while in the northern group of the Eastern Carpathians, during a period of 9 years, between January 2009 and December 2017, a total of 1112 rainwater samples were collected: 286 at Baia Mare (BM), 270 at Bozinta (BZ), 280 at Seini (SE) and 276 at Şomcuţa Mare (SM). In the sampling sites from the Southern and Carpathians, a total of 275 precipitation samples were collected: 81 at Reşiţa, 97 at Moldova Nouă, and also 97 samples at Băile Herculane, from January 1st 2014 to December 31st 2017.

The precipitation chemistry data in the case of Europe and the United States (US) of America were downloaded from regional and national monitoring networks (Vet et al., 2014). The ion composition analysis data used in the case for precipitation samples collected in the European Continent were obtained from the GAW World Data Centre for Precipitation Chemistry, that can be accessed at http://wdcpc.org, while data for the conterminous United States were obtained by accessing the National Atmospheric Deposition Program (http://nadp.slh.wisc.edu), through the National Trends Network (NTN). These databases offer a long-term record of rainwater chemistry across the U.S.

The E-OBS raster dataset (version 19.0) was used in order to extract the annual rainfall amount data for Europe. E-OBS data can be freely accessed at http://www.ecad.eu (Cornes et al., 2018; Keresztesi et al., 2019). In the case of the contiguous US, rainfall amount data for the 1981-2010 climatological period were downloaded from the PRISM Climate Group database (http://prism.oregonstate.edu) (Daly et al., 2017; Keresztesi et al., 2020b).

To conduct the precipitation chemistry analysis in the case of Europe, a total of 27 countries were chosen, between the 2000 and 2017 period: Austria, Belarus, Croatia, Czech Republic, Denmark, Estonia, Finland, France, Germany, Greece, Hungary, Iceland, Ireland, Italy, Latvia, Netherlands, Norway, Poland, Portugal, Serbia, Slovakia, Slovenia, Spain, Sweden, Switzerland, Turkey, and the United Kingdom. After selection, each country was classified into a region: East-Central Europe (Belarus, Czech Republic, Hungary, Poland, Slovakia); Northern Europe (Denmark, Estonia, Finland, Iceland, Ireland, Latvia, Norway, Sweden, United Kingdom); Southern Europe (Croatia, Greece, Italy, Portugal, Serbia, Slovenia, Spain, Turkey); and Western Europe (Austria, France, Germany, Netherlands, Switzerland). To conduct the assessment on precipitation chemistry a total number of 4409 data were processed, having in average from three to 48 measurements/year/country. By calculating the mean value for each country (one value/year/country), resulted in a total of 450 data.

In the contiguous United States, a total number of 86470 data were cleaned, processed, and interpreted collected at 334 sampling sites during the 1978-2017 period.

3.2.2. Quality control

All analytical data used in this thesis were quality control checked using the ion balance method to clean the data, and to remove any possible values that may present measuring error. If the equivalent ratio of the total sum of anions and cations (Σ anions/Σ cations) equals unity, then the data is considered acceptable, mentioning that ion imbalances must not exceed ± 25% (Keene et al., 1986; Wu et al., 2016). Hence a notable anion deficiency was observed at all sampling sites, which may stipulate the existence of HCO_3^- in considerable concentrations, the following equation was used for its calculation (Anatolaki and Tsitouridou, 2009):

$$[HCO_3^-] = 10^{-11.24+pH} \text{ (eq/l)} \quad (1)$$

Ionic balance ratios have changed significantly at all sampling sites, after considering the calculated concentrations of HCO_3^-, showing the following values: in the central group of the Eastern Carpathians 0.6 for CB and GB, 0.7 for OSB and DTP; in the northern group of the Eastern Carpathians 0.90 (BM), 0.78 (BZ), 0.76 (SM) and 0.79 (SE); in the Southern Carpathians 0.82, 0.90 and 0.94 for RS, MN and BH, respectively.

According to Honório et al., (2010) and Xu et al., (2015) additional ionic imbalances might be caused by other unmeasured organic compounds due to analytical limitations.

After checking the quality of the measured data, linear regression analysis was performed between the grand total of anions concentration and the grand total of cations concentration. The results were the following: 0.72, 0.76 and 0.63 for the samples collected in the central group of the Eastern Carpathians, in the northern group of the Eastern Carpathians and in the Southern Carpathians, respectively.

In general, the data accessed through the GAW WDCPC and NADP is verified, however, just to ensure their quality, ion balance method was used, considering the presence of H^+ and HCO_3^- concentrations in samples that have not fulfilled the reliability criteria. The concentration of H^+ was calculated by applying the formula used by Bisht et al., (2017):

$$[H^+] = 10^{-pH} \text{ (eq/l)} \quad (2)$$

By taking into account the concentrations of calculated H^+ and HCO_3^- the number of samples fulfilling the quality criteria increased considerably in the case of the samples from Europe, as well as for the conterminous US. In Europe values exhibited a mean value of 0.98, with the minimum of 0.90 recorded for Estonia and the maximum of 1.22 in Hungary, while for the contiguous US the average value was 0.94, calculated for all 334 sampling sites.

After plotting the grand total of anions against the grand total of cations in a regression analysis, strong correlations were obtained, exhibiting an R^2 value of 0.68 for Europe and 0.90 for the conterminous US.

To verify if the data is normally distributed or not, with the help of IBM SPSS Statistics normality tests were performed, such as skewness and kurtosis z-values, the Kolmogorov-Smirnov test, histograms, Q-Q plots, and boxplots. pH values were selected as dependent variables; hence their values are dependent by the ion concentrations found in the collected samples. Visual outputs (histograms, Q-Q plots and boxplots) showed that the data does not follow the Gaussian distribution, while the Z test showed that values does not fall into the -1.96 and +1.96 interval.

3.2.3. Meteorological data and classification methods of atmospheric circulation types

Atmospheric circulation types (CT) were built with the help of the cost733cat v 1.2 classification software (Philipp et al., 2016) and ERA reanalysis (Interim version). In order to do so, mean sea level pressure (MSLP) and the height of 500 hPa geopotential have been chosen. To put Romania in the center and to consider the specifications of large-scale circulations, the classification domain used has been selected to be between 05° and 45° longitude E; and between 30° and 65° latitude N (Fig. 2).

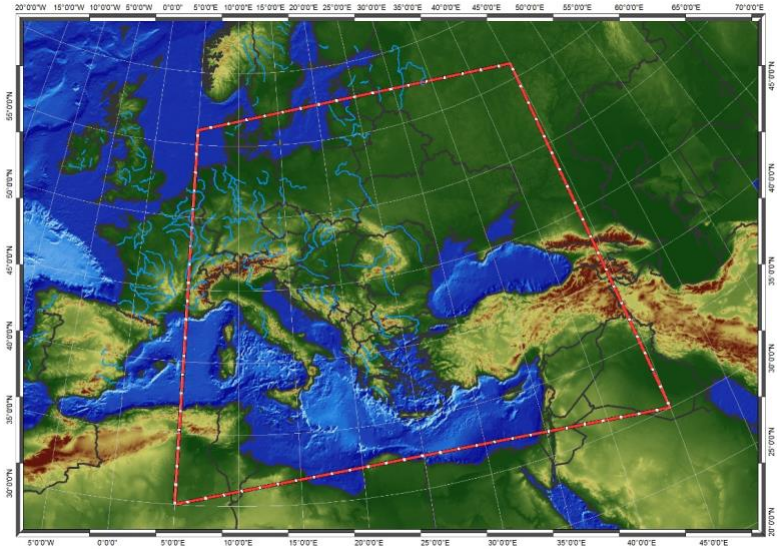

Fig. 2. The classification domain for cost733class.

To show the relationship between precipitation and the mountainous chain of the Eastern Carpathians blocking air masses, weather types were disseminated that led to the development of heavy rainfall periods. This was realized by using the daily rainfall data recorded at weather stations (Table 1) close to the sampling sites in the central group of the Eastern Carpathians. A day is considered high precipitation day if more than 10 mm rain was measured. The data for the 1981-2016 period was obtained from Meteo Romania.

Table 1. Weather stations and their location

Name	Elevation (m.a.s.l.)	Latitude	Longitude	Period used
Batoș (DTP)	415	46°53'10"	24°38'43"	1987-2016
Miercurea-Ciuc (CB)	661	46°22'17"	25°46'21"	1981-2016
Joseni (GB)	759	46°38'56"	25°17'47"	1981-2016
Odorheiu Secuiesc (OSB)	523	46°17'48"	25°17'30"	1981-2016

To build the CT, numerous methods were chosen to verify if related synoptic patterns are characteristic for the days with over 10 mm of precipitation, between 1981 and 2016.

According to Wilks, (2006) equation, the probability of CT leading to a day with more rain than 10 can be assessed:

$$\Pr\left\{\frac{E1}{E2_i}\right\} = \frac{\Pr\{E1 \cap E2i\}}{\Pr\{E2i\}} \quad (3)$$

where {E1} represent the days with high rainfall and {E2$_i$} (*i=1…i*) are the CT. The results are expressed in percent (%), assessing if any links exist between CT and days with high precipitation (Lupikasza, 2010).

The effectiveness of a CT was also determined, using the following relation: Lupikasza, (2010):

$$Pr_{diff} = \Pr\{E1/E2_i\}_{max} - \Pr\{E1/E2_i\}_{min} \quad (4)$$

To construct the CT data were downloaded at a spatial resolution of 0.05 degrees/cell for the period 2005-2014, from CLAAS-2 version of METEOSAT second generation of geostationary satellites; being validated with SYNOP and calibrated with MODIS, moreover the *Liquid water path (LWP)* dataset was also used (Szép et al., 2018). Types that are most related to heavy rainfall were chosen to each classification method, calculating the average of LWP and presenting the possible spreading of LWP values.
Table 2 shows the classification methods using 733class software (Dee et al., 2011) that were selected from the ERA-Interim reanalysis ECMWF (Lupikasza, 2010).

Table 2. Classification methods and their inputs.

No	Method	Name	Abbreviation	No. of classes	Input
1	Threshold	Gross Wetter Types	GWT	24	MSLP
2	Principal Component Analysis	Kruizinga	KRZ	27	MSLP, z500, th850-500, vort500
3	Optimization algorithm	CKMeans	CKM	27	MSLP, z500, th850-500, vort500
4	Leader algorithm	Lund	LND	27	MSLP

As it can be observed in Table 2, the weather types were constructed by applying mean-sea level pressure (MSLP), the height of 500 mb level (z500), the thickness between 850 and 500 mb levels (th850-500) and the relative vorticity at 500 mb level (vort500). The methods were constructed by using the maximum possible number of classes, to

obtain more information on patterns that favor high rainfall events in the studied area. An individual and detailed description about each method and the process of their construction can be found in a study published previously to this thesis (Szép et al., 2018).

To assess the interconnection between various synoptic patterns and rainfall in South-eastern Europe, daily classification of CT was used. To derive the classification of weather types cost722class software was used with MSLP data that were extracted from ERA-Interim. Since the predefined thresholds were used to link each day to a certain CT, the Grosswetter-Types (GWT) classification was selected, resulting in 27 weather types during the 1979-2018 period. Searching for similarities between the weather types and cyclonic formations above the Mediterranean area (close to the sampling site from the Southern Carpathians), that favors the occurrence of rainfall events, six weather types were selected. In contemplation of visualizing the distribution of precipitation upon southeastern Europe, the multiannual average rainfall sums were built for each CT, by using daily gridded E-OBS data at a spatial resolution of 0.1 degrees. To remove uncertainties, the mean from 100-member ensemble from multiple interpolation methods was used (Cornes et al., 2018; Keresztesi et al., 2020a).

3.2.4. Zonal circulations and zonal index construction

To construct the daily zonal index (ZI) ERA Interim MSLP recorded at 12 UTC (Dee et al., 2011) was used, being characterized as the latitudinal difference between MSLP at 56°N and MSLP at 32°N. The meridional index (MI) was built on the same principles, but between 5°E and 45° E longitude, using the method by Kutiel et al., (1996), who used the above-mentioned indices in the Mediterranean area with regard to precipitation. To analyze rainfall that is characteristic to westerly circulations over Romania, the ZI was used, defining the term "strong ZI" as the days with ZI score higher than the 75th % from the overall number of days with ZI greater than 1. The daily gridded precipitation data (at a spatial resolution of 0.1 degrees) for Europe was retrieved from E-OBS to evaluate the interconnections between ZI and rainfall in the European continent. To validate the results, the method used by Jenkinson and Collison in 1977 was applied to build the westerly flow, by using 16 grid points around an area of interest to construct the weather types (Jones et al., 1993). The westerly flow can be calculated according to the following equation, expressing the results in hPa:

$$W = {}^{1}/_{2} * (12 + 13) - {}^{1}/_{2} * (4 + 5) \quad (5)$$

The realize the Jenkinson-Collinson (JC) scheme jcext library in R language was used (Otero et al., 2018).

3.2.5. Air mass trajectory and cluster analysis

In this thesis clustering was used to group trajectories with similarities, using the Hybrid Single-Particle Lagrangian Integrated Trajectory (HYSPLIT) model, developed by NOAA and Australia's Bureau of Meteorology (Draxler and Hess, 1997; Stein et al., 2015).

For the northern group from the Eastern Carpathians, the dominant cluster-mean trajectories were constructed, between 2009 and 2017, using 72-hour back-trajectories arriving at 1500 m AGL, starting new trajectories daily during January 1st, 2009, and

December 31st, 2017, that arrived at the sampling sites, at 0 and 12 UTC. Six clusters were built, taking under account the paths and numbers of trajectories.

In the case of the studied locations from the Southern Carpathians, the main trajectories and paths were generated using 24-h back trajectory during the January 2014 and December 2017 period. To discover the main air parcels, one 24-h back trajectory was generated, starting a new trajectory daily, with an ending height of 2000 m AGL. A total number of 4383 back trajectories were derived, resulting in 1461 back trajectory for each sampling site. Clustering was made by using SPVAR, followed by the selection of the ideal number of clusters with the help of TSV.

3.2.6. Multivariate statistical analysis

To decipher the interconnections between ionic compounds and elements in rainwater, Principal Component Analysis (PCA) was applied, using IBM SPSS Statistics version 23 program. The varimax rotation method was chosen to optimize the variance and to retrieve higher loadings to each principal component.

3.3. Methods used in the assessment of chemical composition of rainwater

3.3.1. The acidic and neutralization potential

The fraction of the acidic (AP) and neutralization potential (NP) can be found by applying using the following equation (Keresztesi et al., 2020c, 2019):

$$AP/NP = (NO_3^- + nssSO_4^{2-})/(NH_4^+ + nss\,Ca^{2+} + nssMg^{2+} + nssK^+) \quad (6)$$

where nss stands for the non-sea salt ratio of the cations mentioned above.

3.3.2. Neutralization factor (NF)

The neutralizing capacity of precipitation was assessed by applying the following formula (Keresztesi et al., 2019; Szép et al., 2018):

$$NF_{xi} = \frac{[X_i]}{[SO_4^{2-}]+[NO_3^-]} \quad (7)$$

where: $[X_i]$ is the concentration of the cations measured in the precipitation samples (Ca^{2+}, NH_4^+, Na^+, K^+, Mg^{2+}) expressed in μeq/L.

3.3.3. Fractional acidity (FA)

Fractional acidity is a renowned and widely applied tool to evaluate the relationship between acidic and alkaline species in precipitation (Keresztesi et al., 2020c; R. Szép et al., 2019):

$$FA = \frac{H^+}{(NO_3^- + SO_4^{2-})} \quad (8)$$

3.3.4. Ammonium Availability Index (AAI)

The AAI shows the fraction between the NH_4^+ concentration and the sum of SO_4^{2-} and NO_3^- (R. Szép et al., 2019):

$$AAI = \frac{[NH_4^+]}{2[SO_4^{2-}] + [NO_3^-]} * 100 \quad (9)$$

When AAI < 100%, there is an NH_4^+ deficit, indicating that sulfate and nitrate are the main acidifying agents; when AAI ≥ 100%, then the rainwater is alkaline, and ammonium can neutralize NO_3^- and SO_4^{2-}.

3.3.5. Wet deposition flux

Wet deposition fluxes are expressed by multiplying the VWM (mg/L concentration) and the annual rainfall (RF) amount (Szép et al., 2017), according to the following equation:

$$WD\ (kgha^{-1}\ yr^{-1}) = VWM\ (mg\ L^{-1}) * \frac{RF}{100} \quad (10)$$

In case of the data for the conterminous US, wet deposition gridded data during 2000-2017 for sodium, potassium, calcium, magnesium, chloride, nitrate, ammonium, and sulfate were used from the National Atmospheric Deposition Program (NADP). The values for deposition data on the NADP were calculated using equation 12, combining the National Trends Network (NTN) measured rainwater chemistry data with rainfall estimates from the Parameter-elevation Regression on Independent Slopes Model (PRISM). After downloading the gridded data for each year during the 2000-2017 period, the multiannual average WD values were assessed for each sampling site, generating concentration maps (Fig. 29).

3.3.6. Marine and crustal enrichment factors

Marine and crustal enrichment factors (EF_{sea}, EF_{crust}) were assessed using the following formula, with Na^+ as the reference element for seawater, and Ca^{2+} as the terrestrial trace ion (Keresztesi et al., 2020b, 2019):

$$EF_{seawater} = [X/Na^+]_{rainwater} / [X/Na^+]_{seawater} \quad (11)$$

$$EF_{crust} = [X/Ca^{2+}]_{rainwater} / [X/Ca^{2+}]_{crust} \quad (12)$$

where X represents the amount of the element of interest in precipitation; X/Na^+ and X/Ca^{2+} of rainwater are the ratios measured in precipitation; X/Na^+ seawater and X/Ca^{2+} crust stand for the ratio of seawater and crustal composition (Keresztesi et al., 2019).

3.3.7. Sea salt and non-sea salt fractions

In order to determine the percentage of seawater and non-seawater sources in rainwater chemistry, the sea salt fractions (SSF) and non-sea salt fractions (NSSF) were calculated, according to the following equations (Das et al., 2005):

$$\%SSF = \frac{100*(Na)_{rain}*(X/Na)_{sea}}{(X)_{rain}} \quad (13)$$

$$\%NSSF = 100 - SSF \quad (14)$$

where, X represents the concentration of the respective ion.

Another method that was used to estimate the relative contributions of seawater, terrestrial and anthropogenic origins to the total chemical composition of precipitation, is described by the following equation (Xing et al., 2017):

$$\%SSF = \frac{Na^+ + ssCl^- + ssSO_4^{2-} + ssCa^{2+} + ssMg^{2+} + ssK^+}{\Sigma ion} * 100 \quad (15)$$

$$\%CF = \frac{nssCa^{2+} + nssMg^{2+}}{\Sigma ion} * 100 \quad (16)$$

$$\%AF = 100 - \%SSF - \%CF \quad (17)$$

where SSF, CF and AF represent sea salt fraction, crust faction and anthropogenic source fraction, respectively, while Σion represents the sum of mean concentration of all cations and anions, except H^+ and HCO_3^-.

To calculate the marine and non-marine fraction values of any particular ion, the following equation was used, considering Na^+ as a reference element (Xing et al., 2017):

$$[ss - X] = [Na^+]_{rainwater} * \left[\frac{[X]}{[Na^+]}\right] seawater \quad (18)$$

$$[nss - X] = [X] - [ss - X] \quad (19)$$

where, [ss-X] and [nss–X] represent the concentration of sea salt (ss) and non-sea salt (nss) concentration of the species X; $[Na]_{rainwater}$ and $([X]/[Na^+])_{seawater}$ are the concentration of Na^+ in rainwater samples and the ratio of ion X and Na^+ in seawater (Xing et al., 2017).

In the case of Europe and conterminous US, where the SSF calculated from Na^+ gives values > 100%, and in most rainwater samples the Na^+/Cl^- ratio has similar values compared to the Na^+/Cl^- seawater ratio (0.86), the seawater and non-seawater contributions can be calculated using Cl^- as a reference element (Keresztesi et al., 2020b, 2019):

$$\%SSF = \frac{100*(Cl)_{rain}*\left(X/Cl\right)_{sea}}{(X)_{rain}} \quad (20)$$

$$\%NSSF = 100 - SSF \quad (21)$$

where X is the concentration of the respective ion.

4. Results and discussion

4.1. Atmospheric circulation and effects of the Eastern Carpathians on precipitation

As it can be observed in Fig. 3, rainfall distribution over Romania shows that on the western side precipitation events are more frequent compared to the eastern side (Szép et al., 2018). The intra-mountain basins of the Carpathians are characterized by lower amounts of rainfall, imposed by the mountainous orographic barrier. This phenomenon can be observed through the orographic convection, leading to more precipitation on the northwestern slopes, also influenced by the prevalent direction of atmospheric circulations, which has effects on the chemical composition of precipitation too. The rainfall amount, temperature and wind direction are also influenced by the adiabatic conditions, hence on the leeward ramps the air becomes more stable.

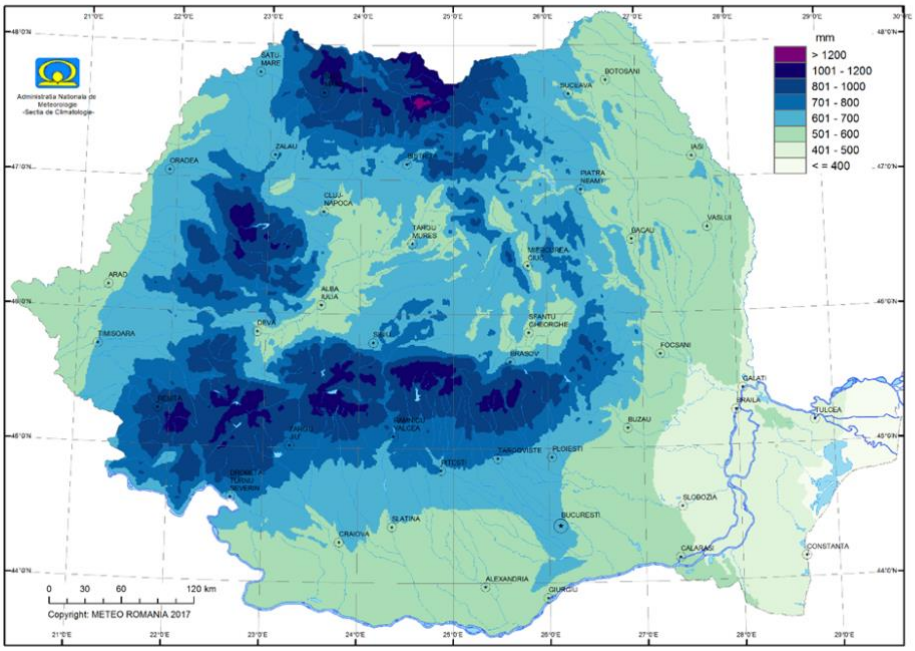

Fig. 3. Multiannual mean precipitation (1981-2016) in Romania.

To study the interconnection between multiannual rainfall amount and elevation, gridded multiannual rainwater data and a digital elevation model were used, the first being provided by the Romanian National Meteorological Administration.

Fig. 4a shows the enlarged spatial domain from 21 to 27 E longitude degrees (to obtain a good coverage) used to assess the connection between precipitation amount and elevation.

The linear regression analysis between rainwater and elevation showed an R^2 of 0.41 at 95% confidence level (Fig. 4b), result sustained by the prediction model too, which showed goodness of fit of the observed vs. the predicted values, from 31660 values included, with a standard error of 54.99.

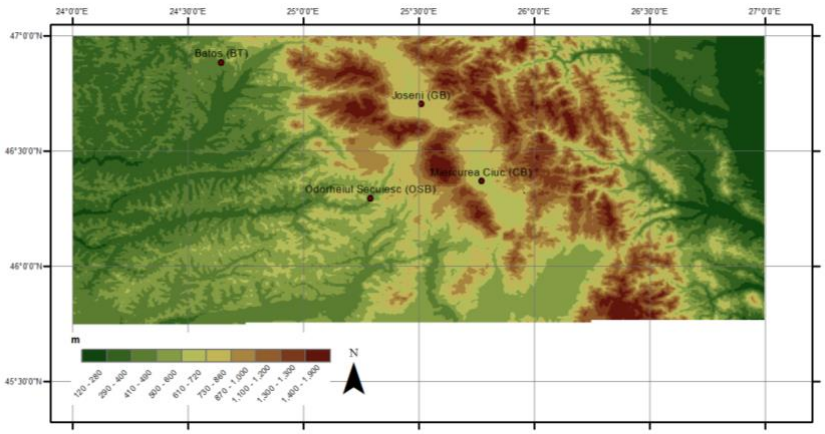

(a)

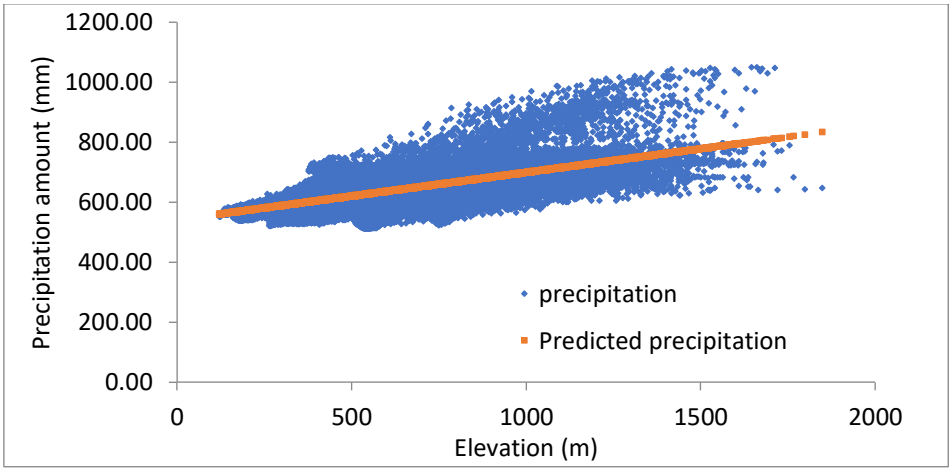

(b)

Fig. 4. Spatial domain for applying linear regression between precipitation and elevation (a); prediction model for observed and predicted precipitation (b).

The barrier effect imposed by the mountainous chain of the Eastern Carpathians can be illustrated by the longitudinal profiles of Joseni and Miercurea Ciuc weather stations, located in GB and CB, respectively, and comparing the rainfall amount and elevation (Fig. 5).

The orographic convection which implies the link between rainfall and elevation is also causing water vapors to be lifted to the condensation level. The atmospheric circulation type characteristic for Romania is the high extent of the Azores High fronting South and Central Europe; yet this pattern is also correspondent to a meridional circulation in the upper levels of the troposphere, with air masses coming from North-Europe to northwest and southeast, carrying more humidity over the studied areas. The mountainous barrier created by the Eastern Carpathians often stands in the way of these air masses, modifying their trajectory, and the wind direction, which also influences the chemical composition of rainwater.

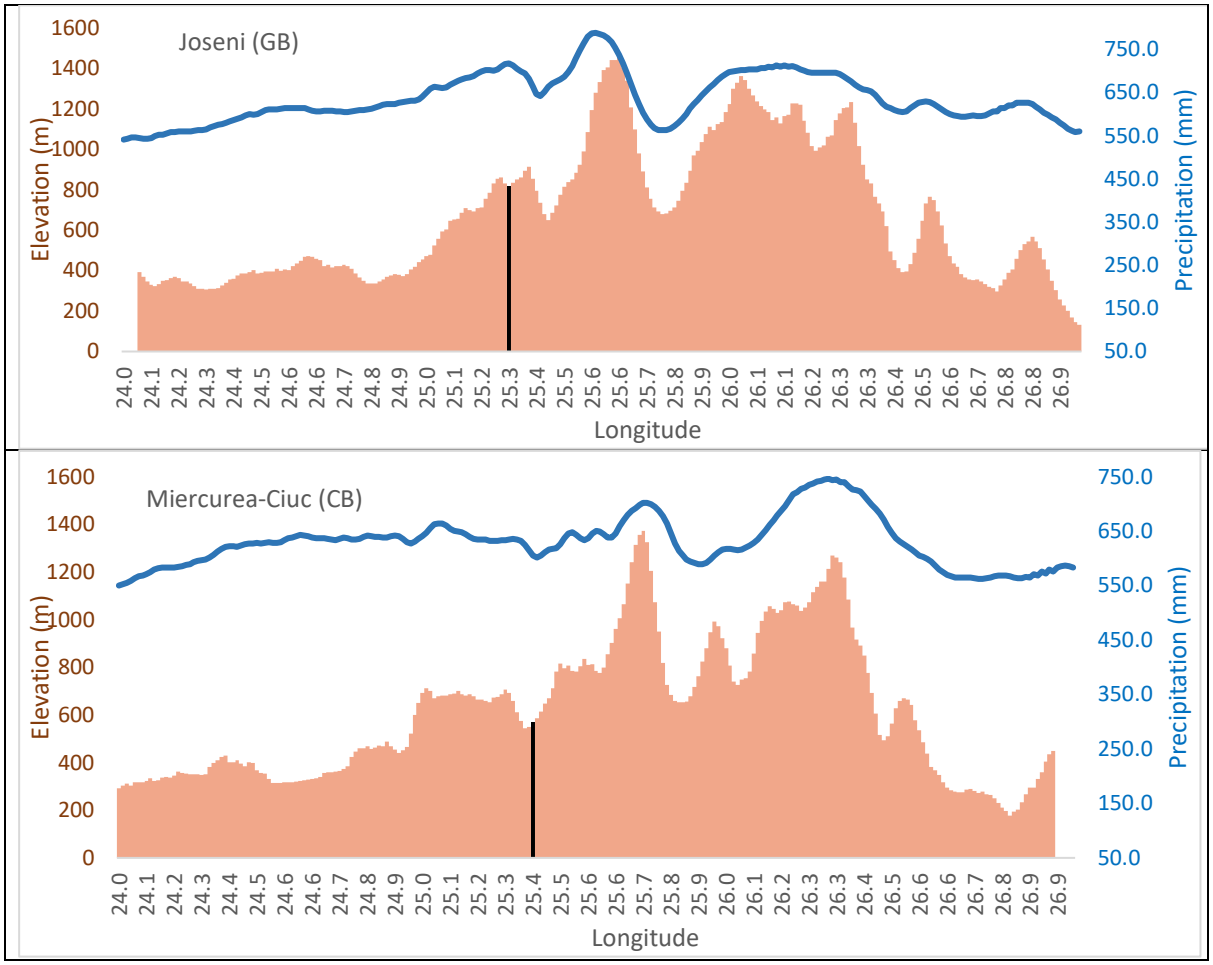

Fig. 5. Longitudinal profile of precipitation amount and elevation.

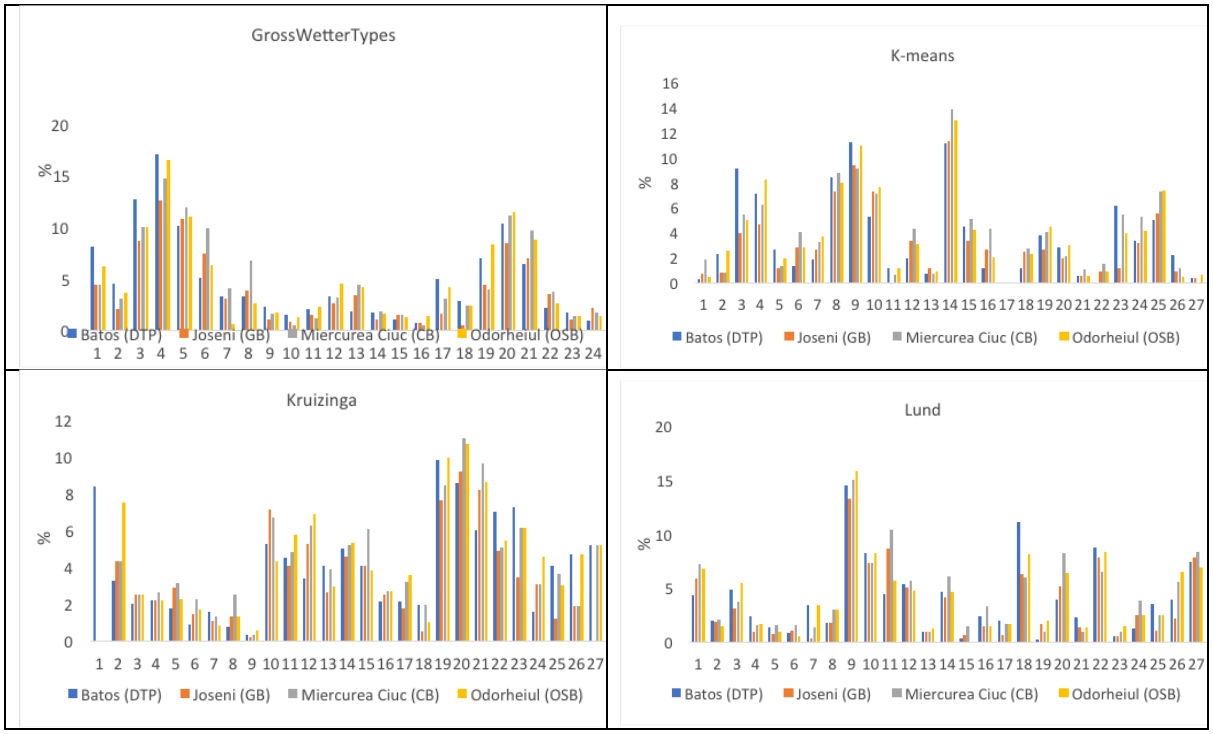

Fig. 6. Conditional probabilities (%) for GWT, K-means, Kruizinga and Lund classification.

Fig. 6 represents the conditional probabilities for each circulation type, exhibiting resembling patterns, with highest probabilities. This high probability observed in case of all methods may be due to an easterly cyclonic type with a low-pressure center placed in the northern part of the Black Sea, while the western part of the European continent influenced by a high-pressure system favoring to cold and wet air masses from the northern Europe to advance to the lower latitudes (Fig. 7), which is characteristic for meridional advections. In the upper troposphere, the polar Jet stream is usually rippled to lower latitudes, leading to cases when separation occur from the main flow to the low boundary situations.

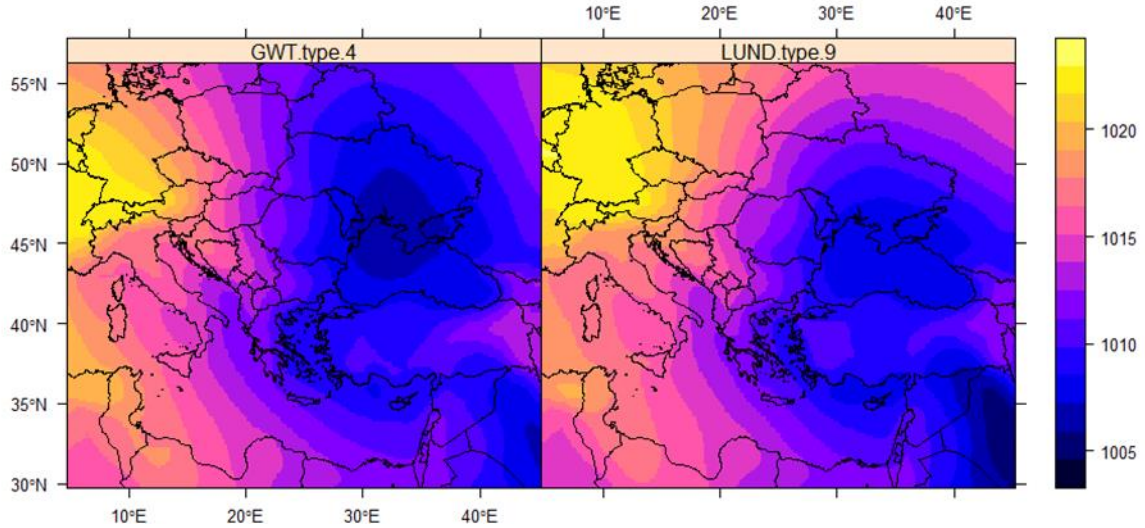

Fig. 7. MSLP centroids for GWT and LUND types leading most frequently to high precipitation.

The above-mentioned phenomenon is also true for polar air masses moving towards the center and south-eastern part of the continent. There are some occurrences, when the polar air masses intersect the warmer and wetter troposphere above the Black Sea, cyclogenesis occurs, which leads to the renewal of the weather front with humidity, and the trajectories change to a NW pattern, advancing towards Romania (Fig. 8).

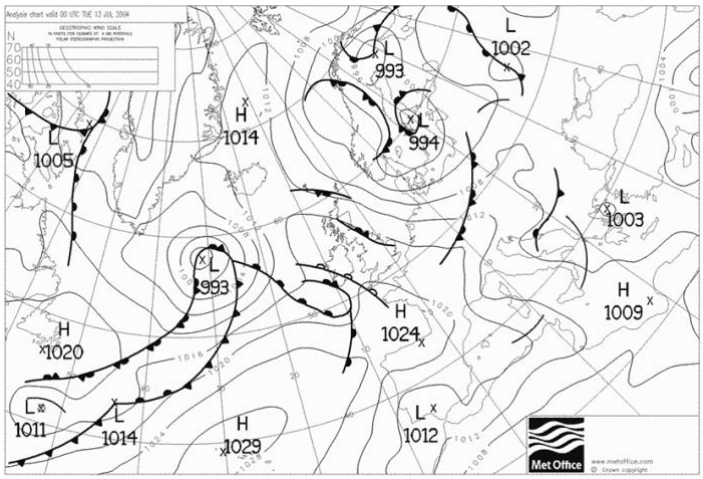

Fig. 8. Mean sea level pressure for 11 July 2004: typical east cyclonic circulation type over the classification domain. Source: metoffice.gov.co.uk.

Amongst the classification methods used, Lund (LND) and GrossWetterTypes (GWT) performed better by having more input parameters. Hence the LND and GWT

methods showed a better result, the average values for liquid water path, all sky liquid water path and cloud optical thickness for the types having the highest probability of high rainfall (type 4 for GWT and type 9 for LUND, both meaning an easterly cyclonic advection) were assessed. Although the sampling sites are placed inside a mountainous depression area, the values for liquid water path, all sky liquid water path and cloud optical thickness didn't exhibit lower values compared to the ones in more elevated proximities (Fig. 9, 10).

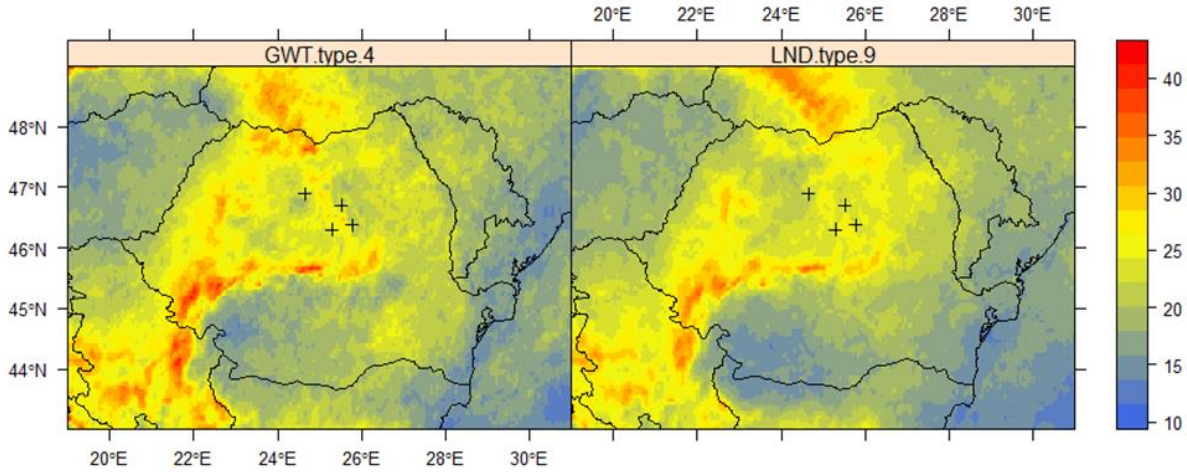

Fig. 9. Mean cloud optical thickness (μm) for CT (GWT) 4 and 9 (LND) for the 2005-2014 period.

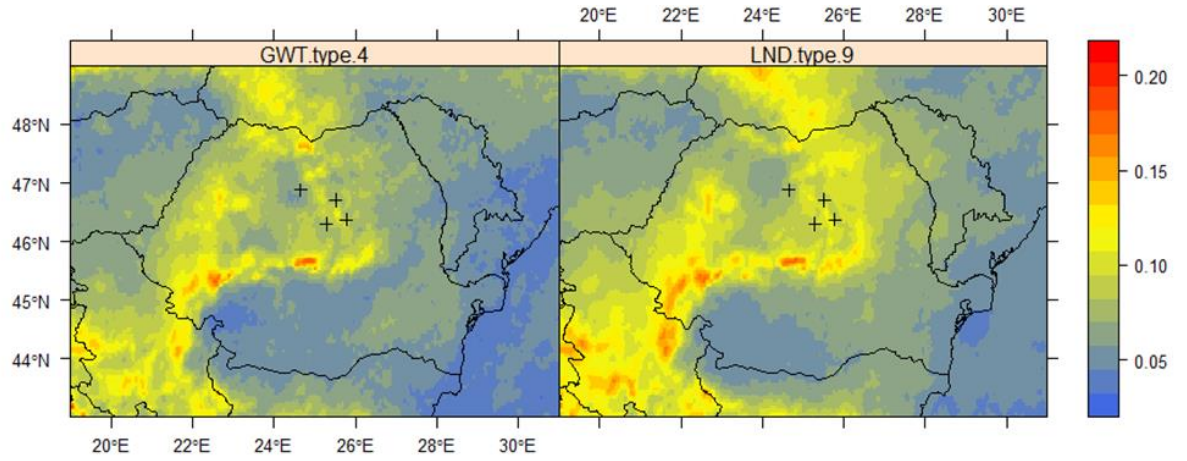

Fig. 10. Mean all sky liquid water path values (kg/m^2) for CT 4 (GWT) and 9 (LND) for the 2005-2014 period.

This result is not surprising, taking into consideration the strong correlation between elevation and rainfall amount, favored by the air's orographic convection. By examining the spatial distribution of cloud products, strong similarities can be observed of the studied parameters. The cloud top height average difference for LND and GWT appears to be lower than the multiannual average, predicting storm intensity.

High-altitude flow and wind shear it is not likely to occur in intra-mountain depressions such as CB and GB, favoring the appearance of deep convection conditions. In the case of an easterly cyclonic type, which is also characteristic to the studied area, the cloud top height values are greater for the areas that are situated further from the low-pressure system (Fig. 11), this may be due to the humidity rate, which is usually more elevated in areas that are in the vicinity of the low-pressure center system.

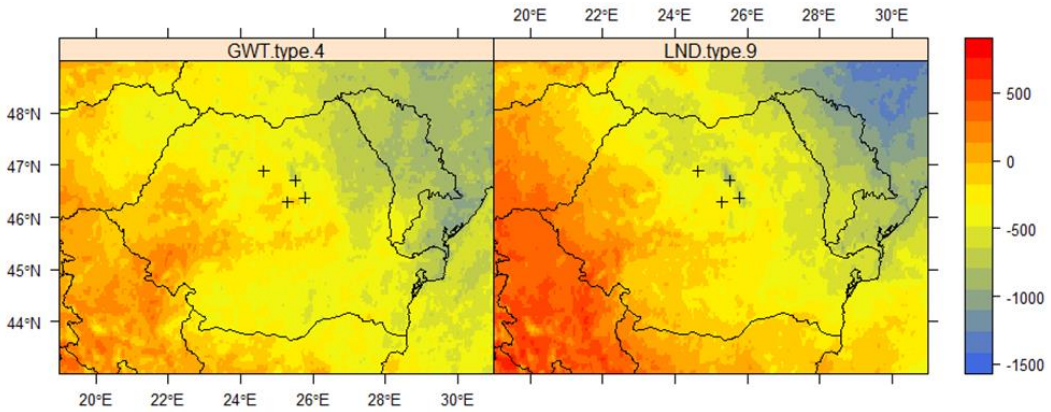

Fig. 11. Mean cloud top height difference against the multiannual mean (m) for CT 4 (GWT) and 9 (LND) for the 2004-2015 period.

4.2. General variability and chemical composition of precipitation

Statistical analyses of precipitation chemistry, such as volume-weighted mean (VWM), average, minimum, maximum, standard error and standard deviation values were performed for all studied regions in the present thesis.

In the case of the central group of the Eastern Carpathians (Table 3), among all assessed ions, NH_4^+ had the highest VWM concentration in CB, GB, and DTP, having an average of 158.0 µeq/l, 224.2 µeq/l, and 407.4 µeq/l, respectively. At OSB, Ca^{2+} presented the greatest VWM concentration (203.1 µeq/l), followed by NH_4^+ with a VWM of 200.6 µeq/l. The downward order for major ions in terms of VWM concentrations was the following in the case of CB: $NH_4^+ > Ca^{2+} > SO_4^{2-} > Cl^- > HCO_3^- > NO_3^- > Na^+ > K^+ > Mg^{2+} > NO_2^- > H^+$, with the ammonium representing ~35% and ~54% of the total ions and cations measured, while Ca^{2+} representing ~17% and ~27% amongst all measured ions and cations, respectively. SO_4^{2-} and Cl^- had the most dominant concentrations amongst anions, with concentrations that accounted for the ~35% and ~25% of the total sum of anions. In the case of GB, the VWM concentrations of major ionic species can be organized in the following order: $NH_4^+ > SO_4^{2-} > Ca^{2+} > HCO_3^- > Cl^- > Na^+ > K^+ > NO_3^- > Mg^{2+} > NO_2^- > H^+$. Amongst all measured ions NH_4^+ and SO_4^{2-} concentrations accounted for ~37% and ~13%, respectively, while in case of cations and anions only, the above-mentioned ions represented ~56% and ~37%, respectively. The following downward order was observed in case of DTP: $NH_4^+ > Ca^{2+} > SO_4^{2-} > HCO_3^- > Cl^- > K^+ > Na^+ > NO_3^- > Mg^{2+} > NO_2^- > H^+$, where NH_4^+ represented the ~46% of all ions, and ~66% of the cations. SO_4^{2-} was observed to be the predominant amongst anions, representing ~37%. For OSB, the measured ionic species were in the $Ca^{2+} > NH_4^+ > SO_4^{2-} > HCO_3^- > Cl^- > NO_3^- > K^+ > Na^+ > Mg^{2+} > NO_2^- > H^+$ downward order, with calcium having the highest concentration and representing ~26% and ~42% amongst all ions and cations. NH_4^+ had similar concentrations, showing values that represented ~25% of the total ions and ~41% of the total cations. The most dominant anion was SO_4^{2-} (159.4 µeq/L), accounting for the~52% of the total measured anions. As it can be observed, in case of CB, GB and DTP, NH_4^+ had the highest concentration amongst the total ionic species in precipitation. According to Xu et al., (2015), elevated concentrations of atmospheric NH_3 may be the result of the heterogeneous reactions involving it, being mainly emitted to the atmosphere from the use of fertilizers, animal waste, anthropogenic activities, such as various industries and wastewater treatments (Wang et al., 2018).

Table 3. Volume-weighted mean concentration of major ion (in μeql^{-1}) and pH along with statistical results in rainwater samples in the central group of the Eastern Carpathians.

Component	pH	Na^+	K^+	Ca^{2+}	Mg^{2+}	SO_4^{2-}	Cl^-	NO_2^-	NO_3^-	NH_4^+	HCO_3^-	H^+
CB												
VWM*	6.5	22.5	19.0	78.5	15.5	54.5	38.4	4.8	26.5	158	32.5	0.9
Mean value	6.6	31.9	25.4	101.2	18.2	64.7	49.7	5.8	33.2	153.1	37.7	0.7
St. deviation	0.5	40.0	32.9	115.3	20.7	72.2	48.7	13.2	28.2	215.7	45.0	2.4
St. error	0.03	2.1	1.7	6.1	1.1	3.8	2.6	0.7	1.5	11.3	2.4	0.1
Minimum	4.5	0.8	0.2	4.2	0.4	0.8	0.7	0.1	0.4	1.9	0.2	0.01
Maximum	7.9	239.6	240.6	1330.9	201.4	501.3	383.9	144.6	177.8	1823.3	407.4	33.9
GB												
VWM*	6.7	38.2	29.5	68.0	21.7	76.0	43.9	4.4	24.7	224.2	51.8	0.4
Mean value	6.6	48.4	34.7	95.1	28.5	99.5	58.5	6.0	30.8	235.4	56.2	0.4
St. deviation	0.5	45.3	32.7	90.6	27.4	103.5	43.6	17.7	22.1	234.7	59.6	0.6
St. error	0.05	4.2	3.1	8.5	2.6	9.7	4.1	1.7	2.1	22.0	5.6	0.1
Minimum	5.5	1.9	1.0	20.0	3.6	7.5	6.2	0.4	2.3	16.9	1.6	0.01
Maximum	7.8	243.4	168.6	623.8	144.6	484.5	216.9	181.8	164.5	1223.3	389.1	3.6
DTP												
VWM*	6.9	34.8	36.5	116.1	24.5	95.0	54.8	12.5	26.2	407.4	71.4	0.8
Mean value	6.9	43.3	41.9	128.7	25.9	109.5	66.4	16.5	32.5	349.8	72.2	0.3
St. deviation	0.5	38.3	68.1	116.4	25.3	88.6	40.1	34.1	23.1	411.6	87.3	0.6
St. error	0.05	3.5	6.3	10.7	2.3	8.2	3.7	3.1	2.1	37.9	8.0	0.1
Minimum	5.2	4.3	4.4	26.0	2.3	11.7	5.7	0.4	3.5	11.6	1.0	0.01
Maximum	8.0	195.6	640.3	782.9	199.1	453.9	240.4	337.4	152.8	1851.9	575.4	5.7
OSB												
VWM*	6.4	26.4	27.7	203.1	19.2	159.4	45.2	7.8	39.1	200.6	54.2	7.4
Mean value	6.6	32.1	30.9	232.7	22.8	193.6	52.7	9.2	47.5	213.5	59.1	5.7
St. deviation	0.9	32.3	34.6	149.8	21.6	199.1	37.2	12.9	35.0	243.7	71.9	24.9
St. error	0.1	3.0	3.2	14.0	2.0	18.6	3.5	1.2	3.3	22.8	6.7	2.3
Minimum	3.6	0.7	0.2	18.0	1.9	9.2	9.4	0.2	1.7	5.5	0.02	0.01
Maximum	8.0	149.2	194.7	910.2	130.5	1160.7	209.3	78.3	183.0	1299.9	562.3	239.9

***** Volume-Weighted Mean

According to the above, OSB the most abundant cation was represented by calcium, which can be attributed to the dissolution of dolomites and calcareous rocks (Szép et al., 2018). The above-mentioned alkaline species controlled the acidity at the studied locations, fact that is also sustained by mean pH values: 6.6, 6.8, 6.89, 6.6 at CB, GB, DTP and OSB, respectively. This is a great example of the theory shown in the study of Wang and Han, (2011), where it is shown that rainwater samples with a pH value > 6, suggest inputs of alkaline species into precipitation.

Inequalities between major ion concentrations in the intra mountain basins (CB, GB, DTP) and the extra mountain areas (OSB) can be caused by the characteristic microclimate and local anticyclone systems, leading to reduced rainwater amount and limited airflow circulation, resulting in pollutant accumulation.

In the Northern group of the Eastern Carpathians, ionic composition of rainwater showed a similarity among sampling sites (Table 4), with calcium being the most dominant, having a VWM concentration of 231.22 μeq/l, 132.14 μeq/l, 178.33 μeq/l and 140.94 μeq/l for SE, at BM, BZ, SM, and SE, respectively. In general, calcium originates from terrestrial sources, and it is present in rainwater due to the dissolution process of dolomitic and calcareous rocks (Szép et al., 2018). Ammonium also presented higher concentrations, with values accounting for 46.11 μeq/l, 69.65 μeq/l, 92.31 μeq/l, and 65.58 μeq/l at BM, BZ, SM, and SE, respectively.

Table 4. Volume-weighted mean concentration of major ion (in μeql^{-1}) and pH along with statistical results in rainwater samples in northern group of the Eastern Carpathians

Component	pH	Na^+	K^+	Ca^{2+}	Mg^{2+}	SO_4^{2-}	Cl^-	NO_3^-	NH_4^+	HCO_3^-	H^+
BM											
VWM*	6.54	27.63	11.18	231.22	25.29	142.66	38.34	29.65	46.11	34.35	0.95
Mean value	6.59	36.00	13.25	250.12	28.10	173.32	47.05	34.90	54.45	35.52	0.87
St. deviation	0.50	81.41	21.53	596.78	19.50	404.68	45.21	51.35	48.43	32.43	3.77
St. error	0.03	4.81	1.27	35.23	1.15	23.89	2.67	3.03	2.86	1.91	0.22
Minimum	4.32	1.26	0.43	18.11	2.88	0.02	4.85	0.48	1.11	0.12	0.02
Maximum	7.63	1194.01	181.08	7440.49	239.46	3667.50	432.83	782.20	359.95	242.66	48.08
BZ											
VWM*	6.80	30.28	20.51	132.14	34.97	65.79	41.00	29.76	69.65	49.34	0.46
Mean value	6.80	35.95	24.56	148.95	39.51	77.95	50.07	33.71	83.94	51.14	0.67
St. deviation	0.44	47.90	32.33	150.37	41.77	117.21	47.38	25.52	69.96	35.50	4.38
St. error	0.03	2.83	1.91	8.88	2.47	6.92	2.80	1.51	4.13	2.10	0.26
Minimum	4.24	2.13	1.59	2.25	7.49	0.77	0.03	1.85	2.27	0.10	0.03
Maximum	7.47	409.75	268.30	1468.64	530.34	788.86	518.29	188.49	699.89	170.61	57.28
SM											
VWM*	6.84	41.15	33.83	178.33	43.99	76.99	49.56	32.47	92.91	60.20	0.40
Mean value	6.82	50.69	39.49	185.22	49.70	84.13	57.80	38.38	101.68	59.03	0.61
St. deviation	0.47	62.93	66.00	191.94	56.75	128.28	44.01	44.63	237.00	61.99	4.37
St. error	0.03	3.78	3.97	11.53	3.41	7.71	2.64	2.68	14.24	3.72	0.26
Minimum	4.20	1.74	2.05	3.19	8.06	0.50	2.43	0.53	5.99	0.09	0.01
Maximum	7.91	398.00	503.09	1813.96	579.30	815.72	331.31	563.87	3032.41	463.45	63.83
SE											
VWM*	6.77	31.83	52.37	140.94	36.23	68.71	50.48	30.75	65.58	45.33	0.58
Mean value	6.78	38.38	64.76	148.75	40.28	75.98	58.78	36.72	81.23	49.14	0.91
St. deviation	0.43	55.15	137.85	189.93	46.31	96.12	51.94	45.70	130.74	50.04	8.59
St. error	0.03	3.26	8.14	11.21	2.73	5.67	3.07	2.70	7.72	2.95	0.51
Minimum	3.89	0.96	2.92	24.00	10.37	0.15	1.75	0.16	0.78	0.04	0.01
Maximum	8.00	472.38	1606.21	2012.58	603.83	697.46	309.48	583.34	1905.65	579.43	129.42

* Volume-Weighted Mean

The elevated NH_4^+ values in in precipitation may be caused by the gas-particle equivalent reactions involving NH_3 (Xu et al., 2015), which is present in the atmosphere from chemical fertilizers, animal manure, natural decomposition, and anthropogenic activities, such as industrial facilities and wastewater treatments (Niu et al., 2016; Shukla and Sharma, 2010; Wai et al., 2008; Wang et al., 2018).

Calcium and ammonium accounted together to 41% at BM, 43% at BZ, 44% at SM and 40% at SE of the total ionic concentration, respectively (Fig. 12). The above-mentioned ions are important in rainwater chemistry, hence of their roles in restraining acidity in the Northern group of the Eastern Carpathians, which leads to higher pH values. The most abundant anion was observed to be SO_4^{2-}, with resembling concentrations at BZ (65.79 μeq/l), SM (76.99 μeq/l) and SE (68.71 μeq/l) and two times higher at BM, accounting for 142.66 μeq/l. The more elevated SO_4^{2-} concentration at BM may be due to a greater industrialization percent, the mining activities characteristic to the surroundings, as well as the emission from coal burning (representing the primary energy source in the area), that are loaded with SO_2 (Huang et al., 2010). Considerable concentrations of Cl^-, HCO_3^- and NO_3^- were also observed amongst anions, presenting an even distribution at all sampling locations. According to (Silva and Manuweera, 2004), the elevated bicarbonate concentrations can be the sign of limestone and dolomite dissolution, contributing to the neutralizing process of rainwater's acidity.

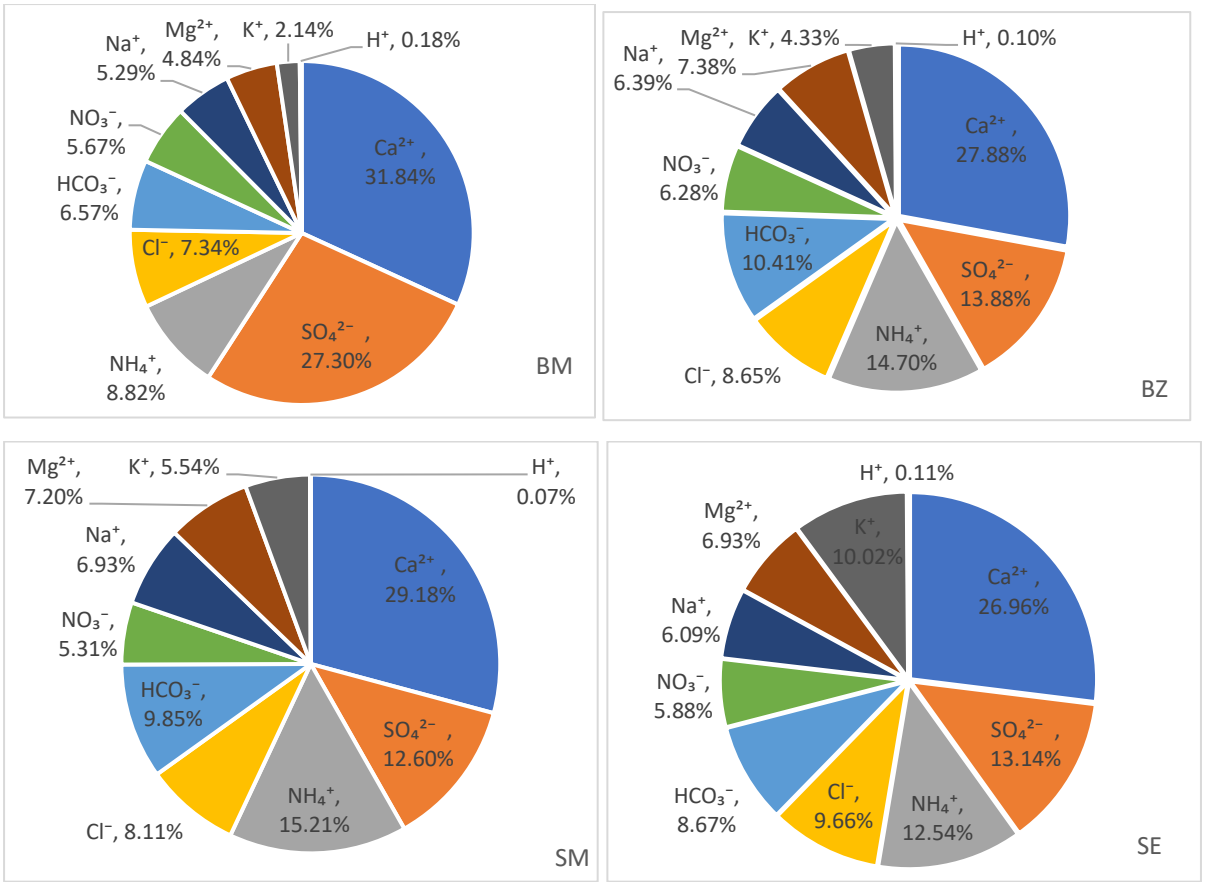

Fig. 12. Chemical composition percentages of precipitation from Baia Mare (BM), Bozinta (BZ), Somcuta (SM) and Seini (SE).

Table 5 shows the statistical results of chemical analysis of precipitation samples collected in the Southern Carpathians, in three different locations.

Table 5. Volume-weighted mean (VWM) concentration of major ions (in μeql^{-1}) and pH along with statistical results in rainwater samples from the Southern Carpathians.

	pH	Na^+	K^+	Ca^{2+}	Mg^{2+}	SO_4^{2-}	Cl^-	NO_2^-	NO_3^-	NH_4^+	HCO_3^-	H^+
RS												
VWM	6.03	37.38	15.13	132.28	68.82	49.72	132.90	2.46	18.80	94.94	24.35	4.55
Average	6.18	38.21	15.77	158.48	78.10	61.87	129.39	2.60	20.65	99.23	31.39	3.17
St. dev.	0.75	40.94	22.96	135.00	73.50	48.61	55.20	3.30	18.87	60.19	98.63	7.02
St. error	0.07	3.69	2.07	12.17	6.63	4.38	4.98	0.30	1.70	5.43	8.89	0.63
Min.	4.33	3.44	0.97	5.29	1.65	10.41	20.03	0.11	0.18	0.33	0.12	0.01
Max.	8.24	247.94	129.42	799.94	473.98	291.48	400.53	22.21	116.06	262.22	1000.00	46.77
MN												
VWM	6.78	7.38	17.50	356.73	189.46	200.35	159.04	5.28	27.81	123.78	57.88	0.29
Average	6.81	35.87	21.20	367.31	219.42	240.91	160.72	5.39	27.73	130.00	68.16	0.45
St. dev.	0.52	54.76	21.13	252.54	234.56	155.92	74.77	6.29	32.00	94.46	106.50	1.58
St. error	0.04	4.63	1.79	21.34	19.82	13.18	6.32	0.53	2.70	7.98	9.00	0.13
Min.	4.76	3.52	1.79	28.44	3.79	20.82	20.03	0.07	0.35	16.63	0.33	0.01
Max.	8.22	430.54	135.40	1574.43	1026.95	874.43	600.80	36.10	212.89	398.04	954.99	17.38
BH												
VWM	7.02	14.17	17.46	382.16	201.86	204.87	162.65	7.25	12.80	93.13	86.44	0.13
Average	7.06	50.88	18.39	422.53	218.05	226.33	162.46	6.25	12.13	86.95	93.67	0.12
St. dev.	0.35	163.42	13.52	382.38	192.82	115.99	91.33	6.64	15.15	382.52	142.09	0.12
St. error	0.03	13.96	1.16	32.67	16.47	9.91	7.80	0.57	1.29	6.45	12.14	0.01
Min.	6.12	5.65	2.81	34.93	4.94	20.82	20.03	0.09	0.35	3.88	7.59	0.00
Max.	8.43	1360.17	72.89	2319.98	789.96	687.05	520.69	30.39	127.89	382.52	1548.82	0.76

The descending order of major ion concentrations measured in rainwater collected at RS was the following: $Cl^- > Ca^{2+} > NH_4^+ > Mg^{2+} > SO_4^{2-} > Na^+ > HCO_3^- > NO_3^- > K^+ > H^+ > NO_2^-$. Calium, magnesium and ammonium presented the highest concentrations, and contributed with 83.84% to the total mass of cations, while chloride accounted for 58.23% of the total sum of anions, being the predominant within anions. At MN the descending order of major ions manifested the following: $Ca^{2+} > SO_4^{2-} > Mg^{2+} > Cl^- > NH_4^+ > HCO_3^- > NO_3^- > K^+ > Na^+ > NO_2^- > H^+$, with calcium being the most abundant cation, presenting 51.32% amongst all cations, while sulfate being the predominant anion, accounting for 44.49% of the total mass of anions. A similar descending order was observed at BH ($Ca^{2+} > SO_4^{2-} > Mg^{2+} > Cl^- > NH_4^+ > HCO_3^- > K^+ > Na^+ > NO_3^- > NO_2^- > H^+$). The most abundant cations were calcium and magnesium, presenting 53.91% and 28.47% between cations. SO_4^{2-} accounted for 43.22%, being the most dominant anion.

The elevated values of Ca^{2+} and Mg^{2+} present in the rainwater samples may be the result of the presence of soil dust originating from the un-rehabilitated tailing dams, as well as from dolomite limestones. The dissolution of calcite ($CaCO_3$), dolomite ($MgCO_3$) and gypsum ($CaSO_4 \cdot 2H_2O$) in the rainwater explains the high concentrations of Ca^{2+}, Mg^{2+} and SO_4^{2-} in the studied areas (Keresztesi et al., 2020a).

To compare the results of the characteristics of precipitation composition found on a local scale with the characteristics on a global scale, the ionic composition of precipitation in Europe and in the Conterminous United States was also assessed.

Fig. 13 presents the spatial distribution and variability of precipitation chemistry across the European continent during 2000-2017.

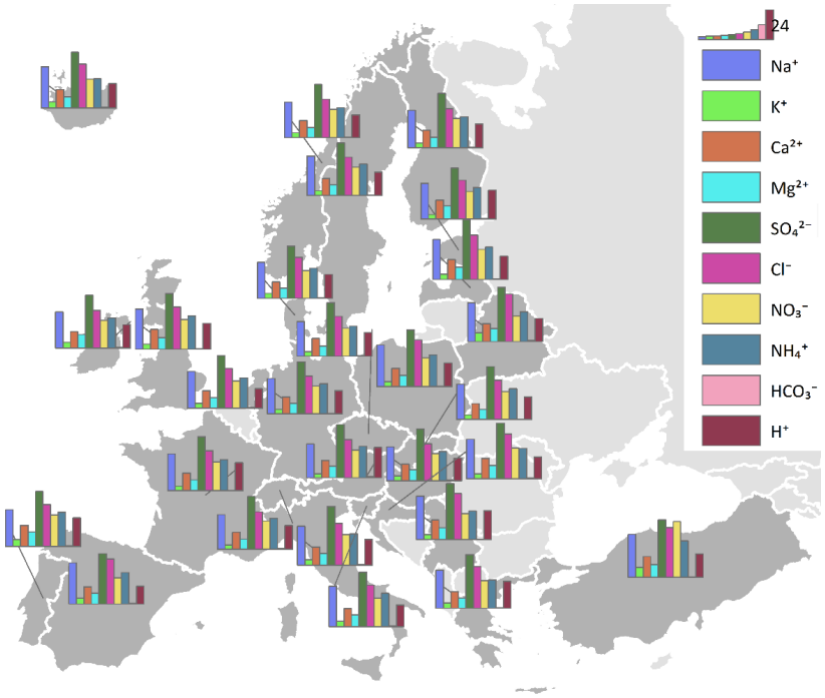

Fig. 13. Volume weighted means of major ions in rainwater samples collected in Europe.

VWM concentration for each major ion are illustrated by a colored bar chart, on a linear scale. In general, ionic concentrations followed the $SO_4^{2-} > Cl^- > Na^+ > NH_4^+ > NO_3^- > H^+ > Ca^{2+} > Mg^{2+} > K^+ > HCO_3^-$ descending sequence, presenting different patterns based on legal framework or industrial activity. Sulfate was the most abundant anion in all 27 countries, exhibiting values between 40.60 μeq L^{-1} (Spain) and 48.38 μeq L^{-1} (Latvia),

representing and 43.51% of the total ions and anions measured, respectively, being ensued by Cl^- and Na^+.

Chloride occupied 16.24% and 32.89% among the total measured ions and anions on average, respectively, while sodium was the most dominant cation, exhibiting 14.95% and 29.54% among all ions and cations, respectively. It was observed that without exception, sodium was succeeded by ammonium.

Hence no major discrepancies have been observed among the VWM concentrations calculated for the 27 European countries, one can say that this indicates the homogeneity of the data, which can be due to the similarity of the applied environmental policies and regulations. It was observed that this results in low emission and pollutant concentration variability at a regional level, however, discordances can be observed locally, as it is shown in the chemical composition of rainwater.

VWM concentrations calculated from data collected between 1978-2017 at 334 sampling sites in the contiguous US are shown in Fig. 14. One can see that major ion concentrations followed in almost every case the $Cl^- > Na^+ > SO_4^{2-} > Ca^{2+} > H^+ > NH_4^+ > NO_3^- > Mg^{2+} > HCO_3^- > K^+$ downward order.

The most abundant concentrations of Cl^- and Na^+ were observed near the coastline, indicating their marine origin. The highest values were observed in Channel Islands, California (153.67 μeq L^{-1} – Cl^-; 136.03 μeq L^{-1} – Na^+) and Nantucket, Massachusetts (155.93 μeq L^{-1} – Cl^-; 128.28 μeq L^{-1} – Na^+). By examining the concentration maps for chloride and sodium, one can see that their dominance drops towards the continental regions, showing the blocking effect of the mountainous regions in front of air masses loaded with marine salts (Keresztesi et al., 2020b). The most elevated VWM values of Ca^{2+} and Mg^{2+} were observed in Green River, Utah (66.09 μeq L^{-1}) and Channel Islands, California (34.38 μeq L^{-1}). In the conterminous US, higher values of Ca^{2+} were registered in the desert areas, such as the Great Basin Desert, the Mojave Desert, the Sonoran Desert, and some parts of the Chihuahuan Desert. According to Xiao et al., (2017), magnesium can originate from both terrestrial and marine sources, fact that is confirmed by the concentration map of Mg^{2+}, where one can see higher magnesium levels near the coastline. NH_4^+ showed the highest VWM concentrations in Huron Well Field, South Dakota (42.43 μeq L^{-1}) and in Logan, Utah (41.50 μeq L^{-1}). High concentrations of ammonium in rainwater may suggest high atmospheric NH_3, that originates from agricultural activities, livestock breeding, cattle waste deposits and use of fertilizers (Keresztesi et al., 2019; Wang et al., 2019; Zunckel et al., 2003). After a detailed examination of the ammonium concentration map, similarities were observed between high NH_4^+ concentrations and the agricultural belts of the studied area, such as the dairy belt and the corn and wheat belts. The main sources of ammonia in the atmosphere from these areas come from livestock breeding (Illinois, Indiana, Michigan, Minnesota, New York, Ohio, Pennsylvania, Wisconsin) and the use of fertilizers for corn and wheatfields, in the regions between the Ohio River and the lower Missouri River, and the areas from Kansas through the Canadian Prairie, respectively (Keresztesi et al., 2020b).

Among anions, sulfate and nitrate exhibited the most elevated values, with maximum concentrations being observed in Tombstone, Arizona (76.76 μeq L^{-1}) and in Channel Islands, California (36.51 μeq L^{-1}).

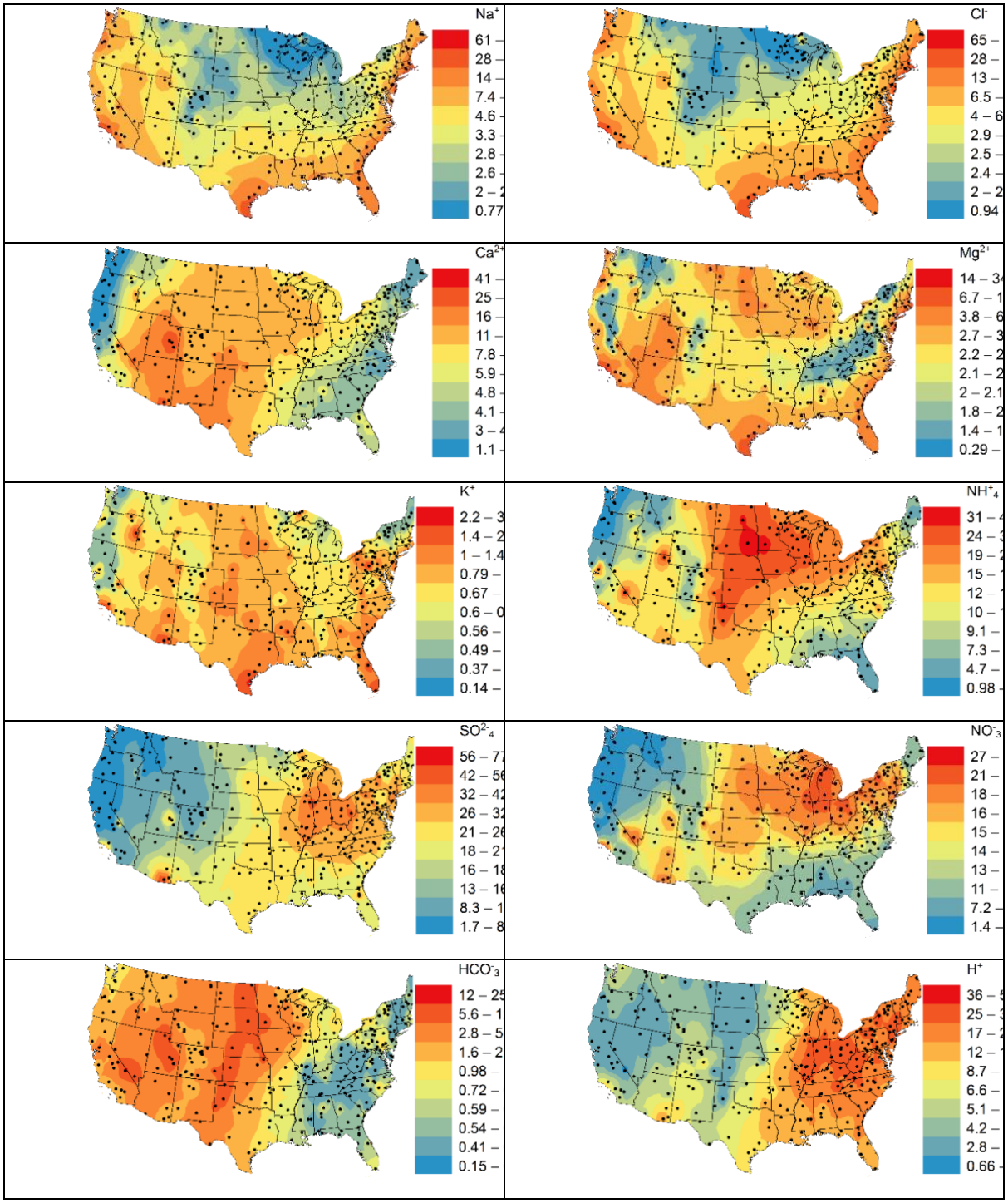

Fig. 14. The spatial variability of volume weighted means (μeq L^{-1}) of major ions in precipitation over the U.S. during 1978-2017.

Common sources of SO_4^{2-} are anthropogenic activities, such as emissions from industrial activities, oil refineries and copper smelters (Herbert and Loel, 1981), and especially in the US energy generating power plants and coal fired electricity are large contributors to sulfate in the atmosphere. Similarities have been observed between the concentration map for sulfate and SO_2 data published by the U.S. Energy Information Administration (EIA), according to which Ohio Valley and the Northeastern region of the conterminous US are the most exposed to sulfate emissions.

The most important NO_3^- emitters are traffic, auto exhaust and industrial combustion processes (Wang and Han, 2011). The US EPA Report on the Environment from 2014 shows that NO_x mainly comes from anthropogenic sources that are combustion related, such as fossil fuel combustion in electric utilities, high-temperature operations at various industrial sources, and motor vehicle emissions. Home heaters and gas stoves are also a great contributor to NO_x emissions. The natural sources of nitrogen oxides are biological decay processes, wildfires, and lightning. As in the case of SO_4^{2-}, NO_3^- concentration in rainwater is the highest in regions that are heavy emitters of nitrogen oxides, namely the Upper Midwest, Ohio Valley, Northeastern and upper part of the Southern regions from the conterminous US.

4.3. Variation of pH

In the studies of Lu et al., (2011); Pu et al., (2017); Tiwari et al., (2016); Xing et al., (2017) and Xu et al., (2015) it is presented that the pH value of precipitation in an unpolluted environment due to the presence of atmospheric CO_2 is around 5.6. In 1982, Charlson and Rhode observed the decreasing trend of this value due to the presence of other naturally occurring acids, stating that the pH values of rainwater in a clean environment can alter between 5 and 5.6 (Charlson and Rodhe, 1982; Hu et al., 2003). According to the above, it can be stated that values below 5.6 indicate acidic rains, while values above 5.6 show the presence of alkaline species in rainwater.

This subchapter presents the multi annual averages and the volume-weighted means for the pH values of rainwater collected in the studied areas from the Romanian Carpathians as well as in Europe and the conterminous US.

The variation of pH values for the central group of the Eastern Carpathians is presented in Fig. 15.

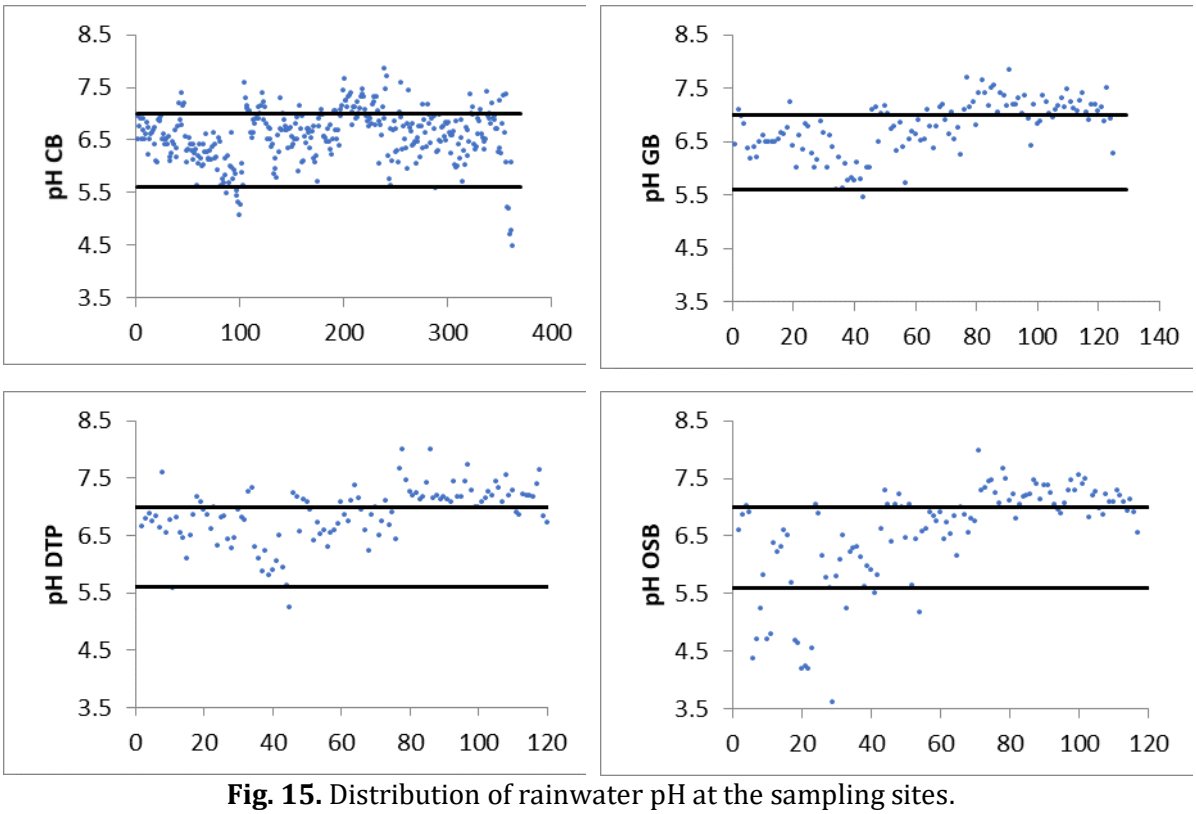

Fig. 15. Distribution of rainwater pH at the sampling sites.

It was observed that for the entire studied period, in the Ciuc basin, the pH values ranged from 4.5 to 7.9. The measured data showed that only 3.3% of the collected rainwater samples had acidic characteristics, situating below the value of 5.6, 78.7% of the samples presented values between 5.6 and 7.0, whilst 18% of the precipitation events had higher pH values then 7.0. The rainwater samples collected in the Giurgeu basin ranged between 5.5 and 7.8, with only the 0.8% of the collected samples had values lower than 5.6, 59% of the samples presenting values between 5.6 and 7.0, and 41% ranging between 7.0 and 7.8.

In the case of rainwater samples collected in DTP, values range between 5.2 and 8.0, with only 1.7% of the samples exhibiting values under 5.6, 51.6% ranging between 5.6 and 7.0, and 46.7% of the samples having values above 7.0. In OSB it was observed that a larger amount of precipitation samples presented acidic character, 12% of the samples ranging between 4.5 and 5.6, while 47% and 41% exhibited values between the 5.6-7.0 and the 7.0-7.9 intervals.

Overall, most rain events have alkaline character, which can be attributed to the presence of calcium carbonate or bicarbonate particles in the atmosphere, along with other neutralizing agents, such as ammonium or magnesium. Similar mean pH values and their homogenous distribution in observed in samples collected in the Central group of the Eastern Carpathians are showing that the atmosphere of the studied areas is in chemical equilibrium, fact that sustains the results of the ionic balance too (Szép et al., 2018).

The precipitation samples in the Northern group of the Eastern Carpathians presented slightly more acidic values. For BM, pH values ranged between 4.32 and 7.63, for BZ between 4.24 and 7.47, for SM between 4.20 and 7.91, while for SE samples exhibited values ranging from 3.89 to 8.0. Fig. 16 shows the distribution of measured pH values at each sampling site.

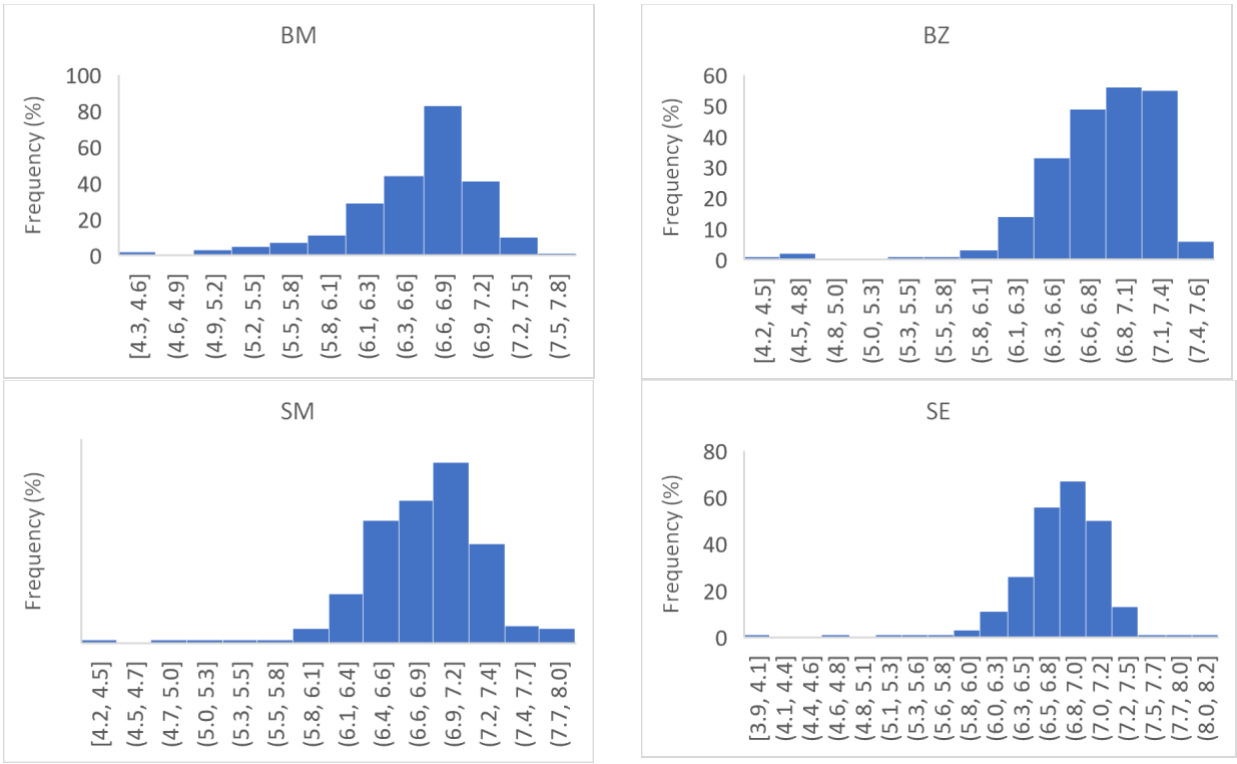

Fig. 16. Frequency distribution of rainwater pH at Baia Mare (BM), Bozinta (BZ), Somcuta (SM) and Seini (SE).

At BM the 79.24% of the total 286 rain events showed pH values ranging between 5.6 and 7, 15.25% situating above the value of 7, while 5.51% of the analyzed samples presented acidic character. The studied area is known for industrial activities using a significant amount of energy, mainly coal combustion and operating thermal power plants that use outdated technologies. The results were similar at BZ, SM and SE, showing that 61.09%, 60.89% and 67.52% of the samples had pH values ranging between 5.6 and 7, while the percentages for the same sampling sites that presented higher pH values than 7 were the following: 37.10%, 36.89% and 30.77%. As in the case of BM, the rate of acidic precipitation was quite small at BZ, SM and SE, exhibiting only ~2% of the total rain events.

The precipitation events recorded in the Southern Carpathians showed pH values varying from 4.33 to 8.43 at all sampling sites, showing a mean value of 6.70 (Fig. 17). Here, the acidity of rainwater was higher, the 7.32% of the rain events having pH values under the 5.6 mark. About 56.83% of the samples presented pH values between 5.6 and 7, while 35.85% of the pH values ranged from 7 to 8.43. Out of all sampling sites, the most acidic precipitation was recorded at RS, with the 20.16% of the pH values being lower than 5.6. At MN, only 2.80% of the total samples exhibited pH values lower than 5.6, while at BH sampling site none of the rain events yielded pH values lower than 5.6. Rain events recorded at RS and MN presented in 72.87% and 59.44% of the cases pH values between 5.6 and 7, while BH showed a more alkaline nature, with 60.87% of the pH values situating in the 7.00-8.43 interval. According to Wu et al., (2012), a possible explanation to higher pH values can be the dissolution of windblown dust, and the weathering of carbonate with elevated $CaCO_3$ concentration.

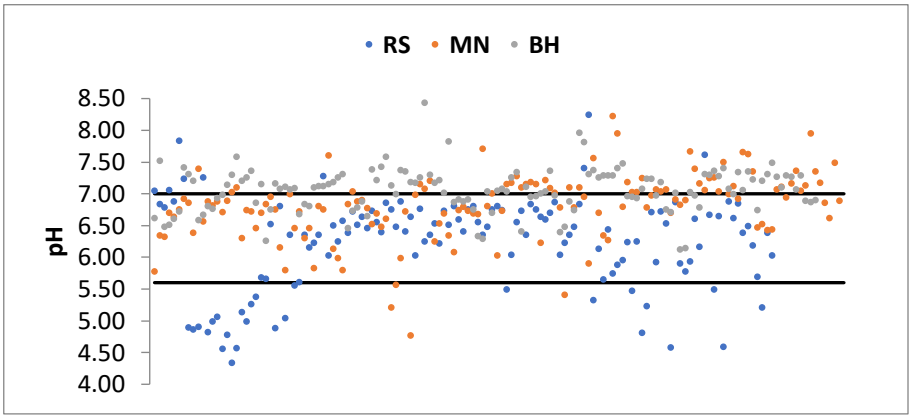

Fig. 17. Distribution of rainwater pH at Resita (RS), Moldova Noua (MN) and Baile Herculane (BH).

In Europe, the pH values of rainwater yielded from 4.19 to 5.82, with a mean value of 4.80. These measurements are significantly lower than the ones measured on a more local scale, in the Romanian Carpathians, which may be due to the presence of more acidic species in the atmosphere, that are derivates of sulfate, chloride and nitrate, showing a lower percentage of neutralizing ones such as calcium, magnesium and ammonium. Measurements showed that the 94.44% of the precipitation samples had pH values lower that 5, 5.11% ranging between 5 and 5.6, and only 0.44% of the samples presenting pH values that are greater than 5.6 (Fig. 18).

The dominance of acidic pH is sustained by the effects of anthropogenic activities, being connected with the VWM concentrations of measured ions, showing the influence of acidic species over the alkaline ones.

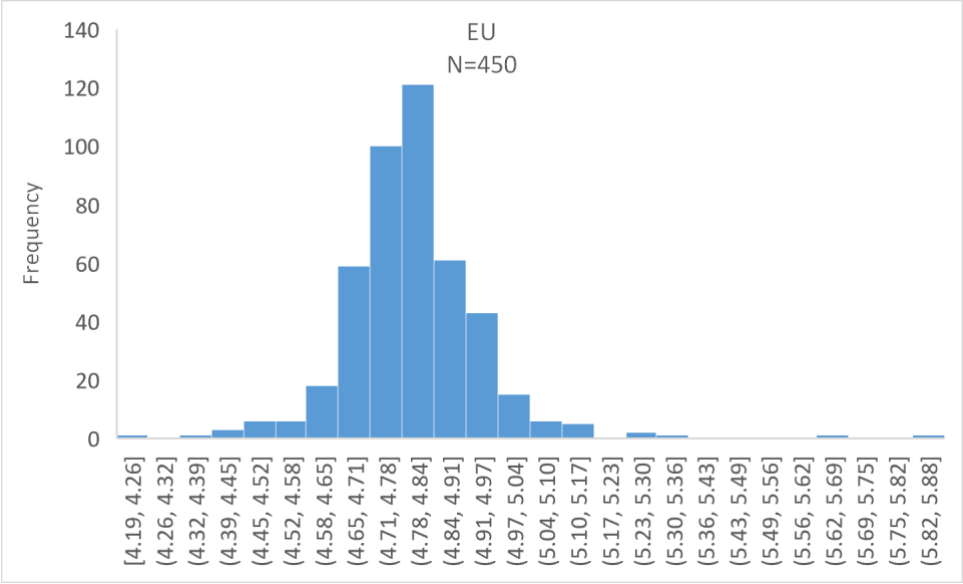

Fig. 18. Frequency distribution of pH for all studied countries during 2000-2017.

Fig. 19a shows distribution of VWM pH value over the conterminous US. pH measurements of rainwater samples showed a minimum value of 3.04 in Wye, Maryland and a maximum of 8.29 at Yosemite National Park – Hodgdon Meadow, California, showing an average of 5.10 and a VWM of 5.02. In general, measured pH values yielded between 3.05 and 5, accounting for 49.12%, 34.97% of the values were situated between 5 and 5.6, while only 15.91% exhibited greater values than 5.6. The VWM pH values yielded between 4.34 in Princeton, New Jersey and 6.36 in Logan, Utah. The acidic character can be also observed in the case of VWM pH values too, hence the 87.90% of the values were under the 5.6 mark, leaving only 12.10% of the values in the alkaline range. To enhance the relationship between rain amount and pH values, the 30-year normal rain amount data were accessed from the PRISM Climate Group website (http://prism.oregonstate.edu) (Daly et al., 2017) (Fig. 19b), for the 1981-2010 climatological cycle. By examining the data (Fig. 23), an inverse relationship was observed, being also sustained by the negative correlation coefficient (R=-0.583) between the measured rain amount and pH.

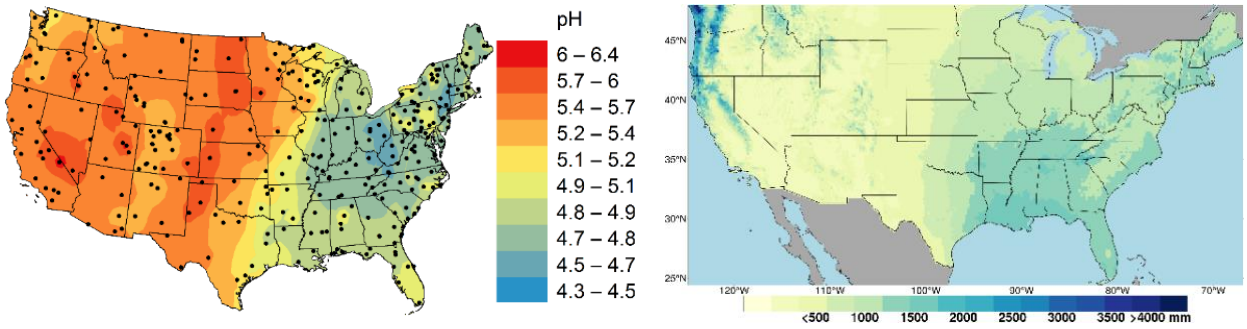

(a) (b)

Fig. 19. Distribution of rainwater volume weighted mean (VWM) pH (a) and the 30-year annual precipitation amounts (1981-2010) at the sampling sites.

The observed interconnection may be since in areas with lower precipitation amount pollutants along with particulate matter often accumulates, which in most of the cases consists of neutralizing components that lowers the acidity, while in areas with heavy rain, which also coincides with highly industrialized regions, the presence of acidic species in the atmosphere are also higher, therefore raising the acidity of precipitation.

4.4. Acid neutralization

The acidity and alkalinity of precipitation is controlled by various factors and chemical compounds, such as H_2SO_4, HNO_3, organic acids and the existence of NH_3 and $CaCO_3$ (Wu et al., 2016; Xu et al., 2015). According to the specialty literature, the concentration of sulfate and nitrate remains constant in the atmosphere regardless of altitude, while the abundance of ammonia and ammonium may decrease fast with height (Harrison and Pio, 1983). Therefore, at cloud level, acidic compounds such as H_2SO_4, HNO_3, NH_4HSO_4 are more abundant than alkaline compounds such as $(NH_4)_2SO_4$ and NH_4NO_3 (Balasubramanian et al., 2001).

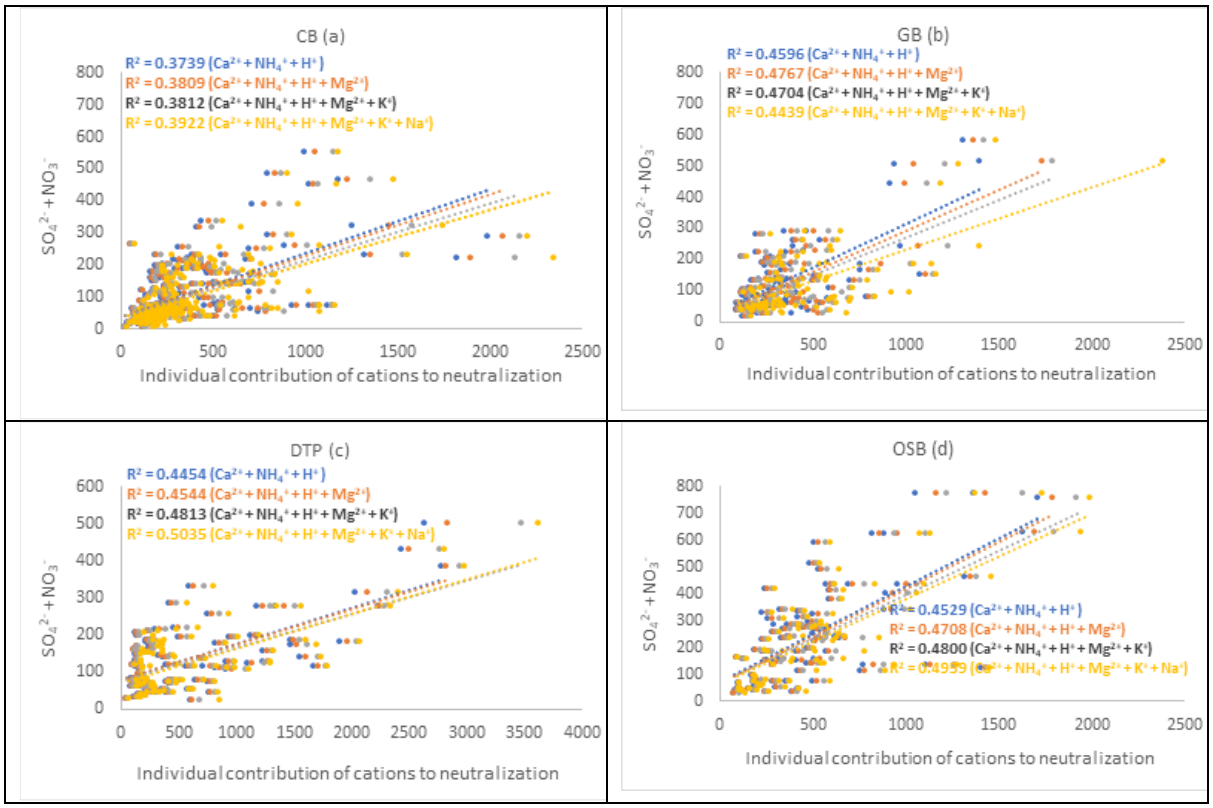

Fig. 20. Linear regressions of (NO_3^- + SO_4^{2-}) vs. the sum of cations.

As it can be observed in the specialty literature, linear regression is often applied to analyze the neutralizing capacity of various alkaline compounds over acidic species (Anatolaki and Tsitouridou, 2009; Báez et al., 2007). The above-mentioned process is usually defined by the proportion between anions (NO_3^- and SO_4^{2-}) and cations (NH_4^+, Ca^{2+}, Na^+, K^+ and Mg^{2+}). The linear regression analysis was applied to the anions and cations measured in the rainwater collected at the sampling sites from the central group of the Eastern Carpathians (Fig. 20). The results show the increasing trend of R^2 when the individual contributions of Mg^{2+}, K^+ and Na^+ are added to the regression when plotting

the sum of (NO_3^- + SO_4^{2-}) against the sum of (H^+ + Ca^{2+} + NH_4^+), in the case of CB (from R=0.37 to R=0.39) (Fig. 20a), DTP (from R=0.45 to R=0.50) (Fig. 20c) and OSB (from R=0.45 to R=0.48) (Fig. 20d). The only exception is observed in the case of GB, where the correlation coefficient decreases with the contribution of potassium and sodium, which may be since the neutralizing ratio of Ca^{2+}, NH_4^+, and Mg^{2+} is more significant.

Neutralization Factors (NF) and the proportions of Acidic Potential (AP) to Neutralization Potential (NP) were assessed at all studied regions from the Romanian Carpathians, Europe, and conterminous US to examine the rate of neutralizing process in rainwater. In the case of NFs, values that are greater than one show the occurrence of neutralization (Chang et al., 2017; Zhang et al., 2007). AP is calculated by summing the non-sea salt SO_4^{2-} and NO_3^- ($nssSO_4^{2-}$ + NO_3^-), while the NP is determined by the sum of non-sea salt Ca^{2+} and NH_4^+ ($nssCa^{2+}$ + NH_4^+).

In general, AP is used to indicate the sources of pollutants that originate from anthropogenic activities, while the NP serves as an index to assess the effect of air masses that have continental origin (Fujita et al., 2003; Wu et al., 2016).

Table 6 shows the results for the NFs and AP/NP ratios for the data collected in the central group of the Eastern Carpathians. One can see that the most relevant neutralizing agent is ammonium at CB, GB and DTP, representing 48%, 46% and 59%, respectively out of all neutralizing cations in rainwater, while at OSB both NH_4^+ and Ca^{2+} contributes largely to the process of acid neutralization, representing 42% and 43% of the total neutralization. Although NF_{Ca} had lower values than NF_{NH4} at CB, GB and DTP, it still can be considered as an important contributor to the neutralizing process.

Table 6. Neutralization factors and acidic/neutralization potential ratio at all sampling sites and their seasonal variations in the central group of the Eastern Carpathians.

	NF_{NH4}	NF_{Ca}	NF_{Na}	NF_K	NF_{Mg}	AP/NP
CB						
Mean value	2.4	1.5	0.5	0.3	0.3	0.3
St. dev.	2.4	1.3	1.0	0.5	0.3	0.4
Range	0.03-14.8	0.06-12.5	0.02-8.7	0.02-5.2	0.02-2.6	-0.01-4.7
GB						
Mean value	2.3	1.2	0.7	0.4	0.4	0.4
St. dev.	2.1	1.5	1.0	0.4	0.6	0.3
Range	0.06-12.2	0.2-12.1	0.04-6.7	0.02-2.2	0.03-5.3	0.02-1.6
DTP						
Mean value	3.1	1.1	0.5	0.3	0.2	0.4
St. dev.	3.7	0.8	0.8	0.3	0.2	0.4
Range	0.07-19.5	0.2-4.8	0.04-6.8	0.05-2.1	0.03-1.0	0.01-2.0
OSB						
Mean value	1.2	1.3	0.2	0.2	0.1	0.5
St. dev.	1.5	0.8	0.2	0.2	0.1	0.4
Range	0.04-7.8	0.3-5.6	0.01-1.2	0.004-1.0	0.02-0.5	0.08-1.8

The AP/NP ratios were lower than unity in all four sampling sites from the central group of the Eastern Carpathians, indicating that all the acidic species in precipitation are being neutralized.

These results indicate that acidic components resulting from fossil fuel combustion are neutralized by the NH_3, NH_4^+ and $CaCO_3$, which are originating from natural and anthropogenic sources, such as dissolution of limestone, fertilizing activities

and biomass burning. The contribution of particulate matter (PM), such as $PM_{2.5}$ and PM_{10}, is also known as reducing agent of acidy in rainwater (Huo et al., 2012).

The higher Na^+ concentrations can be due to the presence of the Icelandic Low, which is a very active cyclone during winter in the Eastern Carpathians, and in contact with the Tropical Cyclone brings heavy snowfall, which is loaded with Na^+. It could be said that the constant increase of the NH_4^+ ion and other alkaline ions are the main causes to the excess alkalization of precipitations which was observed during the past decades. Therefore, more attention should be attributed to the effects of the alkaline precipitations, which have a great impact on the ecosystem. Given that in both intra-mountain basins (CB and GB) and DTP, acidophilic soils are predominant, developed on peat bogs, the excessive alkaline precipitations have negative effects, such as increased N stress in the system and eutrophication of surface waters.

According to Chate and Devara (2009), the concentration of the H^+ ion indicates the raindrop's acidity subsequently to the neutralization by Ca^{2+} and NH_4^+.In their study, Kaya and Tuncel (1997) showed that if the acidity of precipitation is induced by H_2SO_4 and HNO_3 and neutralization does not occur, then the $H^+/(SO_4^{2-} + NO_3^-)$ proportion, which is also known as fractional acidity (FA) (Balasubramanian et al., 2001; Szép et al., 2018), is expected to be one.

The FA values obtained in the central group of the Eastern Carpathians for CB, GB, DTP and OSB were 0.01 ± 0.02, 0.007 ± 0.01, 0.005 ± 0.01 and 0.1 ± 0.59, respectively. These results show that acid neutralization occurred in the studied period in 98.7%, 99.2%, 99.3% and 51.2% of the cases in CB, GB, DTP and OSB, respectively.

The lower neutralization rate in the case of OSB can be explained by its higher industrial activity, but the greater concentration of sulfate in the rainwater samples may be due to the geographical position of OSB, being more exposed in front of air masses loaded with pollutants.

Another method to examine the interconnection between NH_4^+, NO_3^-, and SO_4^{2-} is to calculate the Ammonium Availability Index (AAI). Results showed an AAI value greater than 100% in CB (156.4%), GB (139.9%) and DTP (179.1%). These values are an indicator to the fact that the ammonium ion present in rainwater can neutralize the acidity induced by sulfate and nitrate. However, at OSB the AAI value exhibited less than 100%, being 76.5%, which means that ammonium cannot neutralize all acidic compounds found in the rainwater collected at OSB. However, according to Chu (2004), it is worth mentioning that AAI only indicates the neutralization process over sulfate and nitrate compounds by ammonium, and it does not coincide with the pH value of the analyzed ambient aerosols as a whole. Calcium, magnesium, and sodium can also participate in the neutralization of acidic species.

Another frequent method to analyze the relative contribution of H_2SO_4 and HNO_3 to the acidity of precipitation, along with FA other ratios can be used, such as $(Ca^{2+} + NH_4^+)/(NO_3^- + SO_4^{2-})$, NH_4^+/NO_3^-, NH_4^+/SO_4^{2-}, $(Ca^{2+} + Mg^{2+} + NH_4^+)/(NO_3^- + SO_4^{2-})$, Ca^{2+}/SO_4^{2-}, Ca^{2+}/NO_3^-, $(NO_3^- + Cl^-)/SO_4^{2-}$, SO_4^{2-}/NO_3^- (Chate and Devara, 2009; Tiwari et al., 2016). These ratios are useful in understanding the relative contribution of acidic and alkaline species to the neutralization process, as well as giving an overview of the chemical compounds that can be formed in the atmosphere. According to the above, the ratio of $(NO_3^- + Cl^-)/(SO_4^{2-})$ is an indicator weather HNO_3 and HCl had a greater influence on the rainwaters acidity (if the ratio is greater than 1), or if H_2SO_4 contributed more (if the ratio is smaller than 1) (Khemani et al., 1994). The ratio of NH_4^+/NO_3^- is another indicator of the neutralization process by ammonium, showing if it neutralizes nitrous species, by resulting in NH_4NO_3 in the atmosphere (Seinfeld, 1986). The NH_4^+/SO_4^{2-} ratio

can be used to indicate the relationship between different ions in the atmosphere. According to (Duan et al., 2003) if this ratio is lower than unity sulphates such as $CaSO_4$ and $(NH_4)_2SO_4 \cdot CaSO_4 \cdot 2H_2O$ are formed, if the molar ratio of NH_4^+/SO_4^{2-} is closer to one, it means that both NH_4HSO_4 and $(NH_4)_2SO_4$ are present in the atmosphere (Keresztesi et al., 2019). Use of fertilizers containing $(NH_4)_2SO_4$ and NH_4NO_3, can be converted into NH_3, which in the atmosphere can act as a neutralizing agent (Al-Momani et al., 1995a; Kaya and Tuncel, 1997; Keresztesi et al., 2020a; Migliavacca et al., 2005; Seinfield and Pandis, 1998). Another indicator for acidic species in precipitation is the ratio of $(SO_4^{2-} + NO_3^-)$ / $(Ca^{2+} + Mg^{2+})$ (Jawad Al Obaidy and Joshi, 2006). A ratio lower than unity suggests that the rainwater is alkaline, while a value greater than one is indicating the majority of acidic compounds. (Jawad Al Obaidy and Joshi, 2006). In their study, Tiwari et al., (2012), used the equivalent ratio of $(Ca^{2+} + Mg^{2+} + NH_4^+)/(NO_3^- + SO_4^{2-})$ as an indicator to pollutants originating from anthropogenic activity, and contributing to the acidity of precipitation.

Table 7 shows the results of the above-mentioned ratios for the sampling sites from the central group of the Eastern Carpathians.

Table 7. Ionic ratios of the measured ions over the studied regions from the Central Group of the Eastern Carpathians.

Ionic ratios	CB	GB	DTP	OSB
$H^+/(NO_3^-+SO_4^{2-})$ (FA)	0.01	0.007	0.005	0.1
$(Ca^{2+} +NH_4^+)/(NO_3^- + SO_4^{2-})$	3.9	3.5	4.3	2.5
NH_4^+/NO_3^-	8.7	9.8	21.7	7.6
NH_4^+/SO_4^{2-}	5.0	3.7	4.4	2.1
$(Ca^{2+} + Mg^{2+} + NH_4^+)/(NO_3^- + SO_4^{2-})$	4.1	3.9	4.5	2.6
Ca^{2+}/SO_4^{2-}	3.2	2.1	1.7	2.2
Ca^{2+}/NO_3^-	4.4	4.7	6.4	8.8

The $(Ca^{2+} + NH_4^+)/ (NO_3^- + SO_4^{2-})$ ratio exhibited values greater than 1 at all sampling sites, also showing that at OSB the neutralization of acidity occurs at a smaller rate than at the intramountain areas. The ratios of $(Ca^{2+} + Mg^{2+} + NH_4^+)/ (NO_3^- + SO_4^{2-})$ are also > 1, meaning that Ca^{2+}, Mg^{2+} and NH_4^+ ions contributed at a great extent in neutralizing the acidity of precipitation (Tiwari et al., 2016). The ratios of NH_4^+/NO_3^-, NH_4^+/SO_4^{2-}, Ca^{2+}/SO_4^{2-} and Ca^{2+}/NO_3^- also yielded higher values than unity, indicating an excess over the neutralization value.

Table 8. Neutralization factors of the major ions and AP/NP ratio in rainwater samples from the Northern Group of the Eastern Carpathians.

	Baia Mare (BM)	Bozinta (BZ)	Somcuta (SM)	Seini (SE)
NF_{Ca}	2.05	2.16	2.72	1.89
NF_{NH4}	0.61	1.05	1.04	1.07
NF_{Mg}	0.48	0.64	0.59	0.67
NF_{Na}	0.42	0.57	0.68	0.60
NF_K	0.16	0.30	0.39	0.84
AP/NP	0.61	0.42	0.39	0.46

NFs calculated for the data collected in the northern group of the Eastern Carpathians (Table 8) shows that Ca^{2+} is the most abundant neutralizing ion at all four sampling sites, while NH_4^+ exhibited values higher than one at BZ, SM and SE. NF_{Mg}, NF_{Na},

and NF_K, excepting NF_K at SE, did not had a significant contribution in neutralizing the acidity in comparison with NF_{Ca} and NF_{NH4}. Table 7 also shows the results for the AP/NP ratio, which also confirms that the acidic compounds which can be found in the rainwater due to diverse anthropogenic activities are neutralized by NH_3, NH_4^+ and $CaCO_3$, which may result from agricultural activities, limestone dissolution or biomass burning (Szép et al., 2018).

The FA values calculated for the data collected in the northern group of the Eastern Carpathians (Table 9) showed that ~98% and ~99% of the acidity was neutralized.

Table 9. Ionic ratios among measured major ions.

Ionic ratios	BM	BZ	SM	SE
$H^+/(NO_3^-+SO_4^{2-})$ (FA)	0.02	0.01	0.01	0.01
$(Ca^{2+} +NH_4^+)/(NO_3^- + SO_4^{2-})$	2.68	3.21	3.75	2.97
NH_4^+/NO_3^-	2.80	4.32	6.01	6.43
NH_4^+/SO_4^{2-}	7.92	2.21	2.88	2.26
$(Ca^{2+} + Mg^{2+} + NH_4^+)/(NO_3^- + SO_4^{2-})$	3.16	3.85	4.35	3.64
Ca^{2+}/SO_4^{2-}	14.55	4.78	8.56	4.01
Ca^{2+}/NO_3^-	11.95	7.82	13.64	11.89

As it can be observed in Table 9, the ionic ratios yielded values above unity, indicating that the major cations in rainwater significantly contribute to the neutralization of acidic compounds. These results were also confirmed by the significant correlation coefficient between the sum of Ca^{2+}, Mg^{2+}, and NH_4^+, and the sum of anions ($NO_3^- + SO_4^{2-}$), the R^2 values being 0.692 at BM, 0.361 at BZ, 0.440 at SM and 0.362 at SE.

Table 10. Neutralization factors of the major ions and AP/NP ratio in rainwater samples from the Southern Carpathians.

	NF_{NH4}	NF_{Ca}	NF_{Na}	NF_K	NF_{Mg}	AP/NP
RS						
Mean value	1.51	2.16	0.61	0.23	1.01	0.31
St. dev.	1.12	1.62	0.75	0.29	0.94	0.31
Range	0.01-5.74	0.04-8.67	0.03-4.45	0.01-1.27	0.03-4.15	0.06-1.92
MN						
Mean value	0.60	1.56	0.13	0.10	0.77	0.54
St. dev.	0.50	1.17	0.13	0.10	0.81	0.39
Range	0.03-2.39	0.21-5.57	0.02-0.81	0.01-0.54	0.03-3.08	0.14-1.65
BH						
Mean value	0.52	1.73	0.14	0.09	0.99	0.61
St. dev.	0.62	1.58	0.12	0.07	1.33	0.57
Range	0.02-3.35	0.18-9.60	0.02-0.61	0.01-0.29	0.03-9.20	0.05-2.27

In the Southern Carpathians, according to the results obtained for NF values (Table 10), the dominance of the Ca^{2+} ion as a neutralizing agent can be observed at all three sampling sites. The contribution of Mg^{2+} and NH_4^+ to the neutralization process can also be noted, showing values that ranged between 0.52 and 1.51. The neutralizing capacity of K^+ and Na^+ is insignificant, exhibiting values between 0.09 and 0.61. The AP/NP ratio was also assessed for the sampling sites in the Southern Carpathians (Table

9). AP/NP ratios ranged between 0.31 at RS and 0.61 at BH, showing that alkaline constituents are more abundant than acidic ones in the rainwater collected at RS, MN and BH.

The results for FA and the following ionic ratios can be found in Table 11: $(NO_3^- + Cl^-)/(SO_4^{2-})$, $(Ca^{2+} + Mg^{2+} + NH_4^+)/(NO_3^- + SO_4^{2-})$, SO_4^{2-}/ NO_3^-, NH_4^+/NO_3^- and NH_4^+/SO_4^{2-}.

Table 11. Ionic ratios among measured ions in rainwater collected in the Southern Carpathians.

	$\frac{H^+}{NO_3^- + SO_4^{2-}}$	$\frac{SO_4^{2-}}{NO_3^-}$	$\frac{NH_4^+}{NO_3^-}$	$\frac{NH_4^+}{SO_4^{2-}}$	$\frac{Ca^{2+} + Mg^{2+} + NH_4^+}{NO_3^- + SO_4^{2-}}$	$\frac{NO_3^- + Cl^-}{SO_4^{2-}}$	$\frac{NO_3^- + SO_4^{2-}}{Ca^{2+} + Mg^{2+}}$
RS	0.08	26.47	36.30	2.35	4.68	3.72	0.79
MN	0.002	35.94	15.61	0.68	2.93	1.02	0.90
BH	0.001	68.31	22.44	0.55	3.23	0.98	1.00

The mean FA ratio indicated that almost 99% of rainwaters acidity was neutralized, its values ranging between 0.001 and 0.08. The ratio of $(NO_3^- + Cl^-)/(SO_4^{2-})$ exhibited 0.98 at BH, 1.02 at MN and 3.72 at RS, suggesting that HNO_3 and HCl has a greater influence at RS and MN, while at BH H_2SO_4 contributes the most to the acidity of rainwater. All ionic ratios at all sampling sites from the Southern Carpathians exhibited values that showed the overall dominance of alkaline species over acidic ones.

The neutralizing effect of cations measured in the rainwater collected in European countries was also determined with the help of NFs. Multiannual averages for each studied country are shown in Fig. 21.

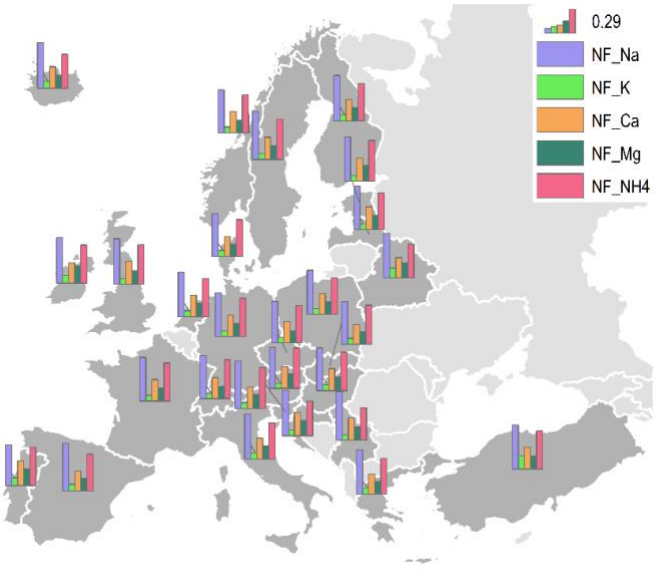

Fig. 21. Neutralization factors of major alkaline ions in precipitation samples collected in Europe.

One can observe that the highest neutralizing potential was delivered by sodium, with a mean value of 0.54 (004-0.98 range), being followed by ammonium with an average of 0.46 and ranging between 0.03 and 1.25. Contrary to the sampling sites in the

Romanian Carpathians, Ca^{2+} did not contribute significantly to the neutralization process. Moreover, the results exhibited values that were lower than one, meaning that the acidity of rainwater collected over Europe is more dominant, and neutralization only occurs at a smaller extent, fact that is also sustained by the results of the AP/NP ratio. The above-mentioned ratio had values greater than unity, with a minimum of 1.24 in Portugal and a maximum value of 2.18 in Turkey, sustaining the results of pH distribution that showed values mostly ranging from 5 to 5.6, which points out the acidic nature of precipitation over Europe.

For the studied countries in Europe, the average FA value is 0.31, yielding values between 0.03 and 1.02, suggesting that on average, the 69% of the inorganic acidity in rainwater is neutralized over Europe. Ionic ratios such as $(NO_3^- + Cl^-)/SO_4^{2-}$, SO_4^{2-}/NO_3^-, NH_4^+/NO_3^-, NH_4^+/SO_4^{2-}, $(Ca^{2+} + Mg^{2+} + NH_4^+)/ (NO_3^- + SO_4^{2-})$ and $(NO_3^- + SO_4^{2-})/(Ca^{2+} + Mg^{2+})$ were also calculated for studied European countries. The average value for the $(NO_3^- + Cl^-)/SO_4^{2-}$ ratio was 1.31, varying from 0.87 in Estonia to 9.72 in Turkey, overall accounting for higher values than 1 in most of the studied countries. The average ratios of SO_4^{2-}/NO_3^- varied between 1.78 in Portugal and 2.83 in Serbia, having an average value of 1.96, indicating that H_2SO_4 had a greater influence on precipitations acidity than HNO_3. Examining the concentrations of ammonium in relation with the concentrations of nitrate, it was observed a minimum value of 0.50 in Serbia and a maximum value of 0.64 in Turkey, with a mean value of 0.58. The average ratio of $(Ca^{2+} + Mg^{2+} + NH_4^+)/ (NO_3^- + SO_4^{2-})$ accounted for 0.73, while the $(NO_3^- + SO_4^{2-})/ (Ca^{2+} + Mg^{2+})$ ratio had a mean value of 2.94, which are clearly the indicators of the significant influence of acidic compounds in the collected rainwater samples in the European countries.

The AAI for the studied European countries did not show significant differences from region to region, exhibiting a mean value of 22.86%, with variations between 3.07% in Turkey and 60.02% in Slovenia, suggesting that there it is not enough NH_4^+ present in the atmosphere to completely neutralize HNO_3 and H_2SO_4 acids.

The results for AP/NP ratios and NFs for the data collected in the conterminous US are shown in Fig. 22. One can observe that the results for the AP/NP ratio are in accordance with the VWM concentrations, exhibiting elevated and very elevated acidifying potential on the Eastern coast, with an overall mean value of 1.95, the maximum of 5.19 being recorded at Waltham, Massachusetts, while the minimum of 0.46 at Logan, Utah.

The multiannual mean values for the NFs of the studied cations showed that NH_4^+, Ca^{2+} and Na^+ were the most powerful neutralizer agents, with averages of 0.46, 0.30 and 0.29, respectively. NF_{NH4} values varied between 0.12 and 1.58, the highest value being registered in Logan Utah, which could be easily explained by the agricultural activities and livestock breeding that are practiced in this area. The maximum NF_{Na} value (2.77) was observed at Alsea, Oregon, followed by the maximum value of NF_{Ca} (1.51) in Green River, Utah. These values can be explained by the geographical characteristics at the location of the sampling sites, since the elevated concentrations of Na^+ show the marine origin transported by air masses from the North Pacific Ocean, while the significant calcium concentrations may be due to the dissolution of calcareous rocks from the neighboring mountainous regions, such as San Rafael Swell and Canyonlands National Park, which are rich in sandstone, shale and limestone; and also to soil resuspension, due to its semi-arid climate. The contribution of magnesium and potassium to acid neutralization was not significant. The results showed that in general, acidic species have a significant influence on alkaline compounds.

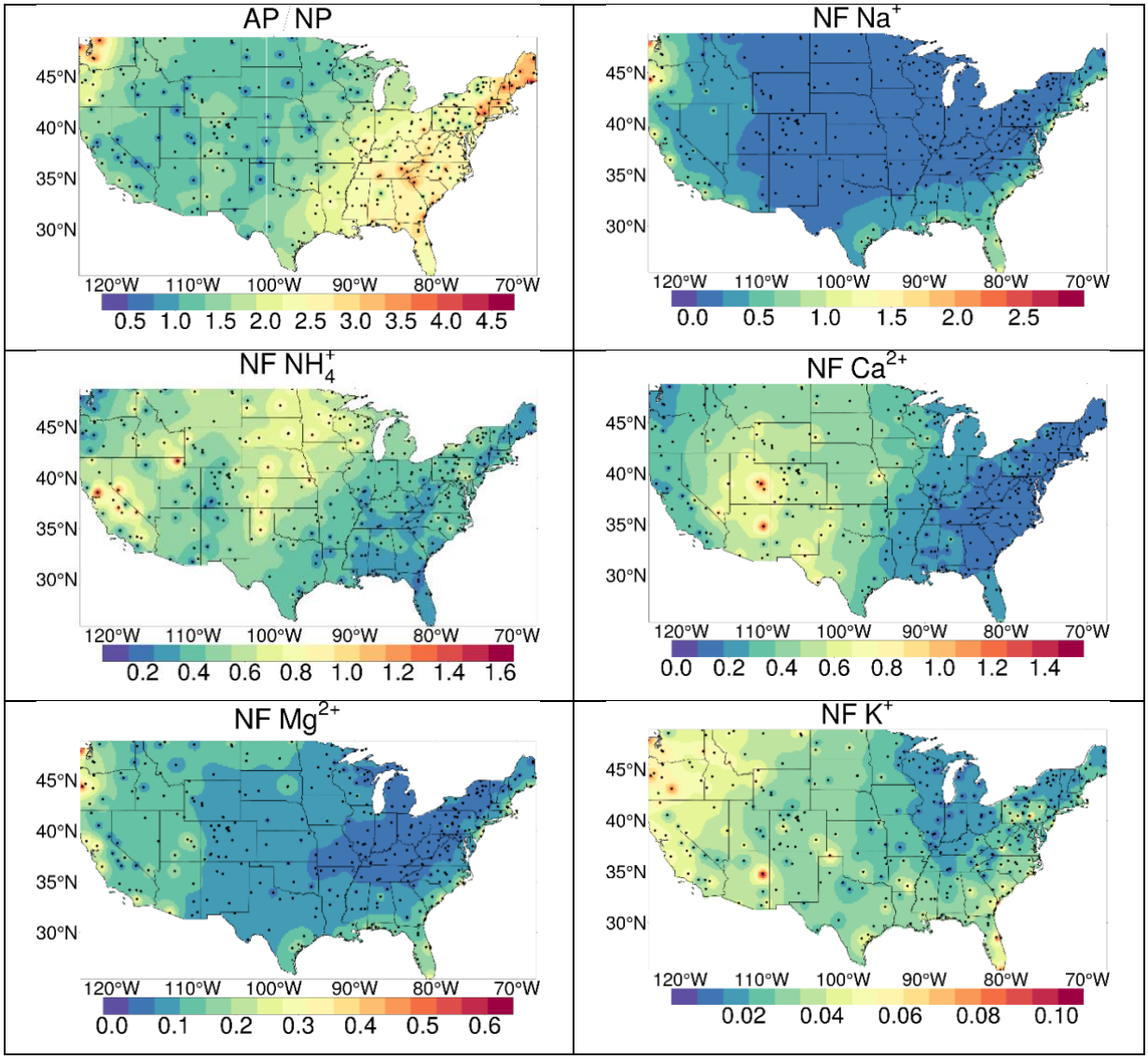

Fig. 22. The mean AP/NP ratios and the neutralization factors of major cations in precipitation for each sampling site over the conterminous US.

FA values in the conterminous US varied between 0.024 (Logan, Utah) and 1.08 (Sagehen Creek, California), accounting to an overall average value of 0.39, which shows that ~61% of rainwaters acidity is neutralized (Fig. 23). Ionic ratios such as SO_4^{2-}/NO_3^-, NH_4^+/NO_3^-, NH_4^+/SO_4^{2-}, $(Ca^{2+} + Mg^{2+} + NH_4^+)/(NO_3^- + SO_4^{2-})$ and $(NO_3^- + Cl^-)/(SO_4^{2-})$ were calculated for conterminous US too. The averages of the SO_4^{2-}/NO_3^- ratio yielded values between 0.62 (Death Valley National Park – Cow Creek, California; Kawuneeche Meadow, Colorado) and 19.63 (Lost Creek, Orlando), with a mean value of 1.74, showing that sulfuric acid dominated over nitric acid in rainwater (Keresztesi et al., 2020c). Mean values of the NH_4^+/NO_3^- (1.04) and NH_4^+/SO_4^{2-} (0.96) ratios, which as one can observe, are very close to one, suggest the presence of NH_4NO_3, NH_4HSO_4 and $(NH_4)_2SO_4$ in the atmosphere over the conterminous US (Duan et al., 2003; Salve et al., 2008). Ratios of $(Ca^{2+} + Mg^{2+} + NH_4^+)/(NO_3^- + SO_4^{2-})$ exhibited values between 0.26 (Stilwell Lake, New York) and 2.49 (Logan, Utah), having a mean value of 0.86. across the conterminous US. The mean ratio of $(NO_3^- + Cl^-)/(SO_4^{2-})$ was 1.47, varying between 0.40 in Tombstone, Arizona and 4.90 in Lac Courte Oreilles Reservation, Wisconsin.

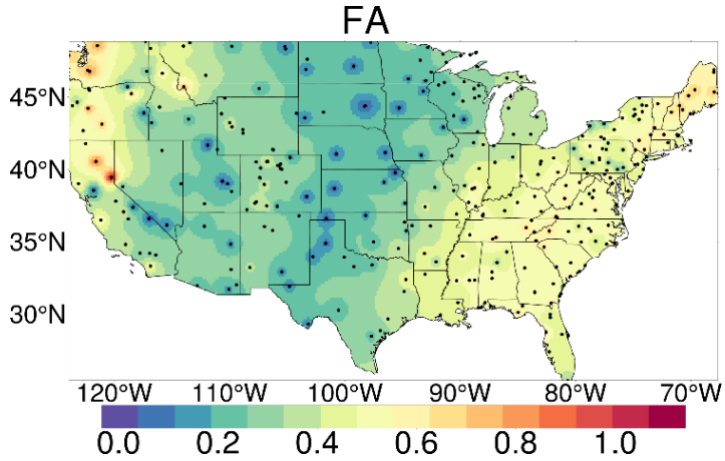

Fig. 23. Average FA values for each sampling site across the conterminous US.

To evaluate the relationship between NH_4^+, NO_3^- and SO_4^{2-}, AAI was assessed. AAI values varied between 6.85% at Saint Simons Island, Georgia and 109.84% at Logan, Utah (Fig. 24). The NH_4^+ excess observed in Logan indicates the influence of agricultural activities and livestock breeding on the precipitation chemistry.

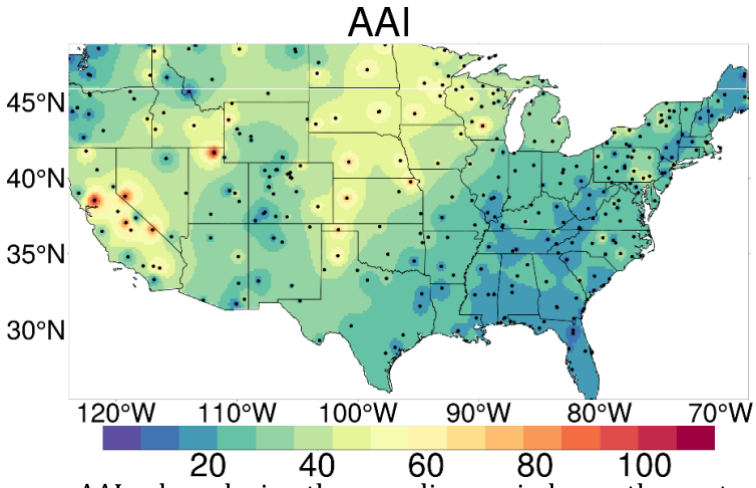

Fig. 24. Average AAI values during the sampling period over the conterminous US.

The results of the methods used to examine the neutralization of acidity showed that the chemical nature of precipitation is largely affected by acidic compounds derived from SO_4^{2-}, which is the main product of green-house-gas (GHG) emissions and refineries. The significant contribution of NH_4^+ and Ca^{2+} to the neutralization process mainly originates from agricultural activities and terrestrial sources, such as livestock breeding, use of fertilizers, dissolution of limestone, calcareous rock weathering and soil resuspension, respectively (Keresztesi et al., 2020b).

4.5. Spatial and temporal variability of Wet Deposition fluxes

Numerous studied have shown that wet deposition may change the rainwater's effect on the ecosystem, also providing information of locally emitted or long-range

transported pollutants, due to its dissolved ionic concentrations (Li et al., 2007). To give a more comprehensive overview of the sources of major ions in rainwater, spatial and temporal variability of wet deposition fluxes were examined.

Fig. 25 shows the multiannual means of major ion deposition fluxed calculated for the rainwater samples collect in the central group of the Eastern Carpathians. Values ranged from region to region, in function of the recorded precipitation amounts (6078.7 mm at CB, 5771.1 mm at GB, 6674 mm at DTP, 6305.2 at OSB) during the 2006 – 2016 period.

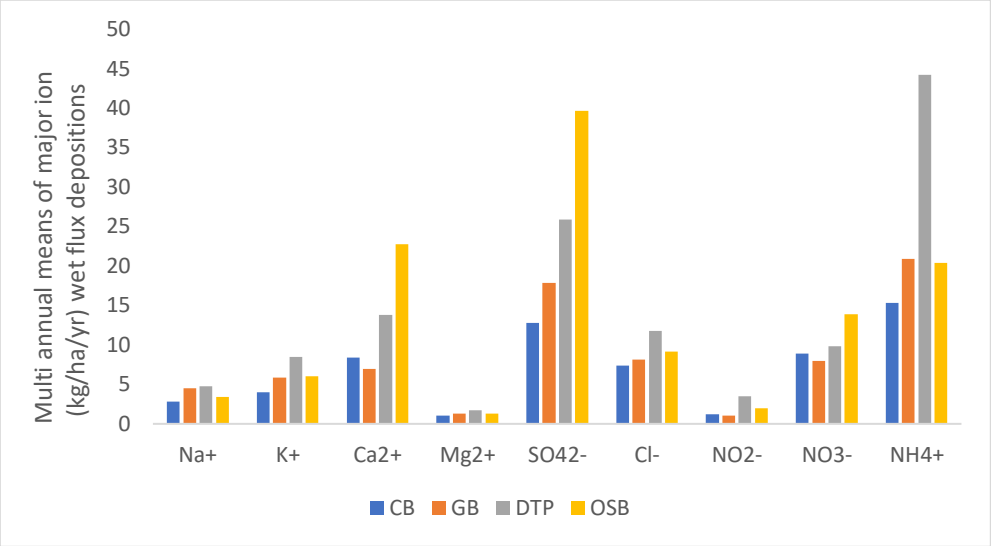

Fig. 25. The average multi annual wet flux depositions (kg $ha^{-1}yr^{-1}$) of major ions at the studied sampling sites from the central group of the Eastern Carpathians.

The average multiannual wet deposition fluxes of Na^+, K^+, Ca^{2+}, Mg^{2+}, SO_4^{2-}, Cl^-, NO_2^-, NO_3^-, NH_4^+ in CB accounted for 2.8, 4.0, 8.4, 1.0, 12.8, 7.4, 1.2, 8.9 and 15.4; in GB were 4.5, 5.9, 6.9, 1.3, 17.9, 8.2, 1.1, 8.0 and 20.9; in DTP were 4.8, 8.5, 13.8, 1.8, 25.9, 11.8, 3.5, 9.9 and 44.2; in OSB were 3.4, 6.0, 22.8, 1.3, 39.6, 9.2, 2.0, 13.9 and 20.4 kg $ha^{-1}yr^{-1}$. It was observed that the annual average concentration of WD for NH_4^+, Ca^{2+} and SO_4^{2-} were higher than the WD fluxes of other major ions. Higher acidic WD fluxes were observed during periods when the precipitation amounts increased, however when the precipitation amount decreased the alkaline species had higher WD fluxes (Tiwari et al., 2016). The highest multi annual average WD flux for SO_4^{2-} (36 kg $ha^{-1}yr^{-1}$) was measured at OSB, followed by the DTP with 23.5 kg $ha^{-1}yr^{-1}$. Cl^- had the highest WD flux at the DTP, accounting for 11.8 kg $ha^{-1}yr^{-1}$. In OSB the higher industrialization rate, thus the emissions of fossil but also the more exposed location is affecting the higher SO_4^{2-} deposition rates. Long – range transported pollutants can be more easily deposited at OSB, than at the other sampling sites, which are protected by the mountain chain from the air masses transporting pollutants. Another cause of higher wet deposition rates of SO_4^{2-}, NH_4^+, and NO_3^- are due to the sizes of these ions in the atmosphere (Samara and Tsitouridou, 2000). Being secondary particles, these ions are produced by the gas to particle conversion process, leading to the formation of ultrafine particles, which can grow via coagulation (Samara and Tsitouridou, 2000). These particles are removed most efficiently by wet deposition, through the in-cloud scavenging mechanism, leading to higher WD fluxes. Chloride may have higher deposition rates in the Central group of the Eastern Carpathians due to the numerous mineral springs and mofette emanations during hydrothermal exhaustion. Moreover, sea-salt spray containing chloride ions being

long-range transported from the Black Sea and the salt mines present in the studied sampling sites may be another cause of higher chloride WD rates. WD rates of major cations showed that ammonium and calcium had the highest multiannual values at all sampling sites, the values for ammonium recorded at DTP being the highest (44.2 kg ha^{-1}yr^{-1}), while the most elevated WD flux for calcium was observed at OSB (22.8 kg ha^{-1}yr^{-1}).

The multiannual wet deposition flux values calculated for BM, BZ, SM, and SE from the northern group of the Eastern Carpathians are given in Fig. 26.

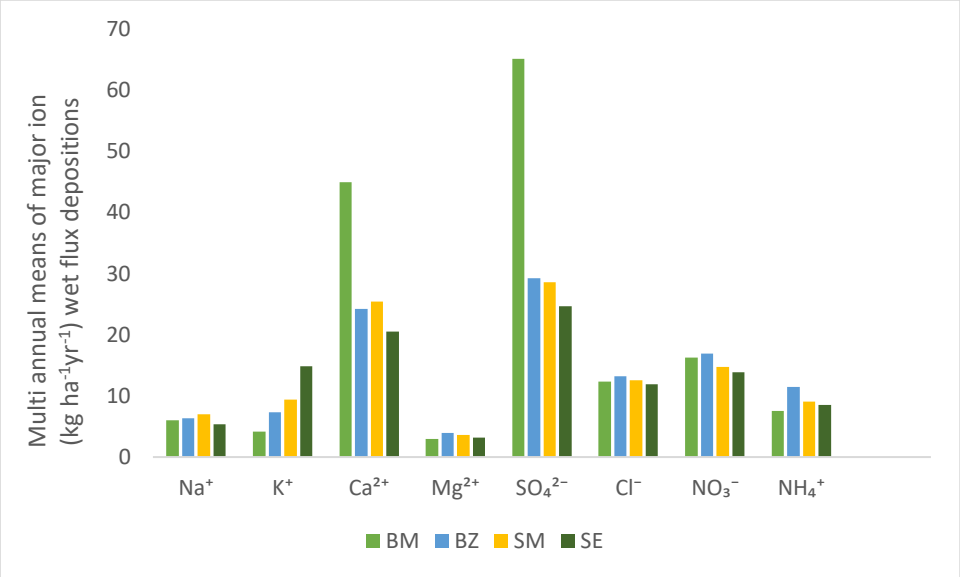

Fig. 26. The average multi annual wet flux depositions (kg ha^{-1}yr^{-1}) of major ions at the studied sampling sites from the northern group of the Eastern Carpathians.

The recorded multiannual means of rainwater amounts for the studied period were the following: at BM – 951.4 mm, at BZ – 917, at SM – 721.8 mm, while at SE – 726.7 mm. In general, WD fluxes were observed to be the most elevated at BM, being followed by a similar distribution at the other sampling sites. Among alkaline species, calcium had the highest values at all sampling sites, while amidst acidic species sulfate exhibited the most elevated WD fluxes. This can be explained by the same process as in the case of the central group. The significant differences between the WD rates recorded for BM and other sampling sites from the northern group of the Eastern Carpathians can be explained by the redundant anthropogenic activities, like mining and industry in the BM area.

Fig. 27 shows the multiannual mean WD rates calculated for the four-year period (2014-2017) at the sampling sites of RS, MN and BH from the Southern Carpathians. WD fluxes for both alkaline and acidic species were the highest in BH, exhibiting 125.86 kg ha^{-1}yr^{-1} for SO_4^{2-} and 73.75 kg ha^{-1}yr^{-1} for Cl^-. Amongst cations, calcium had the highest WD rates, values accounting for 97.95 kg ha^{-1}yr^{-1} at BH, 50.33 kg ha^{-1}yr^{-1} at MN, and 14.63 kg ha^{-1}yr^{-1} at RS.

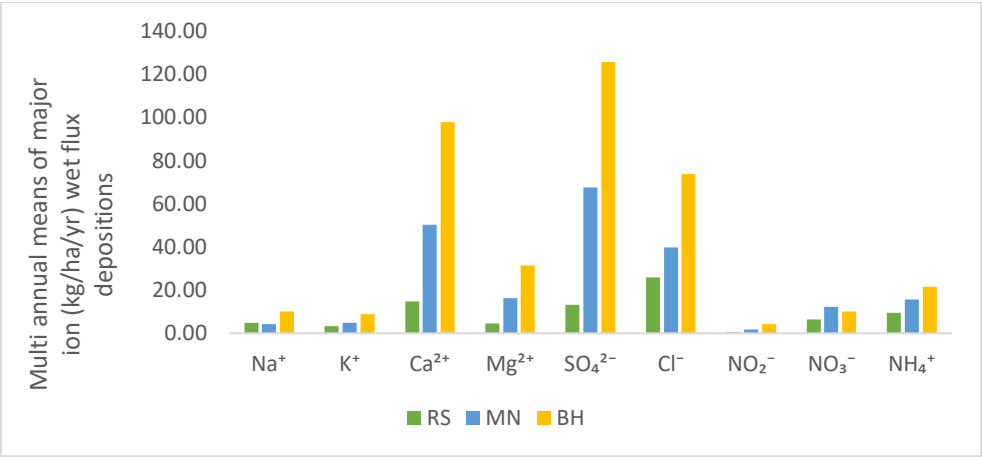

Fig. 27. The average multi annual wet flux depositions (kg ha^{-1}yr^{-1}) of major ions at the studied sampling sites.

The results regarding the WD rates of major ions correlate with the results obtained for NFs, explaining the greater concentration of acidic species at BH and MN, which may be due to coal combustion and the use of chloride in the metallurgic industry. Another cause of higher wet deposition rate of sulfate is due to the size of this ion in the atmosphere (Al-Momani et al., 1995a). Being a secondary particle, this ion is produced by the gas to particle conversion process, leading to the formation of ultrafine particles, which can grow via coagulation (Al-Momani et al., 1995b). Sulfate is removed most efficiently by wet deposition, thru the in-cloud scavenging mechanism, causing higher WD rates.

The multiannual average WD rates calculated for the 2000-2017 period for 27 European countries are displayed in Fig. 28.

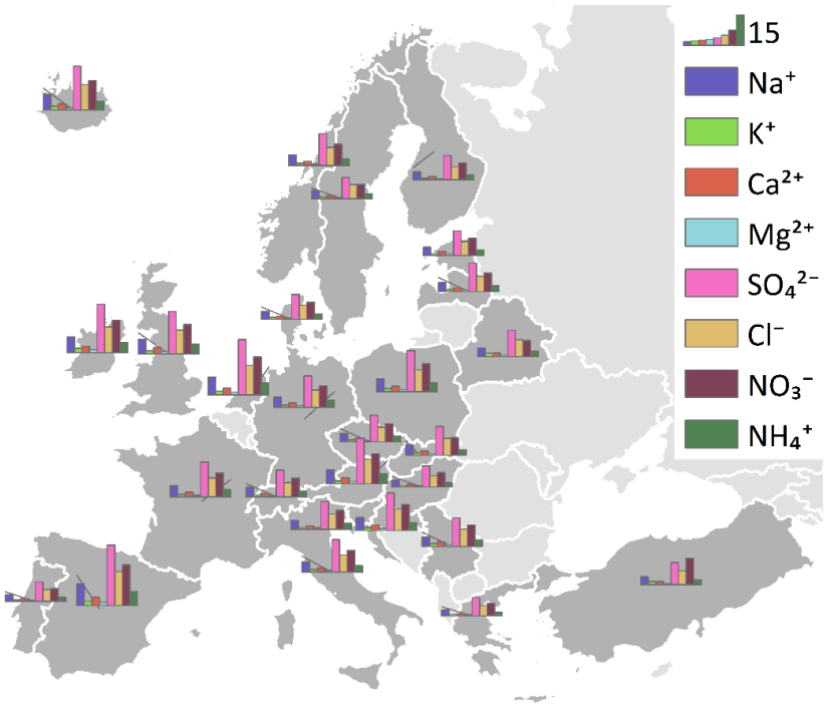

Fig. 28. Average multiannual wet deposition rates (kg ha^{-1}yr^{-1}) of major ions at the studied regions.

The highest deposition fluxes were obtained for SO_4^{2-}, excepting the value for Turkey, where NO_3^- exhibited the highest WD fluxes. The mean WD value for SO_4^{2-} in Europe was 15.88 kg ha^{-1} yr^{-1}, varying between 8.87 kg ha^{-1} yr^{-1} in Greece and 29.64 kg ha^{-1} yr^{-1} in Slovenia. Nitrate and chloride also presented high WD values, with an average of 10.96 kg $ha^{-1}yr^{-1}$ (min. 6.05 kg $ha^{-1}yr^{-1}$ – Greece; max. 20.14 kg $ha^{-1}yr^{-1}$ – Slovenia) and 8.93 kg $ha^{-1}yr^{-1}$ (min. 5.05 kg $ha^{-1}yr^{-1}$ – Greece; max. 16.66 kg $ha^{-1}yr^{-1}$ – Slovenia), respectively. Regarding the alkaline species, the highest WD fluxes were observed in Slovenia, (WD Na^+ = 10.55 kg $ha^{-1}yr^{-1}$; WD NH_4^+ = 6.78 kg $ha^{-1}yr^{-1}$). The average deposition fluxes for sodium and ammonium were 5.32 and 3.43 kg $ha^{-1}yr^{-1}$, respectively. One can observe that Greece has the lowest acidic WD rates, while Slovenia the highest, which can be explained by the climate conditions, hence the Mediterranean climate is characterized with lower amounts of precipitation, while in Slovenia, the moderate continental climate comes with high amounts of precipitation. Another factor may be the pollutant dispersing conditions, which in Greece can cause lower deposition rates, whereas in Slovenia the pollutant accumulation phenomenon is more significant.

In case of the conterminous US, the most elevated WD fluxes were observed in the case of Cl^-, yielding values of ~35 kg/ha/year in areas where chloride is used in the production process (Fig. 29).

Regarding cations, WD rates for calcium were the highest, mainly in the desert areas and in the central region. In a study published in 2013 by Brahney et al., it is stated that Ca^{2+} WD rates had considerably increased in the Western US between 1994 and 2010, referring to the states of Colorado, Utah and Wyoming. These areas are characterized by high Ca^{2+} WD fluxes, caused by their geographical position, being in arid and desert regions, and frequently exposed to dust storms (Vet et al., 2014).

Other factors that contribute to higher calcium WD rates are the coal-fired power plants and cement manufacturers (Brahney et al., 2013). Magnesium WD fluxes were similar to those of calcium, which can be explained by the same source origins in rainwater, such as rock weathering, dust storms, open quarries, etc.).

WD fluxes for sulfur and nitrate exhibited increased values in the Central and Northeastern US, where anthropogenic activities are the most dominant. Ammonium and potassium WD rates were higher in areas with increased agricultural activities (Midcentral and Northeastern regions). WD of potassium can be influenced by biomass burning too, therefore higher values were registered in the Southern industrial area too.

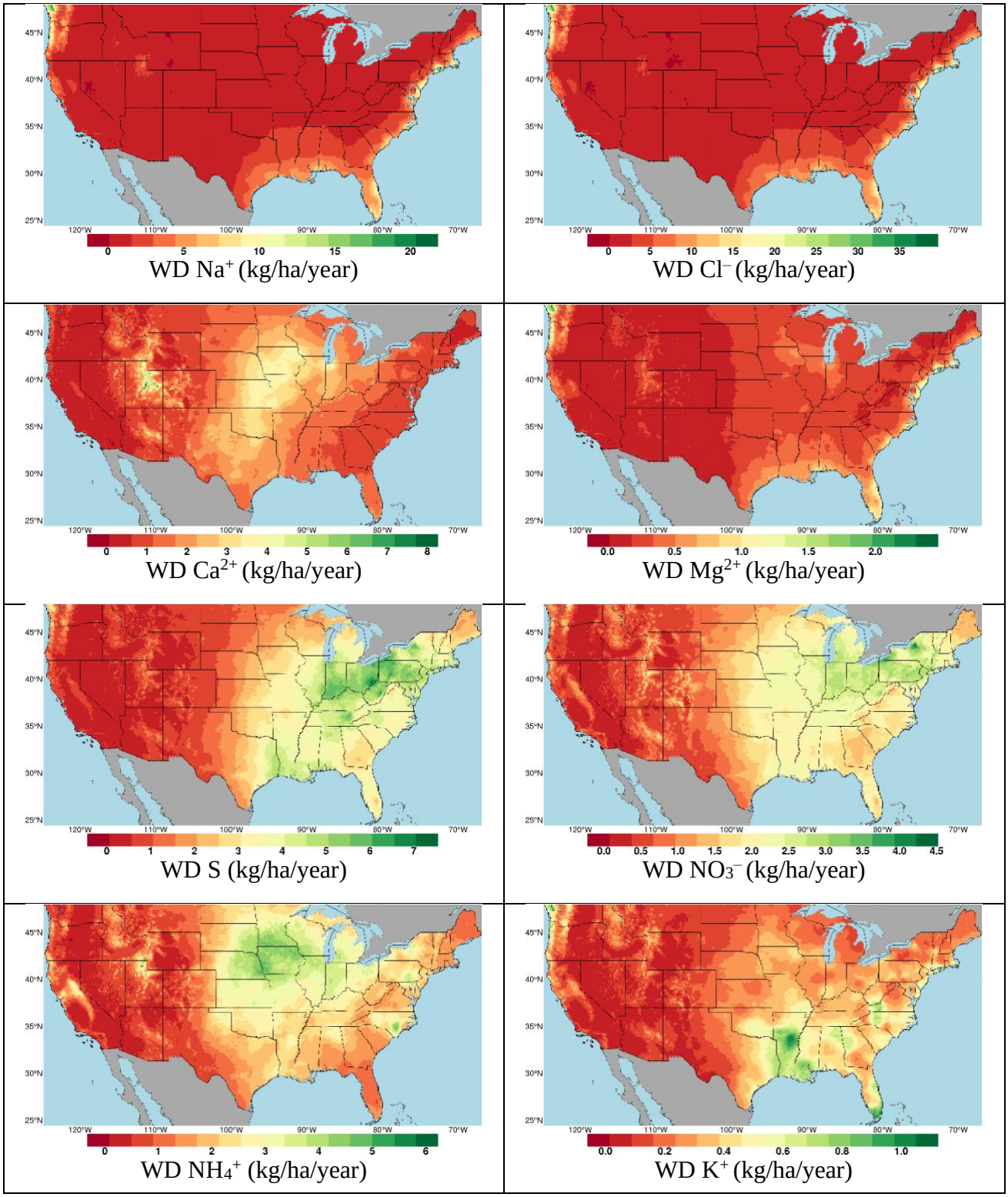

Fig. 29. Multiannual mean wet deposition fluxes of major ions during 2000-2017 over the conterminous US.

4.6. Origins of major ions in rainwater

4.6.1. Ionic correlation using Spearman's Rank Correlation Analysis

Correlation analysis between major anions and cations in precipitation can be a proper method to assess the origins of pollutants and to decipher the interactions and relationships amongst gases, particles, and ionic compounds. The significant correlation coefficients between certain ions can indicate their sources in general, but in most cases the local specificities can also be explained. In most cases, a significant correlation between Na^+ and K^+, Ca^{2+}, and Mg^{2+} indicates the presence of alkali plagioclase feldspars, that are rich in sodium and potassium, phyllosilicates and amphiboles, which can be frequently found in the Eastern Carpathians, showing the volcanic origins of these mountains (Szép et al., 2018). Another significant correlation coefficient can be found between Na^+ and Cl^-, which usually indicates the marine influence in rainwater, moreover, sodium is often used as a marine tracer element, due to its content in seawater, silicate and halite rocks (Szép et al., 2018). In the Eastern Carpathians this correlation coefficient may also indicate the presence of moffette gas, salt mines and mineral springs. According to Rao et al., (2017), chloride can be found in enriched form in seawater, halite rocks and pollutants originated from anthropogenic activities. A good correlation between Cl^- and SO_4^-, NO_3^-, and NO_2^- can indicate the presence of anthropogenic sources (coal combustion, refuse incineration, biomass burning) (Rao et al., 2017). If SO_4^{2-} and Cl^- correlates well in areas where non sea-salt chloride has high values, it may indicate emissions from the metallurgic industry, known for coal combustion and use of Cl^- (Xu et al., 2009). Alkaline ions, such as Ca^{2+}, K^+ and Mg^{2+}, which are known as essential soil components, are very effective neutralizing agents. A significant correlation between calcium and magnesium implies their common origin, such as the dissolution/weathering of calcite, dolomite and limestone, the presence of open quarries, and/or cement factories (Niu et al., 2014; Rao et al., 2017; Szép et al., 2018; Xiao, 2016). Significant correlations between major cations and anions indicate that acid pollutants can be absorbed by the particulate matter and react with alkaline compounds (Pu et al., 2017). Positive correlation between Ca^{2+} and SO_4^{2-} and Na^+ and SO_4^{2-} may be an indicator to the weathering process of gypsum or to the presence of other evaporitic salts, such as mirabilite and thernadite (Stoiber and Rose, 1974; Wu et al., 2014). The above-mentioned compounds are an indicator of volcanic fumaroles and post volcanic activity.

Also, a positive correlation coefficient between cations like calcium, magnesium and potassium may suggest their common origin from terrestrial/ crustal sources (Mouli et al., 2005).

In their study, Jiang and Yan, (2010), suggested that a strong correlation coefficient between conductivity and calcium and bicarbonate indicates the interrelationship among water and rocks, resulting in limestone and dolomite dissolution. The presence of sylvite (KCl) is indicated by the strong correlation between potassium and chloride, which may be present in soil minerals, blown into the atmosphere, and dissolved in rainwater (Rao et al., 2017). Positive correlations between NH_4^+ and SO_4^{2-} may occur due to the chemical reactions in the atmosphere (Zhang et al., 2007). In general, ammonia is present in the atmosphere under the form of $(NH_4)_2SO_4$, NH_4HSO_4 and NH_4NO_3, being the result of chemical reactions with H_2SO_4 and HNO_3 (Gong et al., 2013). In general, a positive correlation between NH_4^+ and K^+ can be attributed to the excessive use of N type fertilizers, cattle waste deposits, agricultural activities and biomass burning. Another tracer of agricultural activities is the significant correlation

between NH_4^+ and NO_3^-. Significant correlations between SO_4^{2-} and NO_3^- are indicators of industrial activities, traffic and coal combustion (Y. Z. Cao et al., 2009). A significant negative correlation coefficient among pH values, sulfate and nitrate may indicate the effects of acidic compounds on pH value and rainwaters acidity.

The Spearman correlation values for all sampling sites in the central group of the Eastern Carpathians are presented in Table 12.

Table 12. Spearman correlation coefficients among ionic constituents in precipitation collected in the central group of the Eastern Carpathians.

CB											**GB***
µeq/l	**Na^+**	**K^+**	**Ca^{2+}**	**Mg^{2+}**	**NH_4^+**	**SO_4^{2-}**	**Cl^-**	**NO_2^-**	**NO_3^-**	**HCO_3^-**	**Cond.**
Na^+	*1*	0.29*	**0.62***	0.48*	-0.09*	0.23*	**0.60***	**0.51***	0.19*	0.16*	0.45*
K^+	**0.50**	*1*	0.38*	**0.71***	**0.57***	0.38*	0.43*	0.35*	0.21*	0.26*	**0.58***
Ca^{2+}	**0.53**	**0.60**	*1*	**0.75***	-0.07*	0.31*	**0.67***	**0.66***	0.38*	0.32*	**0.54***
Mg^{2+}	0.47	**0.77**	**0.78**	*1*	0.32*	0.39*	**0.62***	**0.57***	0.24*	0.40*	**0.67***
NH_4^+	0.36	**0.58**	0.35	**0.53**	*1*	0.38*	0.16*	0.05*	0.28*	0.18*	**0.52***
SO_4^{2-}	0.35	**0.57**	**0.48**	**0.56**	**0.60**	*1*	0.48*	0.48*	**0.57**	0.30*	**0.55***
Cl^-	**0.64**	**0.63**	**0.61**	**0.64**	**0.52**	**0.53**	*1*	**0.60***	0.45	0.02*	**0.67***
NO_2^-	**0.60**	0.43	**0.51**	0.44	**0.57**	0.45	**0.67**	*1*	0.39*	0.12*	**0.59***
NO_3^-	0.48	0.48	**0.62**	**0.58**	**0.50**	**0.58**	**0.64**	**0.58**	*1*	0.10*	**0.50***
HCO_3^-	0.18	0.35	0.36	0.35	0.12	0.24	0.20	0.17	0.10	*1*	0.13*
Cond.	**0.51**	**0.67**	**0.63**	**0.69**	0.29	**0.71**	**0.73**	**0.67**	**0.69**	0.29	*1*
DTP											**OSB**
µeq/l	**Na^+**	**K^+**	**Ca^{2+}**	**Mg^{2+}**	**NH_4^+**	**SO_4^{2-}**	**Cl^-**	**NO_2^-**	**NO_3^-**	**HCO_3^-**	**EC**
Na^+	*1*	**0.72***	**0.68***	**0.63***	0.31*	0.49*	**0.61***	**0.54***	0.33*	0.45*	**0.71***
K^+	0.22	*1*	**0.62***	**0.70***	**0.60***	**0.60***	0.39*	**0.56***	0.22*	**0.64***	**0.74***
Ca^{2+}	0.26	**0.62**	*1*	**0.75***	0.33*	**0.70***	**0.52***	**0.58***	0.38*	**0.55***	**0.77***
Mg^{2+}	0.21	**0.79**	**0.71**	*1*	0.47*	**0.60***	0.44*	**0.56***	0.34*	**0.63***	**0.74***
NH_4^+	-0.14	**0.73**	**0.53**	**0.71**	*1*	0.35*	0.34*	0.31*	0.06*	0.33*	0.48*
SO_4^{2-}	0.37	0.49	**0.53**	**0.53**	0.37	*1*	0.37*	**0.58***	0.20*	**0.58***	**0.73***
Cl^-	**0.75**	0.29	0.38	0.29	0.09	0.44	*1*	0.39*	0.28*	0.17*	**0.60***
NO_2^-	0.34	-0.08	0.23	0.06	-0.24	0.20	**0.52**	*1*	0.23*	**0.52***	**0.68***
NO_3^-	**0.50**	0.10	0.14	0.10	-0.18	0.41	0.43	0.36	*1*	0.18*	0.42*
HCO_3^-	0.32	0.46	0.48	**0.54**	0.40	0.45	0.28	0.14	0.06	*1*	**0.55***
EC	0.41	**0.62**	**0.65**	**0.69**	**0.59**	**0.69**	**0.62**	0.33	0.26	0.49	*1*

Correlation is considered significant if R>0.5 at 99% confidence level. Na^+ and Cl^- presented significant correlation coefficients, R being 0.64 at CB, 0.60 at GB, 0.75 at DTP, and 0.61 at OSB. Sodium and potassium were significantly correlated at CB (R = 0.50) and OSB (R = 0.72), suggesting the presence of alkali felspars. Significant correlation was observed between Na^+ and Ca^{2+} at CB (R = 0.53), GB (R = 0.62) and OSB (0.68), indicating the presence of plagioclase feldspars in the studied area. Positive correlation between Cl^- and SO_4^- (0.53 at CB), NO_3^- (0.64 at CB) and NO_2^- (0.67 at CB; 0.60 at GB; 0.52 at DTP) were also noticed. The significant correlation between Ca^{2+} and Mg^{2+} at all studied areas from the central group of the Eastern Carpathians (0.78 – CB; 0.75 – GB; 0.71 – DTP; 0.75 – OSB) indicates their similar origin (calcite, dolomite and limestone dissolution, quarries, cement factories). There were high correlations between acidic anions and

dust-derived cations, such as Ca^{2+} and SO_4^- at DTP (R = 0.53) and OSB (R = 0.70), Mg^{2+} and SO_4^- at CB (0.56) and DTP (0.53), Mg^{2+} and NO_3^- at CB (0.58), Mg^{2+} and NO_2^- at GB (0.57) and at OSB (0.56). The studied areas are known to be rich in carbonate rocks (limestones and dolomites), explaining the significant correlation coefficients between the above-mentioned ions. Strong correlation among sodium and magnesium (R = 0.63) at OSB indicates their marine origin from long range transported sea salt, while the lack of a significant correlation between the above-mentioned ions at CB, GB and DTP is proof of the barrier effect of the Eastern Carpathians mountainous chain.

Significant correlations between NH_4^+ and SO_4^{2-} (R = 0.60), NO_3^- (R = 0.50) and NO_2^- (R = 0.57) for CB were also observed. Positive correlation can be observed found between NH_4^+ and K^+ in the studied areas (0.58 – CB; 0.57 – GB; 0.73 – DTP; 0.60 – OSB). Positive correlations between SO_4^{2-} and NO_3^- at CB (0.58), at GB (0.57) and between SO_4^{2-} and NO_2^- at OSB (0.58) can also be deciphered.

In the case of the northern group of the Eastern Carpathians results are shown in Fig. 30, correlation being considered significant if R>0.45 at 99% confidence level.

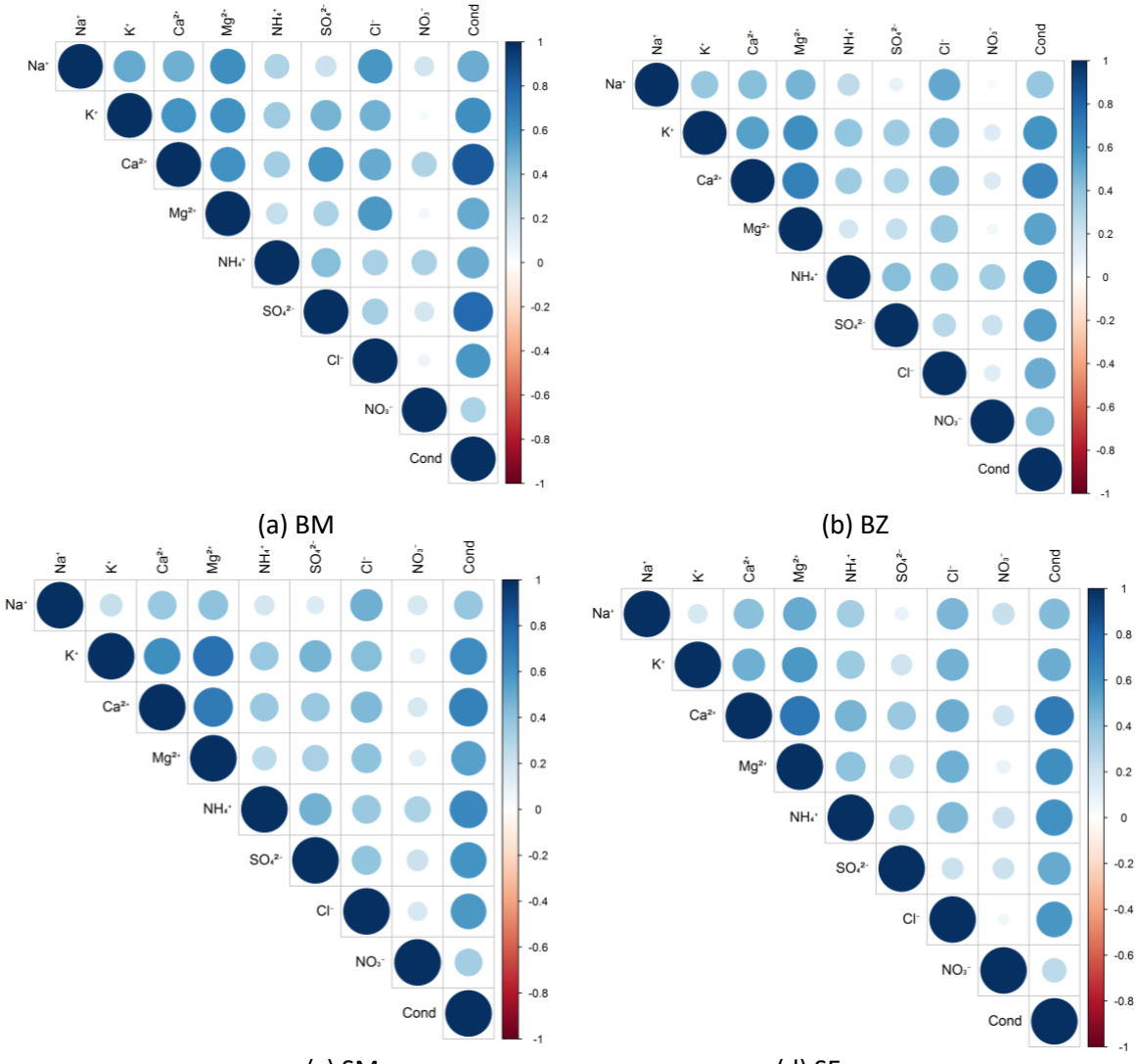

(a) BM (b) BZ

(c) SM (d) SE

Fig. 30. Spearman correlation coefficients of ionic constituents in precipitation.

Na^+ and Cl^- presented significant correlations at all sampling sites, exhibiting a coefficient of 0.52, 0.56, 0.51 and 0.48 at BM, BZ, SM and SE, respectively, indicating the

presence of sea-salt. Strong correlation between Na^+ and K^+ (0.52 at BM), Ca^{2+} (0.48 – BM and BZ), Mg^{2+} (0.64 – BM, 0.51 – BZ, 0.53 – SE) can also be noticed. Significant positive correlations were found between K^+ and Ca^{2+} (0.58 – BM, 0.56 – BZ, 0.57 – SM, 0.48 – SE), K^+ and Mg^{2+} (0.60 – BM, 0.65 – BZ, 0.73 – SM, 0.56 – SE), Ca^{2+} and Mg^{2+} (0.62 – BM, 0.71 – BZ, 0.65 – SM, 0.75 – SE), showing terrestrial influences. This area has a great relief variety, where all main geological formations can be found, such as volcanic and magmatic rocks, crystalline and meso-metamorphic slices and sedimentary rocks. Significant correlations can be found between SO_4^{2-} and Ca^{2+} (0.62), Cl^- and Ca^{2+} (0.51), Cl^- and Mg^{2+} (0.57), suggesting the neutralizing potential of cations. SO_4^{2-} and NH_4^+ also presented a strong correlation coefficient, having an R value of 0.46, 0.40 and 0.46 at BM, BZ and SM, respectively.

Table 13. Spearman correlation coefficients for ionic constituents in precipitation at the sampling sites from the Southern Carpathians.

RS	Na^+	K^+	Ca^{2+}	Mg^{2+}	NH_4^+	SO_4^{2-}	Cl^-	NO_2^-	NO_3^-	HCO_3^-	Cond.
Na^+	1										
K^+	**0.53**	1									
Ca^{2+}	0.28	**0.43**	1								
Mg^{2+}	0.14	0.32	**0.77**	1							
NH_4^+	0.11	**0.41**	**0.39**	0.33	1						
SO_4^{2-}	**0.37**	**0.39**	**0.47**	0.34	**0.35**	1					
Cl^-	0.13	0.10	0.34	0.32	0.12	0.31	1				
NO_2^-	0.27	0.25	0.24	0.15	0.27	**0.35**	0.19	1			
NO_3^-	**-0.35**	0.07	0.07	0.26	0.26	0.03	0.13	-0.10	1		
HCO_3^-	-0.11	0.04	0.12	0.10	0.24	0.14	0.11	0.29	**0.38**	1	
Cond.	**0.36**	**0.62**	**0.57**	**0.48**	**0.49**	**0.68**	0.29	**0.37**	0.18	**0.35**	1

MN	Na^+	K^+	Ca^{2+}	Mg^{2+}	NH_4^+	SO_4^{2-}	Cl^-	NO_2^-	NO_3^-	HCO_3^-	Cond.
Na^+	1										
K^+	**0.56**	1									
Ca^{2+}	0.30	0.17	1								
Mg^{2+}	0.32	0.14	**0.78**	1							
NH_4^+	0.04	0.21	0.32	0.31	1						
SO_4^{2-}	**0.58**	**0.35**	**0.42**	**0.40**	0.22	1					
Cl^-	**0.42**	0.26	**0.49**	**0.43**	**0.36**	0.24	1				
NO_2^-	0.12	0.16	0.21	0.20	**0.71**	0.27	0.04	1			
NO_3^-	-0.09	0.05	0.29	0.27	-0.16	-0.04	-0.06	**-0.39**	1		
HCO_3^-	0.20	0.21	-0.08	-0.13	0.25	0.26	0.01	0.22	-0.24	1	
Cond.	**0.45**	**0.37**	**0.45**	**0.46**	0.22	**0.87**	**0.37**	0.15	0.14	0.22	1

BH	Na^+	K^+	Ca^{2+}	Mg^{2+}	NH_4^+	SO_4^{2-}	Cl^-	NO_2^-	NO_3^-	HCO_3^-	Cond.
Na^+	1										
K^+	0.19	1									
Ca^{2+}	0.25	**-0.45**	1								
Mg^{2+}	0.20	**-0.43**	**0.80**	1							
NH_4^+	-0.31	-0.16	-0.10	0.09	1						
SO_4^{2-}	0.01	0.08	**0.40**	0.11	-0.33	1					
Cl^-	0.18	-0.30	0.24	**0.44**	0.09	-0.11	1				
NO_2^-	-0.23	-0.09	-0.01	0.01	0.19	0.29	-0.07	1			
NO_3^-	-0.21	0.01	0.08	0.22	0.09	0.21	0.22	-0.01	1		
HCO_3^-	0.00	0.30	0.21	-0.11	0.20	0.15	0.17	0.12	0.19	1	
Cond.	0.05	0.19	**0.85**	0.16	0.25	**0.77**	0.13	0.21	0.27	0.34	1

Results of the Spearman's rank analysis for the Southern Carpathians are presented in Table 13. Only correlations with R > 0.35 were considered significant at 99% confidence level.

Significant correlations of conductivity with K^+ (0.620 – RS), Ca^{2+} (0.570 – RS; 0.449 – MN; 0.850 - BH) and Mg^{2+} (0.477 – RS; 0.461 – MN) were observed, indicating the total dissolved solids in rainwater. Strong correlation coefficients were observed between Na^+ and K^+ (0.533 – RS; 0.561 – MN), and between Ca^{2+} and Mg^{2+} at all three sampling sites (0.77 – RS; 0.745 – GB; 0.781 – MN; 0.803 – BH), showing that these ions may originate from same sources. Ca^{2+} and SO_4^{2-} (0.474 – RS; 0.485 – MN; 0.401 – BH) and Na^+ and SO_4^{2-} in the case of MN (R = 0.582) were strongly correlated, indicating the presence of evaporitic salts, like $CaSO_4$ and Na_2SO_4. The lack of correlation between chloride and sodium was also observed.

The fact that in the Southern Carpathians there is no significant correlation between Na^+ and Cl^-, it is of great interest, hence this phenomenon it is not very frequent in the specialty literature regarding precipitation chemistry. This may be due to the fact that the existent chloride and sodium in rainwater is emitted from other sources, such as the industry or coal combustion (Anatolaki and Tsitouridou, 2009; Kaneyasu et al., 1999; Ruprecht and Sigg, 1990). Another possible explanation is the Foehn effect. The air masses that come from the Mediterranean and Adriatic Sea, loaded with sea salts, are blocked by the Dinaric Alps and by the Balkan Mountains. Foehn winds that are travelling across the Adriatic Sea are characterized as dry, and lacking humidity, and when they are blocked by the Dinaric Alps, orographic convection appears. The chloride and sodium concentration in rainwater at the sampling sites from the Southern Carpathians may be explained by the contribution of local sources, such as industrial activities, the presence of thermal waters, mineral springs and mofettas.

In the case of Europe, Spearman rank correlation analysis was performed for each country and for the entire database, considering a correlation significant, if R>0.50 at 95% confidence level (Fig. 31).

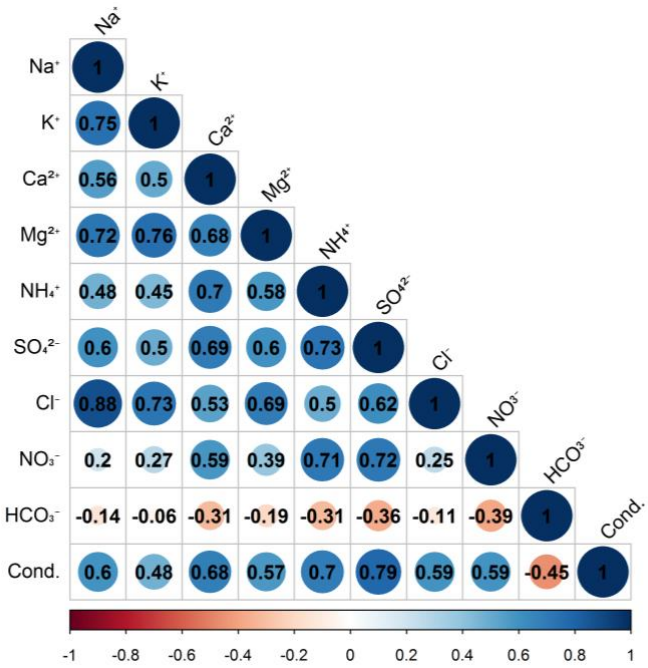

Fig. 31. Spearman correlation coefficients for ionic constituents in precipitation for all studied countries in Europe.

Significant correlation was observed between SO_4^{2-} and NO_3^- (R=0.72). Regarding at the correlation coefficients among sulfate and nitrate at each region, strong interconnections were observed: 0.75 for Northern Europe, 0.70 for Eastern Europe, 0.70 for Southern Europe and 0.67 for Central-East Europe.

SO_4^{2-} and Cl^- were also significantly correlated, exhibiting R=0.62 for all countries and in Northern Europe, 0.66 in Western Europe, 0.56 in Southern Europe and 0.63 in Central-East Europe. The strong correlations amongst Ca^{2+} and Mg^{2+} (R=0.65) for the entire database, as well as for all four regions (0.65 – Northern Europe, 0.69 – Western Europe, 0.75 – Southern Europe and 0.59 – Central-East Europe) were also found. Na^+ and K^+ were significantly correlated, exhibiting 0.75 in Europe and Northern Europe, 0.84 in Western Europe, 0.64 in Southern Europe, and 0.68 in Central-East Europe. The positive correlation coefficients between Ca^{2+} and SO_4^{2-} (R=0.69), Ca^{2+} and Cl^- (R=0.53), Ca^{2+} and NO_3^- (R=0.59), Mg^{2+} and SO_4^{2-} (R=0.60), Mg^{2+} and Cl^- (R=0.69) are implying the neutralizing effects of cations over acidic species. The significant correlation coefficents between Na^+ and Cl^- (R=0.88 – Europe and Northern Europe, R=0.94 – Western Europe, R=0.82 – Southern Europe, R=0.89 – Central-East Europe) are suggesting the presence of marine spray in precipitation.

For the conterminous US, Spearman's rank correlation analysis was performed, considering a correlation coefficient significant, if R > 0.35 at a 95% confidence level (Fig. 32).

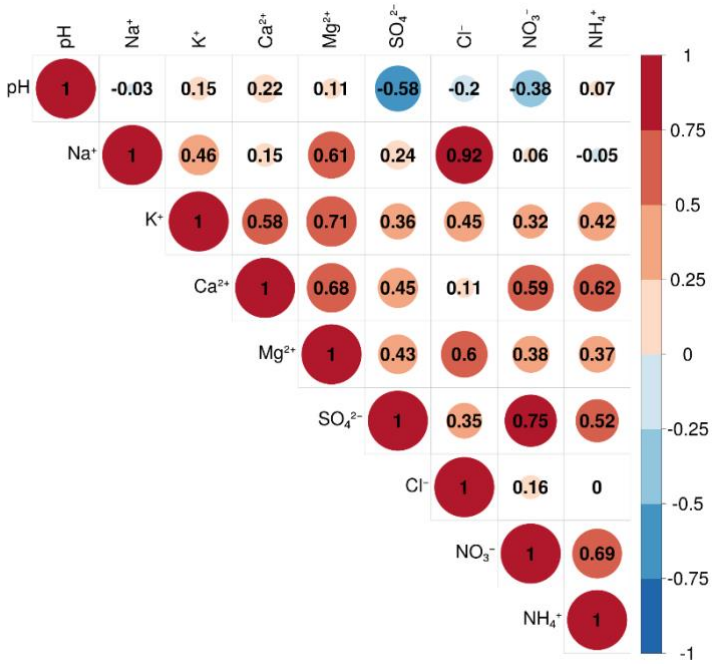

Fig. 32. Spearman's rank correlation analysis performed on major ionic constituents and pH in precipitation samples harvested across the conterminous US.

The strong correlation coefficient of 0.92 amongst Na^+ and Cl^- indicates their origin from sea salts blown in the atmosphere from the Pacific and Atlantic Oceans. The fact that correlation between SO_4^{2-} and Cl^- (R=0.35) was observed indicates the presence of metallurgic industry, which uses chloride and coal combustion. Strong correlation coefficients were found Ca^{2+} and Mg^{2+} (R=0.68), Ca^{2+} and K^+ (R=0.58), K^+ and Mg^{2+} (R=0.71), indicating their common terrestrial sources, while the strong correlation

coefficients between cations and acidic compounds are proof that neutralization occurs. NH_4^+ and K^+, NH_4^+ and Mg^{2+} also presented significant correlation between each other, implying agricultural activities and biomass burning. The same source origin of SO_4^{2-} and NO_3^- is explained by their strong correlation coefficient.

4.6.2. Marine and crustal enrichment factors

Enrichment factors (EF) are a useful tool to assess the possible sources and origins of major ions and species in rainwater (Y. Z. Cao et al., 2009; Yatkin et al., 2016). In order to interpret the results, one should know that an EF value greater or smaller than unity is considered to be enriched or diluted in association to the reference source (Y. Z. Cao et al., 2009; Wu et al., 2016; Zhang et al., 2007).

Table 14 presents the EF values for crustal and marine salt components in the Central group of the Eastern Carpathians. It can be observed that values of $EF_{seawater}$ for Cl^- varied from 1.74 at GB and 3.45 at OSB, while the EF_{soil} exhibited values between 99.23 at OSB and 237.57 at GB, indicating that chloride is enriched relative to marine and crustal sources, but the seawater origin is stronger. Magnesium and potassium $EF_{seawater}$ and EF_{soil} averages calculated for all sampling locations explained that these ions are enriched compared to marine influences and lightly diluted to the Earth's crust. However, these results indicate terrestrial sources, since only in very specific cases the concentration of crustal ions in rainwater can exceed the values of these ions concentrations in soil (Szép et al., 2018). Calcium $EF_{seawater}$ values were situated between 66.9 at GB and 284.8 at OSB, suggesting their crustal origin. For SO_4^{2-}, $EF_{seawater}$ as well as EF_{soil} exhibited significantly enriched values, implying that concentrations of sulfate in rainwater mainly originate from anthropogenic sources and terrestrial and marine sources have an insignificant contribution (J. Cao et al., 2009; Lu et al., 2011).

Table 14. Enrichment factors for soil and sea salt components relative to rainwater.

	Cl^-/Na^+	K^+/Na^+	Ca^{2+}/Na^+	Mg^{2+}/Na^+	SO_4^{2-}/Na^+
Seawater ratio	1.16	0.02	0.04	0.22	0.12
EF_{Marine}					
CB	2.8	67.4	136.0	5.4	32.2
GB	1.7	56.3	66.9	3.9	28.5
DTP	1.9	66.5	111.8	4.4	30.5
OSB	3.5	52.0	284.8	5.0	80.6
	Cl^-/Ca^{2+}	K^+/Ca^{2+}	Na^+/Ca^{2+}	Mg^{2+}/Ca^{2+}	SO_4^{2-}/Ca^{2+}
Soil Ratio	0.0031	0.504	0.569	0.561	0.0188
EF_{Soil}					
CB	220.4	0.6	0.7	0.4	41.8
GB	237.6	0.9	1.0	0.6	67.1
DTP	231.5	0.7	0.9	0.4	53.3
OSB	99.2	0.3	0.3	0.2	44.4

Mean enrichment factors for major ions measured at the sampling locations from the Northern group from the eastern Carpathians (BM, BZ, SM and SE) are shown in Table 15.

Table 15. Enrichment factors for sea salt and soil components relative to rainwater in the Northern Group of the Eastern Carpathians.

	Cl^-/Na^+	K^+/Na^+	Ca^{2+}/Na^+	Mg^{2+}/Na^+	SO_4^{2-}/Na^+
Seawater ratio	1.16	0.02	0.04	0.22	0.12
EF_{Marine}					
BM	1.68	29.81	228.83	5.64	72.31
BZ	1.57	47.00	137.66	6.93	28.07
SM	1.68	62.17	156.98	7.15	27.34
SE	2.08	129.93	145.06	7.20	35.24
	Cl^-/Ca^{2+}	K^+/Ca^{2+}	Na^+/Ca^{2+}	Mg^{2+}/Ca^{2+}	SO_4^{2-}/Ca^{2+}
Soil Ratio	0.0031	0.504	0.569	0.561	0.0188
EF_{Crust}					
BM	112.25	0.20	0.45	0.43	38.72
BZ	156.05	0.41	0.73	0.67	36.69
SM	123.40	0.40	0.59	0.48	29.72
SE	153.97	0.88	0.58	0.62	35.89

The EF values for seawater showed that all major cations are enriched, the highest EF values being registered for calcium, varying between 137.66 at BZ and 228.83 at BM, indicating terrestrial influence. For sulfate, EFs measured 30-70 times higher values than the reference ratios, indicating anthropogenic origin. The EF values for chloride were in all cases greater than 1, but the values calculated for BM (1.68), SM (1.68), BZ (1.57) and SE (2.08) were closer to the seawater reference ration, suggesting that chloride comes from marine sources. The values for EF_{crust} indicated that potassium and magnesium originated from terrestrial sources, hence their values were below one. The 30- and 156-times higher values for SO_4^{2-} and Cl^- indicated that these ions enrichment in rainwater comes from anthropogenic sources and sea spray. Na^+ EF_{crust} values ranged between 0.45 and 0.73, suggesting terrestrial origins too, explained by the presence of halite and silicate rocks in the studied area (Szép et al., 2018).

EF_{marine} and EF_{crust} values are given in Table 16 for the sampling sites from the Southern Carpathians.

Table 16. EFs for sea salt and soil components relative to rainwater in the Southern Carpathians.

	Cl^-/Na^+	K^+/Na^+	Ca^{2+}/Na^+	Mg^{2+}/Na^+	SO_4^{2-}/Na^+
Seawater ratio	1.16	0.02	0.04	0.22	0.12
EF_{Marine}					
RS	5.48	22.87	143.27	13.45	20.38
MN	6.95	42.12	398.44	41.56	87.02
BH	6.82	41.29	422.75	41.72	96.13
	Cl^-/Ca^{2+}	K^+/Ca^{2+}	Na^+/Ca^{2+}	Mg^{2+}/Ca^{2+}	SO_4^{2-}/Ca^{2+}
Soil Ratio	0.0031	0.504	0.569	0.561	0.0188
EF_{Crust}					
RS	723.55	0.47	0.92	0.94	52.16
MN	242.90	0.20	0.24	0.80	54.37
BH	238.69	0.25	0.24	0.86	64.39

EF_{Marine} values for K^+, Ca^{2+}, Mg^{2+} and SO_4^{2-} were considerably enriched, showing the crustal origin of these ions. EF_{Marine} values for Cl^- were also enriched, but still appeared

to be diluted in comparison with other ions, which may indicate a in a small percent marine influence. EFc_{rust} values indicated anthropogenic sources for SO_4^{2-} and Cl^-, while K^+, Mg^{2+}, and Na^+ appeared to be enriched from crustal sources.

The mean values of seawater and terrestrial EFs for Europe are presented in Table 17.

Table 17. Enrichment factors for sea salt and soil components relative to rainwater in Europe.

	$EF_{seawater}$					EF_{crust}				
	$\frac{Cl^-}{Na^+}$	$\frac{K^+}{Na^+}$	$\frac{Ca^{2+}}{Na^+}$	$\frac{Mg^{2+}}{Na^+}$	$\frac{SO_4^{2-}}{Na^+}$	$\frac{Cl^-}{Ca^{2+}}$	$\frac{K^+}{Ca^{2+}}$	$\frac{Na^+}{Ca^{2+}}$	$\frac{Mg^{2+}}{Ca^{2+}}$	$\frac{SO_4^{2-}}{Ca^{2+}}$
Austria	1.29	5.79	14.85	1.77	18.06	738.01	0.46	3.33	1.23	172.22
Belarus	1.11	10.81	11.54	1.55	11.68	1090.18	1.13	4.84	1.58	199.88
Croatia	1.02	5.87	12.17	1.51	11.67	722.55	0.50	3.52	1.20	148.49
Czech Rep.	1.04	6.25	12.12	1.33	13.66	764.52	0.53	3.52	1.03	170.94
Denmark	1.08	6.66	11.06	1.33	13.49	858.23	0.62	3.87	1.12	183.65
Estonia	0.94	6.09	12.17	1.66	12.07	741.85	0.55	3.73	1.37	162.47
Finland	0.91	5.86	11.20	1.29	12.11	727.14	0.54	3.78	1.08	164.61
France	0.95	5.93	11.62	1.37	12.48	740.59	0.53	3.69	1.11	164.43
Germany	0.93	6.13	11.64	1.37	12.52	716.60	0.54	3.64	1.10	163.60
Greece	1.00	7.33	11.14	1.34	14.20	802.12	0.66	3.98	1.13	190.45
Hungary	0.94	6.40	12.00	1.45	13.02	714.80	0.55	3.55	1.17	167.17
Iceland	0.90	6.56	11.33	1.27	12.05	754.74	0.64	3.92	1.08	162.83
Ireland	0.91	7.65	10.57	1.75	12.08	769.16	0.71	3.98	1.50	174.15
Italy	0.94	6.35	11.41	1.40	12.44	778.61	0.61	4.01	1.19	175.54
Latvia	0.96	6.32	12.34	1.53	12.74	716.91	0.54	3.55	1.14	160.32
Norway	0.94	6.53	11.74	1.32	12.88	726.41	0.58	3.65	1.07	167.90
Poland	0.95	5.75	11.01	1.27	11.96	763.16	0.53	3.76	1.08	164.90
Portugal	0.99	9.04	14.26	1.89	12.58	682.75	0.67	3.23	1.27	144.30
Serbia	0.94	5.68	10.88	1.25	11.13	784.42	0.54	3.92	1.09	157.94
Slovakia	0.97	6.27	11.05	1.35	13.02	797.72	0.59	3.88	1.15	180.18
Slovenia	0.88	6.03	10.73	1.33	11.43	747.90	0.58	4.00	1.17	161.96
Spain	1.01	6.67	10.25	1.23	10.69	853.01	0.66	4.18	1.12	157.65
Sweden	0.86	5.81	12.59	1.42	12.96	714.06	0.55	4.03	1.15	165.51
Switzerland	0.94	5.82	11.81	1.33	12.90	711.91	0.51	3.59	1.06	166.21
Netherlands	0.92	6.37	11.32	1.34	11.96	727.58	0.57	3.70	1.10	161.74
Turkey	0.99	13.55	12.02	1.50	11.72	773.77	1.24	3.70	1.18	151.19
UK	0.91	5.69	11.87	1.33	12.00	715.31	0.51	3.68	1.08	155.88

The values of marine EFs for Cl^- ranged between 0.86 1.29 in Sweden and Austria,respectively, while the EF_{Crust} exhibited values between 682.75 in Portugal and 1090.18 in Belarus, indicating that chloride origins from sea spray. Both EF_{Marine} and EF_{Crust} values in the case of potassium indicated crustal origins, EFs being considerably enriched compared to the reference seawater ratio and slightly diluted to the K^+/Ca^{2+} (0.504) reference crustal ratio. Crustal EFs for potassium indicated that in the majority of countries K^+ had terrestrial origins, with the exception of Belarus and Turkey, where the significant difference in enrichment compared to values calculated for other countries may be due to biomass burning and chemical fertilizers (Zhang et al., 2007; Zunckel et al., 2003).

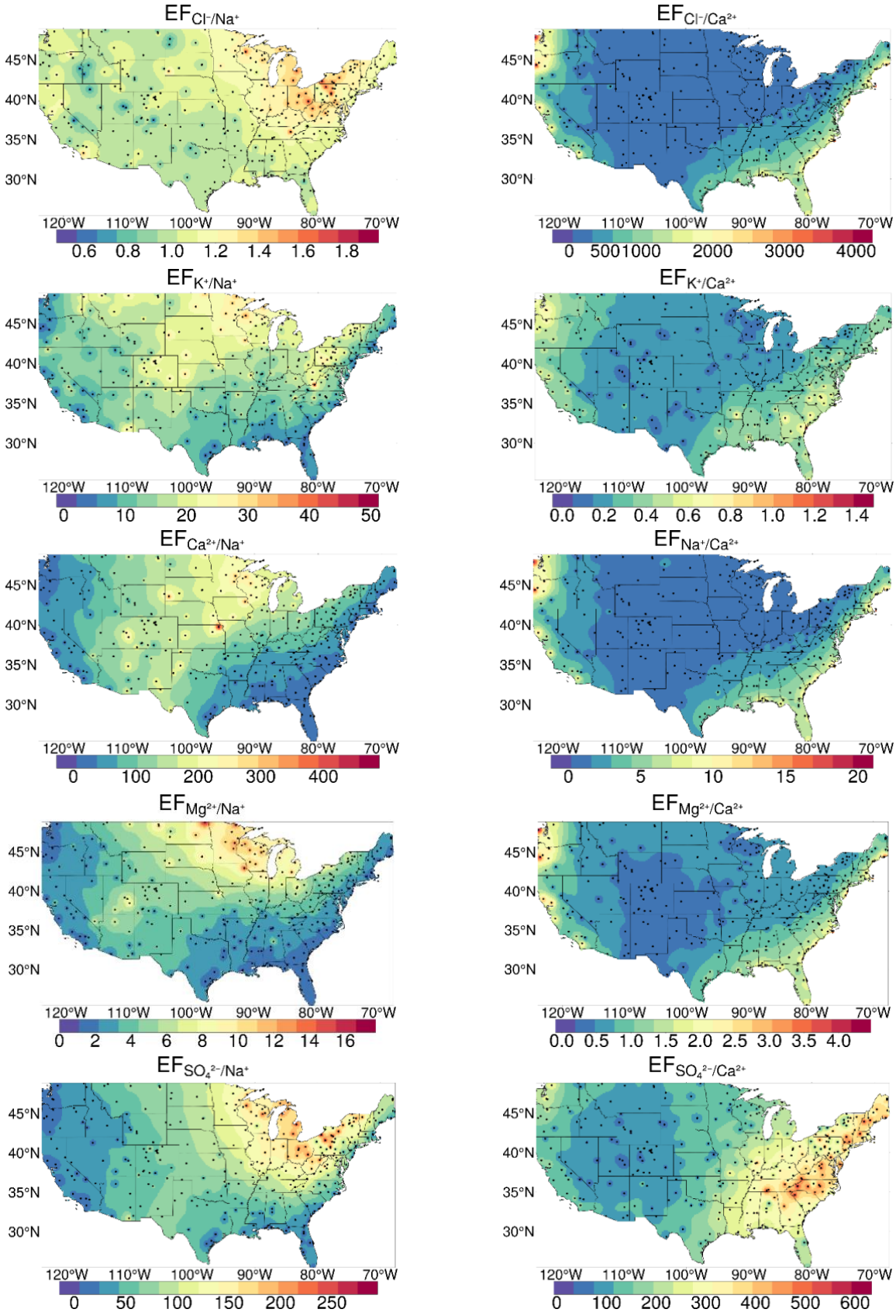

Fig. 33. Marine and crustal enrichment factors with reference to sodium and calcium across the conterminous US.

Crustal EF ratios for magnesium varied between 1.03 in Czech Republic and 1.58 in Belarus, suggesting a relatively small enrichment to the reference Mg^{2+}/Ca^{2+} (0.561) ratio. This indicates mixed sources for Mg^{2+}, which may be derived from both terrestrial and marine sources. EFs for Ca^{2+} indicated its terrestrial origin, while EFs for sulfate showed the relative contribution of anthropogenic sources, with small influences from soil dust and marine spray (Lu et al., 2011). Mean values of crustal and marine enrichment factors for each sampling site in the contiguous US can be observed in Fig. 33. Concentration maps for chloride sustained the results of VWMs, showing that there is an inverse interconnection between $EF_{seawater}$ and EF_{crust}, indicating that in the industrial belts of the conterminous US (Northeastern, Midwestern, Southern and Pacific Coastal regions) where chloride is used in the insdustrial production processes, the EF value for seawater is considerably greater than the reference Cl^-/Na^+ elemental ratio (1.16), suggesting that Cl^- may come from anthropogenic sources too. However, the mean values for $EF_{seawater}$ Cl^- and EF_{crust} Cl^- were 1.10 and 574.49, respectively, indicating that chloride has marine sources in most cases. According to the EF values for seawater (14.60) and crust (0.29) in case of K^+, one can see that potassium mainly originates from crustal sources. $EF_{seawater}$ Ca^{2+} exhibited a mean value of 94.94, implying the crustal sources of calcium. In case of magnesium, the same can be stated, hence its Mg^{2+}/Ca^{2+} ratio average of 0.86 is slightly enriched in comparison to the reference crustal elemental ratio (0.561). The $EF_{seawater}$ and EF_{crust} for SO_4^{2-} ranged between 82.09 and 215.33, respectively. Comparing these results with the reference elemental ratios for both types of EFs (SO_4^{2-}/Na^+ – 0.125; SO_4^{2-}/Ca^{2+} – 0.019), one can see that the anthropogenic origin of sulfate is obvious.

4.6.3. Marine and non-marine salt contributions

The results of equivalent ratios of major ions with reference to Na^+, indicating the sea salt fraction (%SSF) and the non-sea salt fraction (%NSSF) in rainwater measured in the Central group of the Eastern Carpathians are shown in Table 18.

Table 18. Source contributions (in %) for different ions in rainwater from the four sampling sites in the central group of the Eastern Carpathians.

	$\frac{Cl^-}{Na^+}$	$\frac{K^+}{Na^+}$	$\frac{Ca^{2+}}{Na^+}$	$\frac{Mg^{2+}}{Na^+}$	$\frac{SO_4^{2-}}{Na^+}$
CB					
Mean value	52.4	25.6	101.5	18.2	65.2
%SSF	74.8	2.9	1.5	42.3	6.5
%NSSF	25.2	97.1	98.5	57.7	93.5
GB					
Mean value	55.4	32.7	83.2	26.4	92.0
%SSF	87.9	2.8	2.2	36.1	5.7
%NSSF	12.1	97.2	97.8	63.9	94.3
DTP					
Mean value	68.3	43.0	127.3	26.3	105.0
%SSF	77.5	2.3	1.6	39.4	5.4
%NSSF	22.5	97.7	98.4	60.6	94.6
OSB					
Mean value	56.7	31.8	246.7	23.3	204.5
%SSF	70.9	2.4	0.6	33.7	2.1
%NSSF	29.1	97.6	99.4	66.3	97.9

The SSF value for Cl^- exhibited 74.8%, 87.9%, 77.5%, and 70.9% at CB, GB, DTP, and OSB, respectively, while the NSSF% of chloride may originate from different anthropogenic activities. In case of K^+, Ca^{2+} and SO_4^{2-}, high NSSF% can be observed, being above ~94% in all cases. According to the SSF and NSSF values, Mg^{2+} has crustal origins, but compared to other cations the non-sea salt fraction of magnesium is significantly higher than in case of other cations.

Table 19 shows the SSF and NSSF percentages of Cl^-, K^+, Ca^{2+}, Mg^{2+} and SO_4^{2-}, using Na^+ as a reference element for the rainwater samples collected in the Northern group of the Eastern Carpathians.

Table 19. Equivalent ratios of different components with reference to Na^+ in rainwater in the Northern group of the Eastern Carpathians.

	$\frac{Cl^-}{Na^+}$	$\frac{K^+}{Na^+}$	$\frac{Ca^{2+}}{Na^+}$	$\frac{Mg^{2+}}{Na^+}$	$\frac{SO_4^{2-}}{Na^+}$
Seawater	1.16	0.02	0.04	0.22	0.12
BM					
Mean value (rainwater)	1.95	0.66	10.07	1.28	9.04
%SSF	96.23	6.02	0.60	30.06	2.42
%NSSF	3.77	93.98	99.40	69.94	97.58
BZ					
Mean value (rainwater)	1.82	1.03	6.06	1.57	3.51
%SSF	87.22	3.05	1.05	21.14	5.31
%NSSF	12.78	96.95	98.95	78.86	94.69
SM					
Mean value (rainwater)	1.94	1.37	6.91	1.62	3.42
%SSF	99.64	2.78	1.17	25.24	6.93
%NSSF	0.36	97.22	98.83	74.76	93.07
SE					
Mean value (rainwater)	2.41	2.86	6.38	1.63	4.41
%SSF	79.60	1.29	1.15	21.73	5.97
%NSSF	20.40	98.71	98.85	78.27	94.03

As expected, the Cl^-/Na^+ ratio in precipitation presented similar values to the elemental ratio measured in seawater, showing that chloride originates from marine sources at all sampling locations. In contrast to this, calcium and potassium presented NSSF percentages higher than 94% at all sampling sites, showing the terrestrial influences of these ions. On the other hand, Mg^{2+} presented a little lower NSSF percentage, situating between ~69% and ~79%, which indicates that although it mainly originates from crustal sources, its sea spray origin cannot be neglected. SO_4^{2-} exhibited very NFFS% values higher than 93%, indicating the dominance of anthropogenic sources at all sampling stations. Relative contributions of SSF, CF and AF were also calculated, values registering 13.27%, 40.08%, 46.65% for BM, 18.36%, 35.54%, 46.10% for BZ, 21%, 35.88%, 43.12% for SM and 17.53%, 31.35%, 51.12% for SE, respectively. These factors sustain the results of enrichment factors and sea salt/ non-sea salt factors, indicating that ion concentrations in rainwater collected in the northern group of the Eastern Carpathians is mainly influenced by anthropogenic sources, but the contribution of terrestrial ones cannot be ignored. Therefore, it is of great importance to note that the precipitation chemistry is highly affected by the industrial and mining operations and other anthropogenic activities in the studied area.

The results of SSF% and NSSF% calculated for the sampling locations in the Southern Carpathians are shown in Table 20.

Table 20. Equivalent ratios of different components with reference to Na^+ in rainwater in the Southern Carpathians.

	$\frac{Cl^-}{Na^+}$	$\frac{K^+}{Na^+}$	$\frac{Ca^{2+}}{Na^+}$	$\frac{Mg^{2+}}{Na^+}$	$\frac{SO_4^{2-}}{Na^+}$
Seawater	1.16	0.02	0.04	0.22	0.12
RS					
Mean value (rainwater)	6.35	0.50	6.30	3.05	2.55
%SSF	34.91	5.20	1.08	12.26	7.81
%NSSF	65.09	94.80	98.92	87.74	92.19
MN					
Mean value (rainwater)	8.06	0.93	17.53	9.43	10.88
%SSF	26.77	3.57	0.43	3.94	1.88
%NSSF	73.23	96.43	99.57	96.06	98.12
BH					
Mean value (rainwater)	7.91	0.91	18.60	9.47	12.02
%SSF	20.23	3.28	0.31	3.20	1.44
%NSSF	79.77	96.72	99.69	96.80	98.56

The results observed for the Southern Carpathians were unique amongst all sampling sites discussed in this thesis, hence the SSFs and NSSFs showed that analyzed ions had non-marine origins. One can see that Cl^- had the highest SSF at RS (35%), while at BH and MN its values were even smaller, exhibiting 20.23% and 26.77%, respectively. In this area, iron and steel production is common, hence the chloride concentration in rainwater can be attribute to this, among other anthropogenic activities, such as traffic emissions, etc. (Wu et al., 2016; Xu et al., 2009). Among natural sources of NSSF chloride are the halite and sylvite, which through the dissolution process end up in rainwater (Xu et al., 2009). Sulfate also exhibited high NSSF percentages (92.19% - BH, 98.12% RS, 98.56% - BH), indicating anthropogenic sources (coal combustion, industry). High values of NSSF% for K^+, Ca^{2+} and Mg^{2+} can be explained by the presence of un-rehabilitated tailing dams, through which soil dust gets dissolved in rainwater. The dissolution of limestones, dolomites, but also the agricultural activities from the area are sustaining the crustal origin of the above-mentioned cations.

One possible explanation to the he absence of sea salts present in the rainwater collected in the Southern Carpathians, also sustained by the weak correlation coefficient Na^+ and Cl^-, is the distance between the sampling sites and Adriatic (540 km) and Mediterranean Sea (1240 km). Another possible cause is the Foehn effect, which is explained below more in detail. The precipitation amounts and their distribution upon the Balkan peninsula is analyzed (Fig. 34), taking under consideration the cyclonic circulations too in the eastern Mediterranean basin (Fig. 35) during the 1979-2018 period.

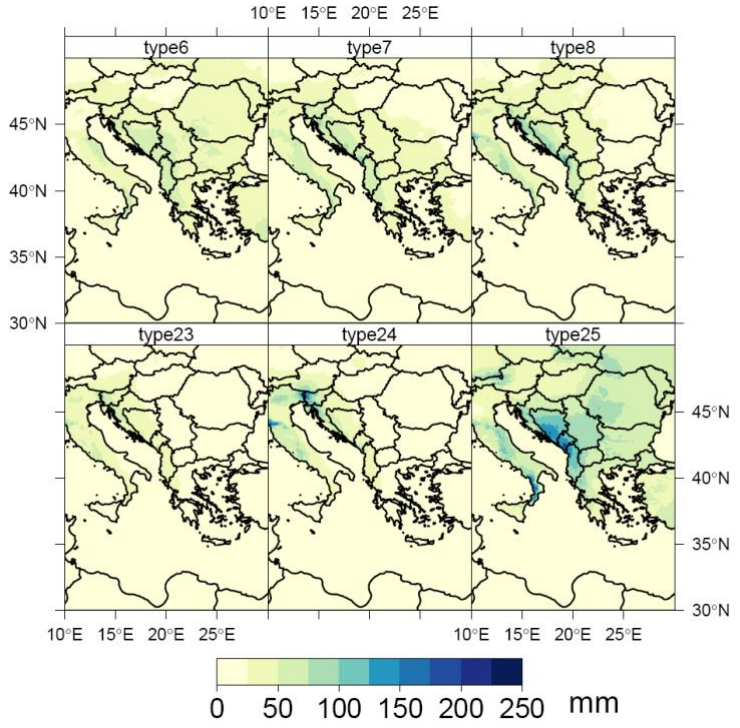

Fig. 34. Multiannual means of precipitation sums according to each cyclonic weather type.

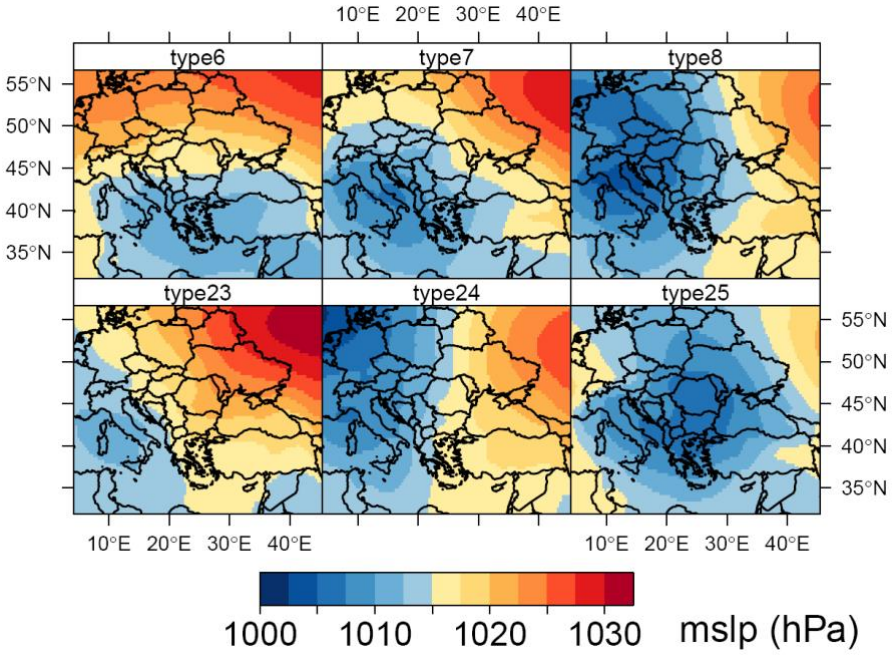

Fig. 35. GWT circulation types resembling to Mediterranean lows upon Balkan peninsula.

Usually, these synoptic patterns consist into frontal passages moving from northern Europe towards the Mediterranean Sea. When these fronts reach southern Europe (usually the vicinity of the Gulf of Genova), they often lead to cyclogenesis, enhancing the existent baroclinic conditions (Keresztesi et al., 2020a). The cyclones born in this area usually follow a west to east trajectory, across the Dinaric Alps towards the Balkans inland.

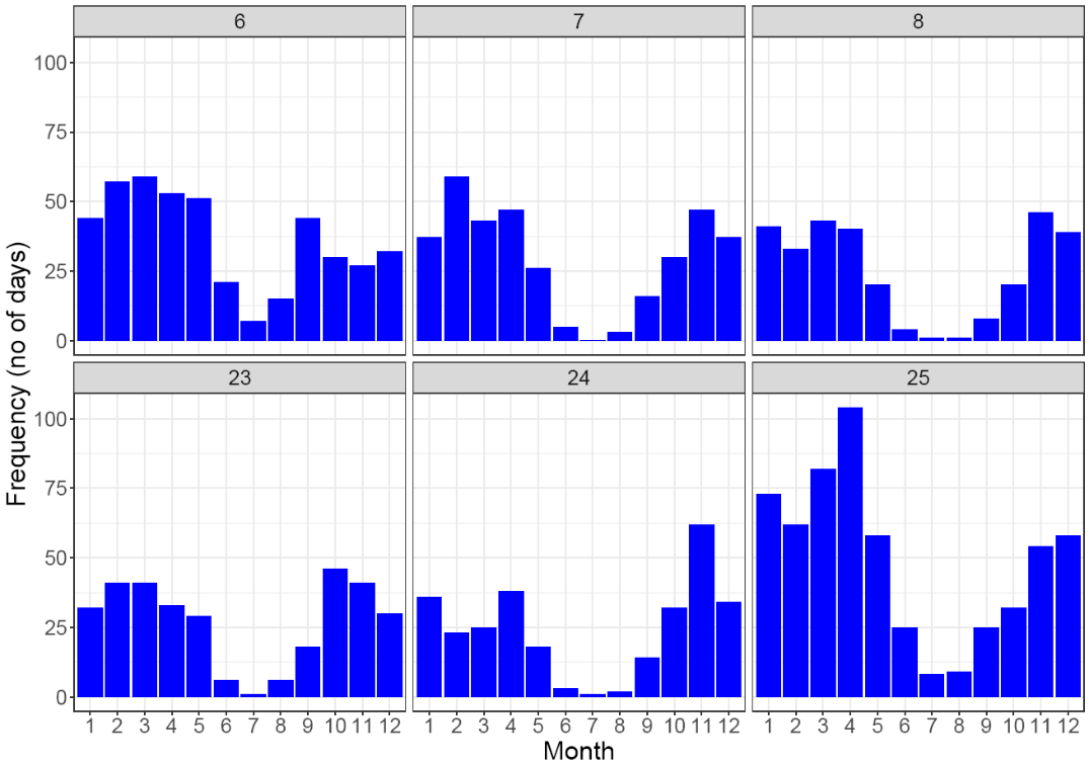

Fig. 36. Monthly frequency of cyclonic weather types in southern Europe.

As they travel towards the east, their humidity content is constantly decreasing due to the orographic barrier imposed by the high elevated terrain in this area. In terms of absolute frequency, these synoptic types are more frequent in the winter, spring and autumn and less in the summertime, when anticyclonic conditions are usually prevalent upon Europe (Fig. 36) (Keresztesi et al., 2020a).

As a result of the orographic lifting the sea salts concentration in the precipitation is affected due to the adiabatic processes on the windward slopes of Dinaric Alps. This also has effects upon the temperature in the airmass since the descending air on the leeward side will be warmer and subsequently drier due to the adiabatic compression (Keresztesi et al., 2020a).

For Europe and the contiguous US, in order to apportion the sea salt and non-sea salt fractions to different major ions in rainwater, chloride was used as a reference element when calculating the SSF% and NSSF%, hence in the majority of the collected precipitation samples the Na^+/Cl^- ratio exhibited values more similar to the Na^+/Cl^- marine ratio (0.86) (Herut et al., 2000).

As in all previous cases, Ca^{2+}, K^+ and SO_4^{2-} are clearly of non-marine origin, as it can be observed in Fig. 37.

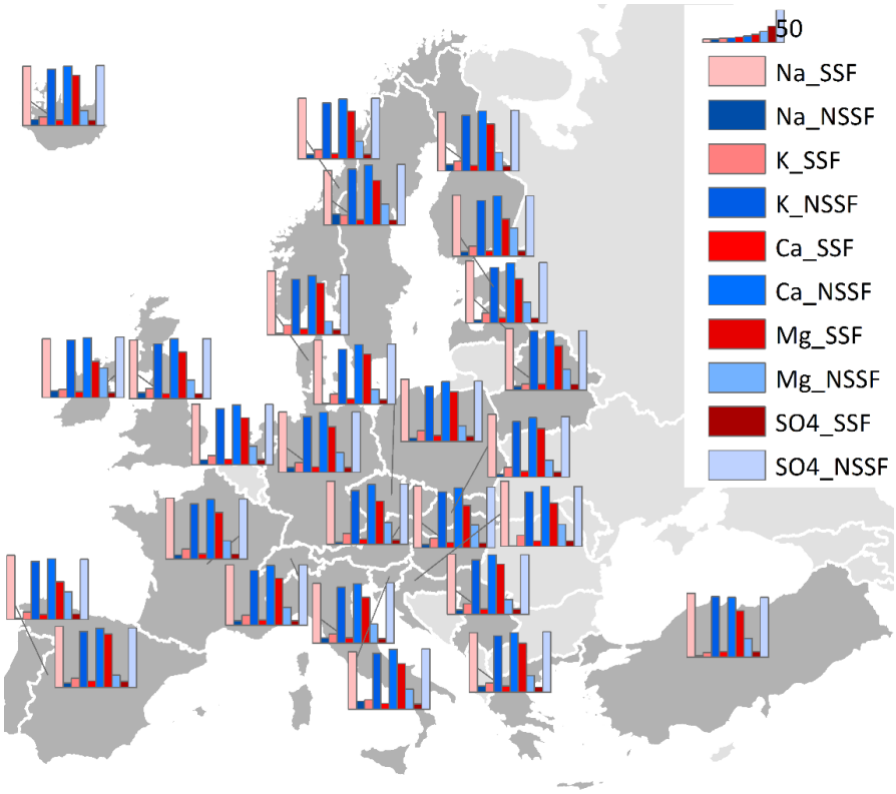

Fig. 37. Source contributions of different components in precipitation over Europe with reference to Cl^-.

In average, the 91.42% of Ca^{2+}, 85.60% of K^+ and the 92.13% of SO_4^{2-} in rainwater can be attributed to other sources than sea spray. The fast pace of industrialization is sustained by the nss-SO_4^{2-} percentage, while almost all calcium is originated from crustal sources, like dolomite and limestone weathering, remote transport of soil dust, open quarries, cement factories, or dirt roads. The non-sea salt origin of potassium can be attributed to soil particles, as well as to fine particulates that may appear due to biomass burning and agricultural activities. In case of magnesium, SSF% exhibited 70.43%, indicating that in most cases magnesium has marine origins. In their study, Xiao et al., (2017) found that in certain remote ocean areas, magnesium can present higher concentrations in comparison to calcium, which explains the average of 70.43% of Mg2+ that can be attributed to marine spray in the rainwater collected over Europe. Cl– was clearly attributed to marine origin, exhibiting a mean SSF% value of 93.26%, the minimum of 83.22% being recorded in Sweden, while the maximum of 99.63% in Croatia.

The results for sea salt fractions calculated for the samples collected in the contiguous US are shown in Fig. 38. Regarding at the concentration maps, one can notice that Ca^{2+} and SO_4^{2-} clearly originates from crustal sources, along with K^+ (avg. SSF = 16.30%), which only exhibited higher marine fractions (~60-70%) near the coastline.

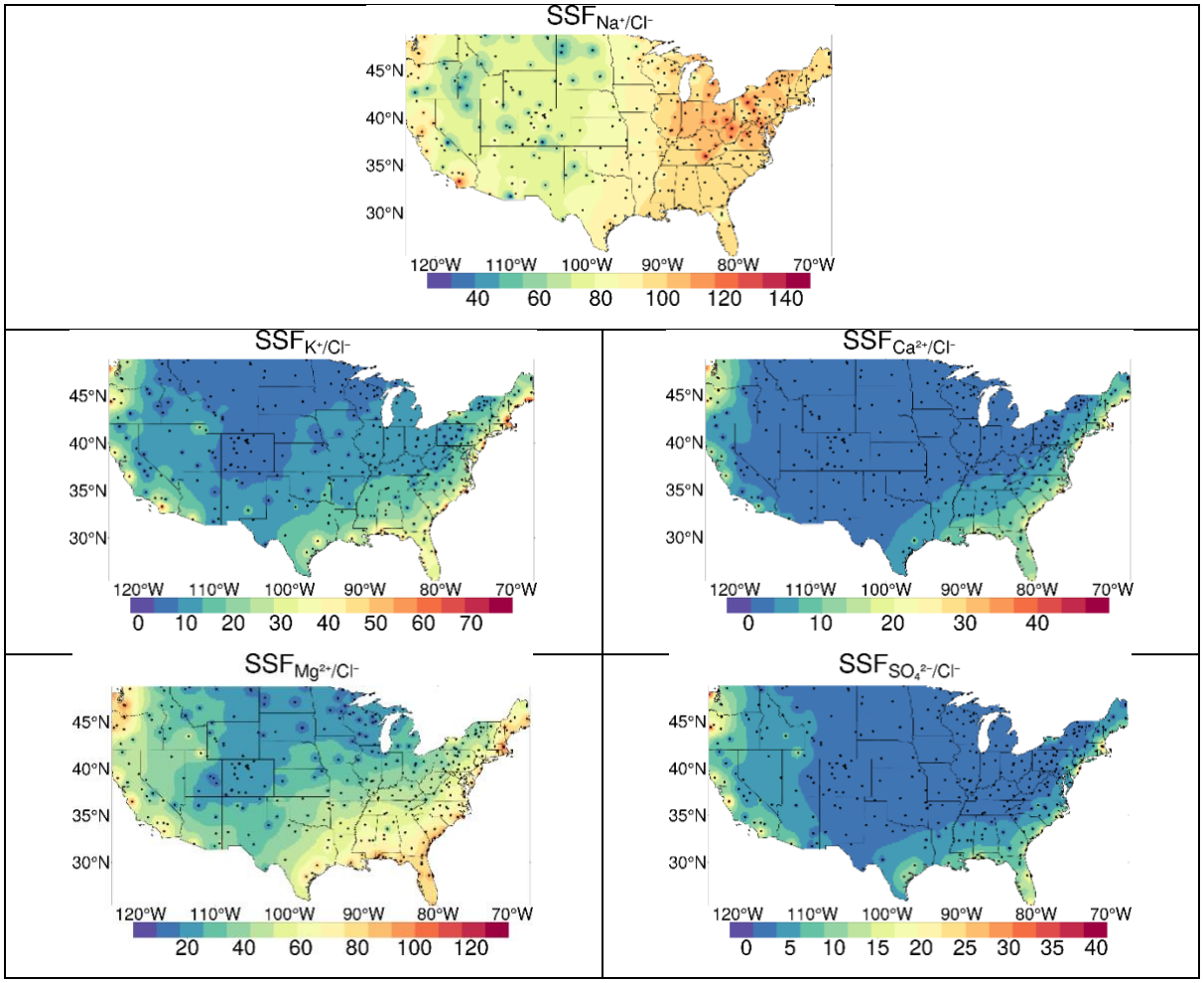

Fig. 38. Sea salt contributions (expressed in %) of different components in precipitation with reference to Cl^- in the contiguous US.

Results showed that SSF Ca^{2+}/Cl^- varied between 0.21 and 51.04%, with a mean value of 5.14%, while the SSF SO_4^{2-}/Cl^- ranged between 0.68% and 46.40%, with a 4.67% average. Marine fraction percentages for Mg^{2+} situated between a minimum of 8.76 and a maximum of 131.90%, with an average of 45.07%, showing values than 100% near the coastline, suggesting that magnesium may have a marine origin, in the form of evaporites, but it can also originate from terrestrial sources, such as dolomite dissolution. The SSF for sodium indicated 72.75%, but in heavily industrialized areas sodium appears to have non marine sources, which can be explained by the higher than 100% SSF values, indicating an enrichment of this element. This phenomenon can be explained by the air mass circulations, when the NaCl from sea spray reacts with sulfuric acid in the atmosphere, over highly industrialized areas, resulting in sodium sulfate and hydrogen chloride (Keresztesi et al., 2020b). In their study, Panno et al., (2005) showed that sodium and chloride in the midcontinent region of the US may originate from natural and anthropogenic sources such as soil/rock-water interactions, basin brines, as in the case of the Great Salt Lake, atmospheric deposition, and from agricultural chemicals and fertilizers, effluents from private and municipal septic systems, animal waste from livestock breeding, as well as from municipal landfills, respectively. Inland chloride may also be a product of biomass and coal combustion, smelting operations and road deicing agents (Keresztesi et al., 2020b; Thornton et al., 2010). If one compares the industrial belts of the U.S. (New England, New York and Mid-Atlantic, Southern and Pacific Coastal)

with the areas where > 100% SSF Na^+/Cl^- fraction was noted, it can be observed that these areas correspond, hence the major industries use Cl^- in the production process (fabricated metals, steel production, electrical machinery, petrochemicals, heavy chemicals, etc.) NSSF values coincided with the SSF values, exhibiting the following percentages for Na^+/Cl^-, K^+/Cl^-, Ca^{2+}/Cl^-, Mg^{2+}/Cl^- and SO_4^{2-}/Cl^-: 10.19%, 83.70%, 94.86%, 54.93%, and 95.33%, respectively.

4.6.4. Principal Component Analysis (PCA)

PCA is a useful tool to decipher and associate the eventual sources of major elements in precipitation. PCA operates by transforming a set of (possibly) correlated variables into a (smaller) set of uncorrelated variables, called principal components. After this, the principal components that have eigenvalues >unity are subjected to Kaiser Normalization Varimax rotation method, yielding a number of factors depending on the analyzed dataset, which can be attributed to various sources depending on the associated factor loadings in case of each principal component. In the specialty literature for precipitation chemistry numerous studies can be found where the origins of various major ions are discussed, by associating them in different groups (Celle-Jeanton et al., 2009; Facchini Cerqueira et al., 2014; Herut et al., 2000; Pu et al., 2017; Rao et al., 2016; Tiwari et al., 2016; Zhang et al., 2007). Ca^{2+} and Mg^{2+} are often associated, having crustal origins, being present in rainwater through the weathering of calcareous rocks, like limestones and dolomites (Rao et al., 2016; Tiwari et al., 2016; Xiao, 2016). It has also been observed, that Ca^{2+} may appear in rainwater as a result of anthropogenic activities and due to its re-suspension, from dirt roads, open quarries or cement factories (Tiwari et al., 2012). Also, magnesium may have marine origins too. Potassium in most cases is present in coarse particles in soil, while fine particulate K^+ can be the result of biomass burning (Zhang et al., 2007). Potassium may originate from agricultural activities too since it is frequently used in chemical fertilizers. According to Khare *et al.*, (2004), potassium may be considered as a chemical signature of biomass burning, but is also present in complex chemical fertilizers, such as NPK (Róbert Szép et al., 2019; Zunckel et al., 2003). The correlations between SO_4^{2-}, NO_3^- and NH_4^+ can be due to their chemical reactions in the atmosphere (Zhang et al., 2007), their sources being usually anthropogenic, such as traffic, industry, coal burning, or agricultural activities, including fertilizer factories, livestock breeding, use of animal manure or biomass burning. N is excreted in the form of urea (in mammals) or uric acid (in birds), which through decomposition (vaporization) can form NH_3 and NH_4^+ in the atmosphere (Behera et al., 2013). The reduction of NO_x to molecular nitrogen in catalytic convertor-fitted vehicles can contribute to the formation of NH_3 gas, which in the atmosphere appears under the form of NH_4^+ (Kumar et al., 2014). Given that the CB and the GB has numerous peat bogs, which in periods of summer often ignite, the high loading of NH_4^+ and K^+ also originates from peat fires and stubble burning. The increased occurrence and severity of wildfires in the last decades is known as a large contributor to the sources of ammonium in precipitation via PM emissions (Knorr et al., 2017).

Na^+ and Cl^- are usually associated with sea spray, however, both sodium and chloride can have other origins too, such as geological or industrial activities, traffic emissions.

In the case of the Central group of the Eastern Carpathians, four number of factors were extracted, explaining about 87.6% at CB, 91.1% at GB, 90.6% at DTP and 86.6% at OSB of the total data variance (Table 21).

Table 21. Varimax rotated factor loadings, total variance, and ionic sources at the studied sampling sites.

	F1	*F2*	*F3*	*F4*
CB				
Cl^-	0.28	**0.85**	0.30	0.13
SO_4^{2-}	0.42	0.13	**0.75**	0.16
NO_3^-	0.08	0.24	**0.86**	0.22
Na^+	0.10	**0.89**	0.11	0.33
K^+	**0.83**	0.34	0.09	0.26
Ca^{2+}	0.02	0.36	0.25	**0.85**
Mg^{2+}	0.51	0.14	0.20	**0.76**
NH_4^+	**0.89**	0.06	0.27	0.05
% Total variance	**25.02**	**23.06**	**19.98**	**19.56**
Possible Source	Biomass burning & fertilization	Marine	Anthropogenic	Crustal
GB				
Cl^-	0.37	**0.88**	0.15	0.09
SO_4^{2-}	0.22	0.10	0.17	**0.92**
NO_3^-	**0.86**	0.21	0.03	0.26
Na^+	0.30	**0.93**	0.04	-0.02
K^+	0.13	0.23	**0.98**	0.11
Ca^{2+}	**0.91**	0.36	-0.04	0.003
Mg^{2+}	**0.83**	0.27	0.26	0.11
NH_4^+	0.003	-0.17	**0.67**	0.59
% Total variance	**32.75**	**24.68**	**17.60**	**16.94**
Possible Source	Mixed	Marine	Biomass burning & fertilization	Anthropogenic
DTP				
Cl^-	0.28	**0.86**	0.22	0.20
SO_4^{2-}	0.33	0.21	**0.73**	0.46
NO_3^-	0.10	0.22	0.08	**0.94**
Na^+	0.10	**0.95**	-0.04	0.13
K^+	**0.80**	0.18	0.34	0.22
Ca^{2+}	**0.91**	0.22	0.06	0.09
Mg^{2+}	**0.86**	0.18	0.40	0.08
NH_4^+	**0.62**	-0.05	**0.68**	-0.20
% Total variance	**35.08**	**23.27**	**16.33**	**15.66**
Possible Source	Mixed	Marine	Anthropogenic	Combustion
OSB				
Cl^-	0.16	0.24	**0.91**	0.09
SO_4^{2-}	**0.87**	0.28	0.04	-0.05
NO_3^-	0.05	-0.03	0.09	**0.97**
Na^+	0.60	0.13	**0.6e mo5**	0.13

	F1	*F2*	*F3*	*F4*
K^+	0.42	**0.83**	0.13	0.30
Ca^{2+}	**0.78**	0.12	0.44	0.14
Mg^{2+}	**0.58**	0.36	0.32	0.44
NH_4^+	0.09	**0.93**	0.21	-0.01
% Total variance	**28.49**	**23.11**	**20.26**	**14.76**
Possible Source	Mixed	Biomass burning & fertilization	Marine	Combustion

At CB, the first factor (F1) explained ~25% of the total variance and exhibited high loads of K^+ and NH_4^+, which may be attributed biomass burning, livestock breeding, fertilization, and agricultural activities. The second factor (F2) represented ~23% of the total variance, having loadings of Na^+ and Cl^-, indicating seawater contribution. Factor 3 (F3) and factor 4 (F4) explained the 19% of the total variation, F3 having high loadings of SO_4^{2-} and NO_3^-, while F4 exhibiting elevated loadings of Ca^{2+} and Mg^{2+}. F3 may be attributed to anthropogenic sources, such as industry, traffic, and waste combustion. The fourth factor is representative for terrestrial sources, magnesium and calcium mainly originating from dolomites and limestone weathering.

For GB the first factor showed the dominance of NO_3^-, Ca^{2+} and Mg^{2+}, accounting for the ~38% of the total variance and suggesting mixed sources. F2 explained the ~25% of the total variance and presented high loads of Na^+ and Cl^-, indicating marine influence. F3 exhibited high loadings of K^+ and NH_4^+, and explained 18% out of the total variance, showing that potassium and ammonium may come from agricultural sources and/or biomass combustion. The fourth factor accounted for the 17% of the total variance, and presented greater loads of SO_4^{2-}, indicating anthropogenic activity.

F1 in DTP represented ~35% of the total variance, indicating high loadings of K^+, NH_4^+, Ca^{2+} and Mg^{2+}, characteristic to mixed sources. F2 with the total variance of ~23% and the high loads of Na^+ and Cl^- indicates the influence of marine sources. F3 is dominated by SO_4^{2-} and NH_4^+, accounting for ~16% of the total variance and indicating anthropogenic sources. The fourth factor presented high loadings of NO_3^-, explaining ~16% of the total variance, and indicating traffic/ automobile combustion for the presence of nitrate in rainwater.

In case of OSB, F1 presented high loads of SO_4^{2-}, Ca^{2+} and Mg^{2+}, accounting for 28.49% of the total variance. The second factor explained 23.11% of the total variance, with elevated concentrations of K^+ and NH_4^+, implying biomass combustion and use of fertilizers. The third factor explained ~20% of the total variance, presenting high concentrations of sodium and chloride, indicating the long-range transport of marine salts. F4 presented the dominance of NO_3^-, exhibiting ~15% of the total variance, and indicating as sources for this pollutant traffic, including vehicle combustion, diesel powered automobiles and tractors, the latter being used in agricultural activities.

The results from the PCA showed that the difference between total variances of principal components can be attributed to the air masses from N and NW, transporting various pollutants, that are discharged along with precipitation in front of the Carpathian Mountainous chain, resulting in different major ion concentrations in rainwater depending on extra- or intra-mountain areas.

The results from the PCA applied to the Northern Group of the Eastern Carpathians can be consulted in Table 22. During the analysis, five factors were extracted from the database, having a total variance of 83%.

F1 accounted for 21.06% of the total variance, having high concentrations of K^+ and NH_4^+, implying their origin from agricultural activities and biomass combustion. F2 explained 18.54% of the total variance and exhibited high loadings of Ca^{2+} and SO_4^{2-}, indicating mixed source origin for the above-mentioned ions. The third factor suggested influences from sea spray, having high loadings of Na^+ and Cl^-, and accounting for 17.22% of the total variance. F4 and F5 explained 13.15% and 13.10% of the total variance, having elevated concentrations of NO_3^- and SO_4^{2-}, indicating anthropogenic sources, mainly traffic and industrial activities. The PCA results for the Northern group of the Eastern Carpathians coincide with the results obtained from the Spearman correlation analysis used to apportion the possible sources of major components in precipitation.

Table 22. Varimax rotated factor loadings, total variance, and ionic sources for the Northern Group of the Eastern Carpathians.

	F1	***F2***	***F3***	***F4***	***F5***
Na^+	-.120	.127	**.736**	.313	.363
K^+	**.806**	.093	.101	-.010	.312
Ca^{2+}	.095	**.850**	.106	-.033	.023
Mg^{2+}	.302	.044	.139	.008	**.902**
SO_4^{2-}	.026	**.854**	-.014	.085	.041
Cl^-	.342	.012	**.866**	.051	-.025
NO_3^-	.061	.039	.183	**.969**	.011
NH_4^+	**.894**	.051	.108	.068	.054
% Total variance	21.06	18.54	17.22	13.15	13.10
Possible Source	Agricultural & biomass burning	Mixed	Marine	Traffic	Industry

PCA results revealed a total of four factors for the data collected in the Southern Carpathians, In the Southern Carpathians, a total of four factors were extracted, having a total variance of 77.39%, 75.17% and 77.42% at RS, MN and BH, respectively. Table 23 presents the results of factor loadings for each sampling site. In case of RS, the results showed that F1 had significant loadings of Ca^{2+} and Mg^{2+}, accounting for 21.94% of the total variance, and indicating the terrestrial influence over the precipitation chemistry. F2 indicated anthropogenic sources, showing high loadings of SO_4^{2-} and Cl^-, and explaining 19.11% of the total variance. The third factor (F3) exhibited high loadings of K^+ and NH_4^+ and explained 19.07% of the total variance, indicating agricultural activities and fertilizer use. F4 is characterized by high loadings of NO_3^-, explaining 17.26% of the total variance, which may be considered as an indicator to sources such as traffic and coal combustion. Similar results were found in case of MN and BH, including factor loadings, variance percentages and possible source apportionment. Both at MN and BH, F1 had high loadings of Ca^{2+}, Mg^{2+} and SO_4^{2-}, representing mixed/crustal origins, and explaining 27.15% and 27.95% of the total variance, respectively. F2 is attributed in both cases to anthropogenic sources, explaining the 18.23% of the total variance in MN and 19.28% of the total variance in BH, with high loadings in both cases of NO_3^-, NH_4^+ and K^+. The third factor both in MN and BH suggests marine sources, exhibiting 15.97% and 16.86% of the

total variance, respectively. In this case, such low variances sustain the results of SSF analysis, indicating a very low contribution of sea spray to the rainwater chemistry of this area. F4 at MN accounted for 13.82% of the total variance, suggesting agricultural sources, due to the high loading of K^+, while at BH, F4 explained 12.33% of the total variance, showing the significant contribution of NH_4^+, which indicates the influence of agricultural activities.

Table 23. Varimax rotated factor loadings, total variance, and ionic sources at the Southern Carpathians.

RS	***F1***	***F2***	***F3***	***F4***
Na^+	.041	.274	.384	-.681
K^+	.195	-.128	**.899**	-.150
Ca^{2+}	**.865**	.291	.116	-.127
Mg^{2+}	**.916**	.096	.063	.173
SO_4^{2-}	.224	**.729**	.212	-.336
Cl^-	.261	**.730**	-.099	.274
NO_3^-	.088	.190	.135	**.798**
NH_4^+	-.047	.494	**.694**	.157
% Total variance	21.94	19.11	19.07	17.26
Possible Source	Crustal	Anthropogenic	Agricultural	Traffic
MN	***F1***	***F2***	***F3***	***F4***
Na^+	.134	.515	**.575**	.374
K^+	.063	.007	.048	**.976**
Ca^{2+}	**.758**	-.038	.327	.069
Mg^{2+}	**.896**	-.084	.006	.083
SO_4^{2-}	**.699**	.188	.144	-.004
Cl^-	.219	-.203	**.881**	-.013
NO_3^-	.363	**.736**	.014	.021
NH_4^+	.321	**-.752**	.199	.034
% Total variance	27.15	18.23	15.97	13.82
Possible Source	Mixed/Crustal	Anthropogenic	Marine	Agricultural
BH	***F1***	***F2***	***F3***	***F4***
Na^+	-.132	.359	**.767**	-.227
K^+	-.447	**.662**	.214	.067
Ca^{2+}	**.829**	-.123	.223	.075
Mg^{2+}	**.803**	-.205	.079	.082
SO_4^{2-}	**.762**	.433	-.159	-.135
Cl^-	.317	-.182	**.795**	.177
NO_3^-	.063	**.832**	-.018	.036
NH_4^+	.030	.066	-.016	**.973**
% Total variance	27.95	19.28	16.86	12.33
Possible Source	Mixed/Crustal	Anthropogenic	Marine	Agricultural

For Europe, the PCA extracted 5 factors that had a total variance of 91.64% (Table 24). F1 exhibited high concentrations of NH_4^+, SO_4^{2-} and Ca^{2+}, and explained 26.47% of

the total variance, suggesting the influence of mixed sources, dominated by anthropogenic activities. F2 presented significant concentrations of Na^+ and Cl^-, accounting for 25.71% of the total variance, and suggesting the influence of maritime breeze on the precipitation chemistry. F3 had high loadings of Ca^{2+} and Mg^{2+}, explaining 13.70% of the total variance, and indicating terrestrial sources. F4 explained 12.92% of the total variance and presented high loads on nitrate, which is an indicator to vehicular emission. F5 exhibited high loadings on K^+, accounting for 12.84% of the total variance and indicating biomass burning as a possible source.

Table 24. Varimax rotated factor loadings, total variance, and possible sources over Europe.

Europe	***F1***	***F2***	***F3***	***F4***	***F5***
Na^+	0.26	**0.87**	0.27	-0.07	0.12
K^+	0.14	0.14	0.09	0.02	**0.98**
Ca^{2+}	**0.70**	0.22	**0.52**	0.20	0.04
Mg^{2+}	0.29	0.39	**0.82**	0.11	0.13
SO_4^{2-}	**0.76**	0.51	0.10	0.17	0.07
Cl^-	0.27	**0.89**	0.20	0.07	0.11
NO_3^-	0.09	0.01	0.07	**0.99**	0.02
NH_4^+	**0.89**	0.19	0.17	0.05	0.15
% of Total variance	26.47	25.71	13.70	12.92	12.84
Possible Source	Anthropogenic and mixed	Marine	Terrestrial	Traffic	Biomass burning and fertilization

PCA was also performed in the case of the contiguous US, analyzing the data for all 334 sampling sites and resulting in the extraction of five major factors, which accounted to a total variance of 92.52% (Table 25).

Table 25. Varimax rotated component matrix, total variance, and possible major ion sources over the contiguous US.

Conterminous US	**F1**	**F2**	**F3**	**F4**	**F5**
Na^+	**.933**	.009	.183	.147	.103
K^+	.198	.169	.154	.060	**.949**
Ca^{2+}	.226	.133	**.905**	.243	.146
Mg^{2+}	.666	.146	**.557**	.275	.178
SO_4^{2-}	.234	.176	.296	**.891**	.064
Cl^-	**.961**	.011	.095	.087	.123
NO_3^-	.078	**.868**	.054	.275	.022
NH_4^+	-.021	**.897**	.124	-.048	.180
%Of total variance	29.86	20.70	16.26	12.99	12.71
Possible sources	Marine	Traffic and agriculture	Terrestrial	Anthropogenic	Fertilizers and biomass burning

The first factor presented high loadings of Na^+ and Cl^-, explaining 29.86% of the total variance and indicating the influence of maritime sources on the precipitation chemistry, which were more highlighted in the coastal areas, flanked by the North Pacific

Ocean and North Atlantic Ocean. F2 presented high loadings on NO_3^- and NH_4^+, and accounted for the 20.70% of the total variance, indicating as sources traffic emissions and agricultural activities. The third factor (F3) appeared to be as of terrestrial influence, with high loadings of Ca^{2+} and Mg^{2+}, explaining the 16.26% of the total variance. F4 presented high loads of SO_4^{2-}, accounting to the 12.99% of the total variance, and indicating anthropogenic activities. The last factor, F5, explained 12.71% and had a significant concentration of potassium, suggesting biomass combustion and use of complex fertilizers, like NPK.

4.7. Zonal circulations, zonal index, and chemical composition of air masses

The use ZI and MI in precipitation chemistry studies is an innovative technique. In this thesis, the influence of airmasses travelling from NW, NE, SW and SE Europe, and the contribution of long-range transported pollutants on rainwater collected in the Northern group of the Eastern Carpathians, is assessed using ZI and MI daily values, which are subsided in 8 groups depending on their direction. In general, trajectories such as N-S or W-E are given by the positive or negative phases of ZI and MI, while for directions such as NE, NW, SE, and SW, secondary directions are observed. For example, the NW direction is characterized by a positive ZI and a negative MI, while SE direction can be recognized by a negative ZI and a positive MI. By using the above-mentioned method, precipitation chemistry data was examined in case of each direction for BM sampling site in the Northern group of the Eastern Carpathians. To do so, rainfall events were grouped into four groups, depending on their ZI and MI value. Therefore, 82 rainwater events were counted to be originating from NW, 12 as originating from NE, 51 as originating from SW and 56 as coming from SE, while 85 events were catalogued as of mixed/uncertain origin, accounting to the total of 286 rainfall events recorded at BM.

Regarding rainfall amounts, multiannual means, and monthly multiannual mean percentages (Fig. 39) were registered in accordance with various advection types. If one studies the entire studied period, one can observe that the majority of rainfall amounts originated from NW and SW, summing up 30.29% and 32.29%, respectively. Advections coming from SE accounted for 27.65%, while the smallest contribution was recorded from NE, with a value of 9.77%.

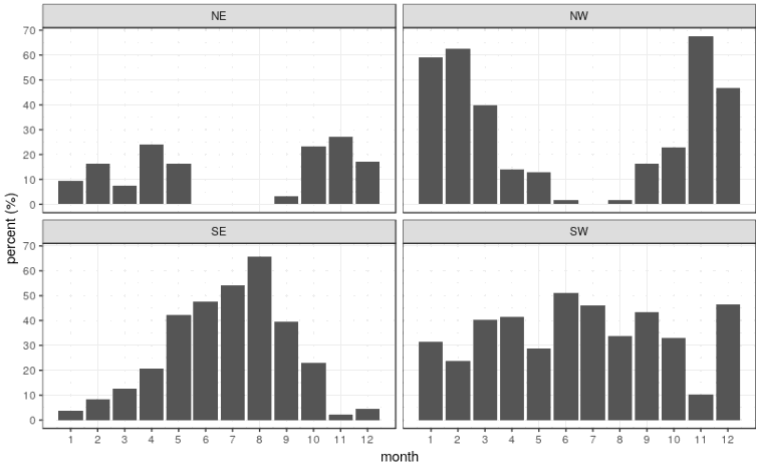

Fig. 39. Monthly multiannual percentages of precipitation recorded on days with different advections.

In the studied area from the Northern group of the Eastern Carpathians, the principal wind directions came from to N, NW, W and SW in all seasons (Fig. 40). It was observed, that during the winter, advections originating from E-Europe are also frequent.

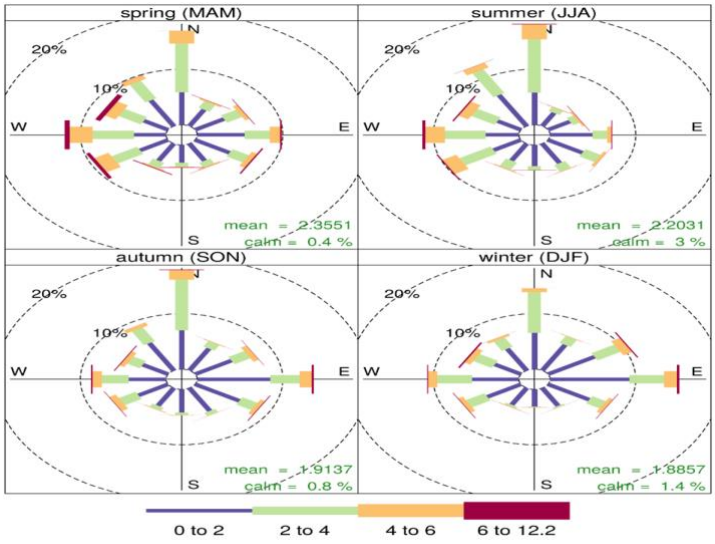

Fig. 40. Multiannual seasonal wind direction frequency.

The above-mentioned air masses are accompanied by low temperatures and low or no rainfall amounts, caused by their continental nature. These air masses can be associated with the Siberian High, that extends upon eastern and Central Europe. Advections originating from West were observed when the ZI values were positive, occurring in general during the winter, when the Azoric High is present above the Atlantic. These occurrences lead to westerly advections, due to the significant pressure differences between the above-mentioned formations. Fig. 41 illustrates the monthly average frequency of days with westerly flow. The annual distribution shows that the Jenkinson-Collinson classification has fewer days with zonal circulation, however, the MSLP difference and the JC scheme also shows a similar pattern, mostly during the January-March and September-December period, when more days with westerly flow occur.

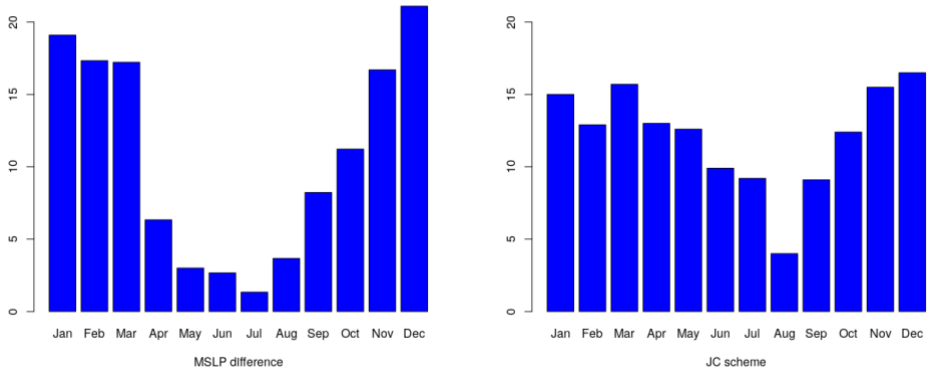

Fig. 41. Averaged monthly number of days with strong westerly component (>8 hPa difference between the minimum and maximum latitude) according to the MSLP method (left) and the JC scheme (right).

Fig. 42 shows the rainfall percent on days with a significant ZI value taking under consideration the total monthly averages. During the winter period, 30-40% of the monthly averages are registered on days with westerly flow.

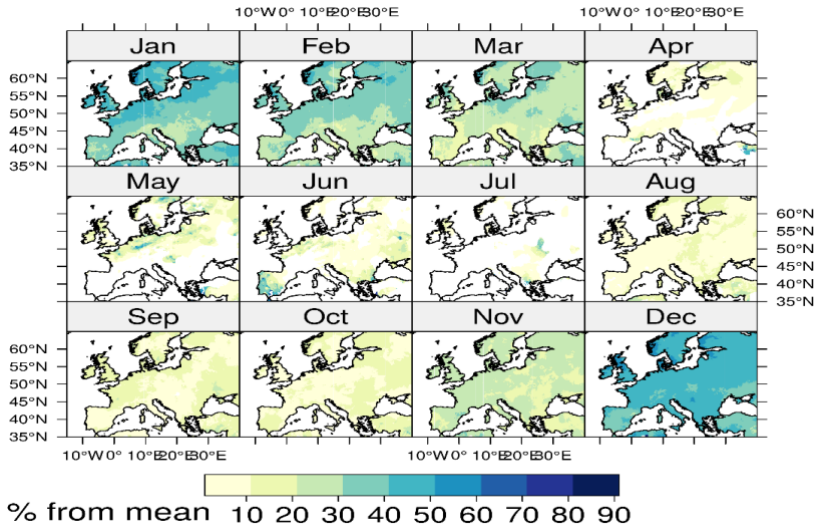

Fig. 42. Rainfall quantities recorded during strong ZI (percent from seasonal mean).

To assess the imprint of long-range transported pollutants, the volume weighted means of major ions measured under each above-mentioned direction were compared to the VWMs of major ions measured for the entire database. The VWMs of sulfate registered in case of SE and NE directions exhibited 184.38 μeq l^{-1} and 155.76 μeq l^{-1}, respectively, which are significantly higher than the VWM for the entire studied period (142.66 μeq l^{-1}). The NW and SW advection types presented more similar sulfate VWM values to the overall VWM, measuring 132.66 μeq l^{-1} and 135.82 μeq l^{-1}, respectively, showing that although SE and NE advection types are the least dominant. Air masses coming from these directions transport more acidifying pollutants than the NW and SW directions. A possible explanation to these differences may be the industrial activities in non-EU member countries (Ukraine, Russia), which operate under different environmental laws and regulations, while the air-masses originating from the Balkan Peninsula and southwestern Romania can be loaded with higher concentrations of acidic compounds due to the presence of unmodernized industrial sites. Calcium exhibited with 48.21% higher VWM values for air masses coming from NW, than the VWM calcium value calculated for the entire study period. The above-mentioned increased calcium values may be due to the air masses that are travelling through the North European Plain, which is known for having numerous agricultural lands, that favor the remote transport of soil dust. The use of ZI and MI can help to evaluate the pollutant concentration of air mass directions, therefore contributing to the prediction of pollution levels arriving to a certain area through long-range transport.

Spearman correlation analysis was also applied to the data extracted with the use of MI and ZI values. Strong correlation coefficient (r=0.56) was observed between chloride and sodium for NW advection type, sustaining the air masses that originate from the Atlantic Ocean.

Spearman's rank correlation analysis was also performed on the data extracted according to different advections. Significant correlation was found between Na^+ and Cl^-

(r=0.56) for NW, implying the presence of air masses originating from the Atlantic. In case of SW direction, significant correlation was observed between magnesium and calcium (r=0.65), sustaining the air masses that are travelling through the North European Plain, and are loaded with terrestrial compounds. The data extracted accounting to the NE advection type showed significant correlation coefficients of 0.98 and 0.83 among sea salts and soil derived compounds, implying the imprint of the North Sea and the Russian Plain. Marine and non-marine fractions were also assessed, sustaining that chloride is originated from sea spray, having the following values for NW, SW, SE and NE directions: 93.54%, 91.49%, 65.90% and 84.30%. As it can be observed, lower values of SSF were registered for SE and NE directions, which may be due to the continental influences, such as the Siberian Anticyclone, hence the variability of rainwater chemistry is largely controlled by the magnitude of dominant air masses.

4.8. Cluster analysis. General air flow transport patterns

To highlight and sustain the observed Foehn effect in the Southern Carpathians, cluster analysis was used, establishing 5 trajectory groups for each sampling site during January 1st 2014, and December 31st 2017 (Fig. 43). The cluster analysis examined general air flow pathways, taking under account direction and wind speed at 2000 m AGL. The prevailing transport patterns were similar at all sampling sites, and were classified into NW, W, SW, S flows and regional recirculation. Fig. 48 shows the air mass percentages for each location. Air flows originating from NW and W accounted for 41% at RS, 32% at MN and 24% in case of BH, respectively. Air masses coming from S and SW summed up to 29% at RS, 35% at MN and 31% at BH, respectively, being also known as Foehn winds, which induces dramatic temperature increases, leading to desiccation in the lee of the mountain range, or it can negatively impact human health. Foehn winds are also responsible to the lack of correlation between chloride and sodium in rainwater samples collected in the Southern Crapathians. It was observed that the 40% of air masses originated from regional recirculation, coming from Central and Eastern Romania, and it was applicable to all sampling sites from the Southern Carpathians, having eastern tendency and relatively short distance transport.

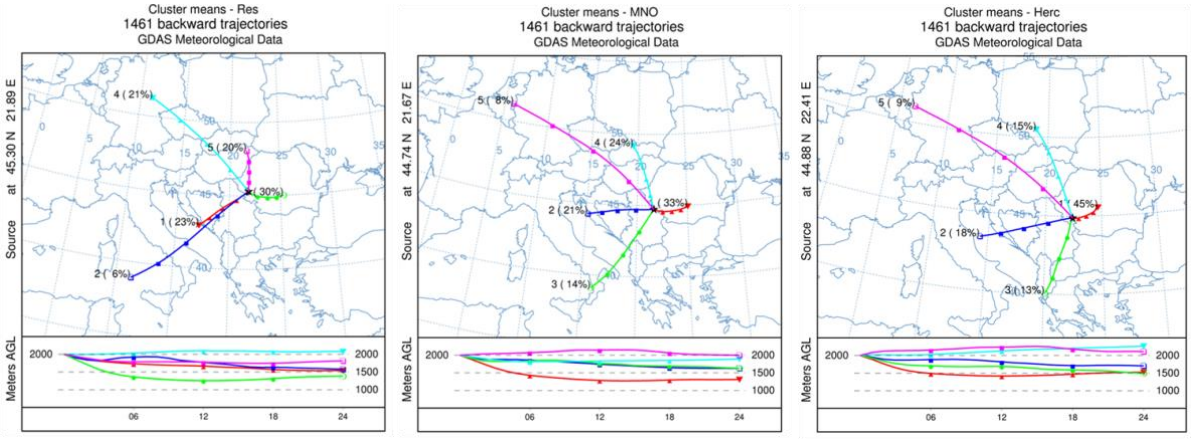

(a) RS (b) MN (c) BH

Fig. 43. Backward trajectory distribution obtained with HYSPLIT for the three locations for the 2014-2017 period in the Southern Carpathians.

Potential atmospheric loads were also taken under account, classifying the transport patterns of clusters as follows: air masses that have anthropogenic origin being influenced by terrestrial sources (clusters 1, 3, 4 and 5 for RS; clusters 1, 2, 4 and 5 for MN; clusters 1, 3, 4 and 5 for BH), and air masses that have anthropogenic origin, but are influenced by marine sources and crustal sources as well (cluster 2 at RS, 3 at MN and 2 at BH, respectively). Taking under consideration the above-mentioned facts, it can be said that the 60% of the long-range transported pollutants are coming from N, NW, and SW, while the ~30% of the aerosols are coming from local sources, emitted into the atmosphere from sources that are close to the sampling sites, such as the coal mines, with their numerous tailing dams and ponds. The above-mentioned information can be noticed in the air mass trajectory distribution as well.

5. Conclusions

This thesis presents a comprehensive analysis on the chemical composition of precipitation, performed in the Romanian Carpathians, Europe, and the contiguous U.S.

Analyzing the data collected in four different sampling sites during the 2006-2016 period in the central group of the Eastern Carpathians, the differences imposed by the effects of the orographic barrier and atmospheric circulations can be easily observed. In general, intra mountain areas are characterized by lower amounts of rainwater, caused by the barrier formed of the mountainous chain in front of air masses loaded with precipitation. This phenomenon is followed by the orographic convection, which leads to heavy rainfall on the northwestern slopes of the Carpathians, fact that can influence the chemical composition of rainwater. The methods used in the current thesis highlighted the differences between intra mountain and extra mountain areas, hence the impact of acidic compounds was more intensely felt in areas that are exposed in front of air masses, this also explains the fact why long-range transported pollutants are more easily deposited in extra mountain areas. The western rim of the Eastern Carpathians creates a barrier in front of NW air masses, that are carrying long-range transported pollutants, leading to differences between the chemical composition of rainwater measured in extra and intra mountain regions.

In the northern group of the Eastern Carpathians data collected at four sampling sites over 9 years from 2009 to 2017 shows the influence of long-range transported pollutants on the rainwater chemistry, by applying a meteorological technique (the zonal and meridional index) in the field of precipitation chemistry. Zonal circulations and determining the zonal index can be useful to show the effect of different polluting sources in countries outside the European Union, that have different environmental legislation and regulations. By analyzing the chemical composition of air masses that are classified in different groups depending on their direction, the influence of long-range transported pollutants (originating from the North European Plain, East European Plain and the Balkans) on the rainwater chemistry can be observed.

In the Southern Carpathians, the assessment of rainwater chemistry over a period of four years (2014-2017) showed that in some relief conditions, atmospheric circulations and the main air mass transport routes may be influenced by meteorological phenomena, as in this case the Foehn effect. The orographic convection also plays a key part in this area's precipitation chemistry, having a considerable effect on the sea salt concentration measured in the collected rainwater samples. This occurs due to the adiabatic processes that can be frequently observed on the leeward slopes of the Dinaric Alps, when air masses travelling thru the mountainous chain and Balkan Peninsula are desiccated of their humidity, fact that is also felt in the chemical composition of precipitation. Local polluting sources, such as the result of mining activity (surface mines, tailings ponds and dams) significantly contribute to the rainwater chemistry of the Southern Carpathians.

The comprehensive assessment targeting 27 European countries over a period of 18 years highlighted the importance of environmental protection and the unitary appliance of environmental legislation, hence the analyzed chemical compounds present in precipitation were rather homogenously distributed. Local characteristics occupied an important place, but it was observed that dominant atmospheric circulations can often diminish or enhance them, especially if their transporting other pollutants from long distances. The most abundant within acidic species was SO_4^{2-}, followed by nitrogenous

compounds, that can originate from various anthropogenic activities, such as industry or agriculture; traffic emissions being also important to note. Since S and N compounds can negatively affect the environment, by harming vegetation and fauna as well, damaging water and soil, it is of great importance that policy and decision makers take under consideration the pollutant concentrations in rainwater, which in their dissolved form can have a more immediate effect on the environment.

The analysis made on the data collected in the contiguous US over a period of 40 years, highlighted the interconnections and differences between the studied areas, that appear due to the geographical location of monitoring stations, climate, precipitation and atmospheric chemistry. All relevant methods used in precipitation chemistry were applied to the data collected from 334 monitoring stations, in order to get a long-term analysis of rainwater chemistry, studying the pH variation, acidic and neutralizing compounds, wet deposition, enrichment factors and the contribution of sea-salts and different pollutants. The results that were obtained may provide an overview to environmental specialists and political decision makers of the current situation and may be of great help in further analyses or studies, that evaluate the effects of the implementation of environmental regulations on the chemical composition of the atmosphere and precipitation.

Overall, the conclusions of the studies presented in this thesis show that a greater importance should be given to the chemical composition of rainwater, hence pollutant concentration in precipitation can be considered as a more sensitive indicator showing the changes effective immediately, since the chemical composition of rainwater is more intensely influenced by the local and regional emission sources. It is also important to note, that although a greater importance is given to acid rain, rainwater that is alkaline can be equally harmful to an ecosystem with acidophilic vegetation, hence the intake of compounds having alkaline characteristics can increase the stress in terrestrial and aquatic ecosystems.

Perspectives

In the future, we want the results obtained from the models applied in this thesis to be extrapolated and quantified from an economic point of view. The application of macroeconomic models that include precipitation chemistry can be indicators and forecasts of economic crises or of medium-term GDP trends.

6. References

Aiuppa, A., Bonfanti, P., D´Alessandro, W., 2003. Rainwater Chemistry at Mt . Etna (Italy): Natural and Anthropogenic Sources of Major Ions. J. Atmos. Chem. 46, 89–102.

Al-Momani, I.F., Ataman, O.Y., Anwari, M.A., Tuncel, S., Köse, C., Tuncel, G., 1995a. Chemical composition of precipitation near an industrial area at Izmir, Turkey. Atmos. Environ. 29, 1131–1143. https://doi.org/10.1016/1352-2310(95)00027-V

Al-Momani, I.F., Tuncel, S., Eler, Ü., Örtel, E., Sirin, G., Tuncel, G., 1995b. Major ion composition of wet and dry deposition in the eastern Mediterranean basin. Sci. Total Environ. 164, 75–85. https://doi.org/10.1016/0048-9697(95)04468-G

Anatolaki, C., Tsitouridou, R., 2009. Relationship between acidity and ionic composition of wet precipitation. A two years study at an urban site, Thessaloniki, Greece. Atmos. Res. 92, 100–113. https://doi.org/10.1016/j.atmosres.2008.09.008

Báez, A., Belmont, R., García, R., Padilla, H., Torres, M.C., 2007. Chemical composition of rainwater collected at a southwest site of Mexico City, Mexico. Atmos. Res. 86, 61–75. https://doi.org/10.1016/j.atmosres.2007.03.005

Báez, A.P., Padilla, H., Cervantes, J., Pereyra, D., Belmont, R., 1997. Rainwater chemistry at the eastern flanks of the Sierra Madre Oriental, Veracruz, Mexico. J. Geophys. Res. 102, 23329–23336.

Balasubramanian, R., Victor, T., Chun, N., 2001. Chemical and statistical analysis of precipitation in Singapore. Water. Air. Soil Pollut. 130, 451–456. https://doi.org/10.1023/A:1013801805621

Behera, S.N., Sharma, M., Aneja, V.P., Balasubramanian, R., 2013. Ammonia in the atmosphere: A review on emission sources, atmospheric chemistry and deposition on terrestrial bodies. Environ. Sci. Pollut. Res. 20, 8092–8131. https://doi.org/10.1007/s11356-013-2051-9

Bisht, D.S., Srivastava, A.K., Joshi, H., Ram, K., Singh, N., Naja, M., Srivastava, M.K., Tiwari, S., 2017. Chemical characterization of rainwater at a high-altitude site “Nainital” in the central Himalayas, India. Environ. Sci. Pollut. Res. 24, 3959–3969. https://doi.org/10.1007/s11356-016-8093-z

Brahney, J., Ballantyne, A.P., Sievers, C., Neff, J.C., 2013. Increasing Ca2+ deposition in the western US: The role of mineral aerosols. Aeolian Res. 10, 77–87. https://doi.org/10.1016/j.aeolia.2013.04.003

Cao, J., Shen, Z., Chow, J.C., Qi, G., Watson, J.G., 2009. Seasonal variations and sources of mass and chemical composition for PM10 aerosol in Hangzhou, China. Particuology 7, 161–168. https://doi.org/10.1016/j.partic.2009.01.009

Cao, Y.Z., Wang, S., Zhang, G., Luo, J., Lu, S., 2009. Chemical characteristics of wet precipitation at an urban site of Guangzhou, South China. Atmos. Res. 94, 462–469. https://doi.org/10.1016/j.atmosres.2009.07.004

Celle-Jeanton, H., Travi, Y., Loyle-Pilot, M.D., Huneau, F., Bertrand, G., 2009. Rainwater chemistry at a Mediterranean inland station (Avignon, France): Local contribution versus long-range supply. Atmos. Res. 91, 118–126. https://doi.org/10.1016/j.atmosres.2008.06.003

Chang, C. Te, Wang, C.P., Chuan, J.H., Wang, L.J., Liu, C.P., Lin, T.C., 2017. Trends of two decadal precipitation chemistry in a subtropical rainforest in East Asia. Sci. Total Environ. 605–606, 88–98. https://doi.org/10.1016/j.scitotenv.2017.06.158

Charlson, R.J., Rodhe, H., 1982. Factors controlling the acidity of natural rainwater. Nature 295, 683–685. https://doi.org/10.1038/295683a0

Chate, D.M., Devara, P.C.S., 2009. Acidity of raindrop by uptake of gases and aerosol pollutants. Atmos. Environ. 43, 1571–1577. https://doi.org/10.1016/j.atmosenv.2008.06.031

Chate, D.M., Rao, P.S.P., Naik, M.S., Momin, G.A., Safai, P.D., Ali, K., 2003. Scavenging of aerosols and their chemical species by rain. Atmos. Environ. 37, 2477–2484. https://doi.org/10.1016/S1352-2310(03)00162-6

Chu, S.H., 2004. PM2.5 episodes as observed in the speciation trends network. Atmos. Environ. 38, 5237–5246. https://doi.org/10.1016/j.atmosenv.2004.01.055

Cornes, R.C., van der Schrier, G., van den Besselaar, E.J.M., Jones, P.D., 2018. An Ensemble Version of the E-OBS Temperature and Precipitation Data Sets. J. Geophys. Res. Atmos. https://doi.org/10.1029/2017JD028200

Daly, C., Slater, M.E., Roberti, J.A., Laseter, S.H., Swift, L.W., 2017. High-resolution precipitation mapping in a mountainous watershed: ground truth for evaluating uncertainty in a national precipitation dataset. Int. J. Climatol. 37, 124–137. https://doi.org/10.1002/joc.4986

Das, R., Das, S.N., Misra, V.N., 2005. Chemical composition of rainwater and dustfall at Bhubaneswar in the east coast of India. Atmos. Environ. 39, 5908–5916. https://doi.org/10.1016/j.atmosenv.2005.06.030

Dee, D.P., Uppala, S.M., Simmons, A.J., Berrisford, P., Poli, P., Kobayashi, S., Andrae, U., Balmaseda, M.A., Balsamo, G., Bauer, P., Bechtold, P., Beljaars, A.C.M., van de Berg, L., Bidlot, J., Bormann, N., Delsol, C., Dragani, R., Fuentes, M., Geer, A.J., Haimberger, L., Healy, S.B., Hersbach, H., Hólm, E. V., Isaksen, L., Kållberg, P., Köhler, M., Matricardi, M., Mcnally, A.P., Monge-Sanz, B.M., Morcrette, J.J., Park, B.K., Peubey, C., de Rosnay, P., Tavolato, C., Thépaut, J.N., Vitart, F., 2011. The ERA-Interim reanalysis: Configuration and performance of the data assimilation system. Q. J. R. Meteorol. Soc. 137, 553–597. https://doi.org/10.1002/qj.828

Dentener, F., Drevet, J., Lamarque, J.F., Bey, I., Eickhout, B., Fiore, A.M., Hauglustaine, D., Horowitz, L.W., Krol, M., Kulshrestha, U.C., Lawrence, M., Galy-Lacaux, C., Rast, S., Shindell, D., Stevenson, D., Van Noije, T., Atherton, C., Bell, N., Bergman, D., Butler, T., Cofala, J., Collins, B., Doherty, R., Ellingsen, K., Galloway, J., Gauss, M., Montanaro, V., Müller, J.F., Pitari, G., Rodriguez, J., Sanderson, M., Solmon, F., Strahan, S., Schultz, M., Sudo, K., Szopa, S., Wild, O., 2006. Nitrogen and sulfur deposition on regional and global scales: A multimodel evaluation. Global Biogeochem. Cycles 20. https://doi.org/10.1029/2005GB002672

Draxler, R.R., Hess, G.D., 1997. Description of the HYSPLIT4 modeling system. Techreport 24pp. https://doi.org/Tech. Memo. ERL ARL-224

Duan, F.K., Liu, X.D., He, K.B., Lu, Y.Q., Wang, L., 2003. Atmospheric aerosol concentration level and chemical characteristics of water-soluble ionic species in wintertime in Beijing, China. J. Environ. Monit. 5, 569–73. https://doi.org/10.1039/b303691j

European Environmental Agency (EEA), 2018. Air quality in Europe — 2018 report, Report. https://doi.org/10.2800/62459

Facchini Cerqueira, M.R., Pinto, M.F., Derossi, I.N., Esteves, W.T., Rachid Santos, M.D., Costa Matos, M.A., Lowinsohn, D., Matos, R.C., 2014. Chemical characteristics of rainwater at a southeastern site of Brazil. Atmos. Pollut. Res. 5, 253–261. https://doi.org/10.5094/APR.2014.031

Fagerli, H., Tsyro, S., Denby, B.R., Gauss, M., Simpson, D., Wind, P., Benedictow, A., Jonson, J.E., Klein, H., Schulz, M., Griesfeller, J., Aas, W., Hjellbrekke, A., Solberg, S., Platt, S.M., Fiebig, M., Yttri, K.E., Rud, R.O., Mareckova, K., Pinterits, M., Tista, M., Ullrich, B., Posch, M., Imhof, H., Putaud, J., Cavalli, F., Poulain, L., Schlag, P., Heikkinen, L.M., Swietlicki,

E., Martinsson, J., Vana, M., Smejkalova, A.H., Kouvarakis, G., Mihalopoulos, N., 2017. Transboundary particulate matter,photo-oxidants, acidifying and eutrophyingcomponents - EMEP Status Report 2017. EMEP Status Rep. 2017.

Fujita, E.M., Stockwell, W.R., Campbell, D.E., Keislar, R.E., Lawson, D.R., 2003. Evolution of the magnitude and spatial extent of the weekend ozone effect in california's south coast air basin, 1981–2000. J. Air Waste Manag. Assoc. 53, 802–815. https://doi.org/10.1080/10473289.2003.10466225

Gong, L., Lewicki, R., Griffin, R.J., Tittel, F.K., Lonsdale, C.R., Stevens, R.G., Pierce, J.R., Malloy, Q.G.J., Travis, S.A., Bobmanuel, L.M., Lefer, B.L., Flynn, J.H., 2013. Role of atmospheric ammonia in particulate matter formation in Houston during summertime. Atmos. Environ. 77, 893–900. https://doi.org/10.1016/j.atmosenv.2013.04.079

Greaver, T.L., Sullivan, T.J., Herrick, J.D., Barber, M.C., Baron, J.S., Cosby, B.J., Deerhake, M.E., Dennis, R.L., Dubois, J.J.B., Goodale, C.L., Herlihy, A.T., Lawrence, G.B., Liu, L., Lynch, J.A., Novak, K.J., 2012. Ecological effects of nitrogen and sulfur air pollution in the US: What do we know? Front. Ecol. Environ. 10, 365–372. https://doi.org/10.1890/110049

Harrison, R.M., Pio, C.A., 1983. Size-differentiated composition of inorganic atmospheric aerosols of both marine and polluted continental origin. Atmos. Environ. https://doi.org/10.1016/0004-6981(83)90180-4

Herbert, B., Loel, R., 1981. Rainwater Quality in Southeastern Arizona Rangeland. Hydrol. Water Resour. Arizona Southwest 155–160.

Herrera, J., Rodríguez, S., Baéz, A.P., 2009. Chemical composition of bulk precipitation in the metropolitan area of Costa Rica, Central America. Atmos. Res. 94, 151–160. https://doi.org/10.1016/j.atmosres.2009.05.004

Herut, B., Starinsky, A., Katz, A., Rosenfeld, D., 2000. Relationship between the acidity and chemical composition of rainwater and climatological conditions along a transition zone between large deserts and Mediterranean climate, Israel. Atmos. Environ. 34, 1281–1292. https://doi.org/10.1016/S1352-2310(99)00291-5

Honório, B.A.D., Horbe, A.M.C., Seyler, P., 2010. Chemical composition of rainwater in western Amazonia - Brazil. Atmos. Res. 98, 416–425. https://doi.org/10.1016/j.atmosres.2010.08.001

Hu, G.P., Balasubramanian, R., Wu, C.D., 2003. Chemical characterization of rainwater at Singapore. Chemosphere 51, 747–755. https://doi.org/10.1016/S0045-6535(03)00028-6

Huang, X.F., Li, X., He, L.Y., Feng, N., Hu, M., Niu, Y.W., Zeng, L.W., 2010. 5-Year study of rainwater chemistry in a coastal mega-city in South China. Atmos. Res. 97, 185–193. https://doi.org/10.1016/j.atmosres.2010.03.027

Huo, M., Sun, Q., Bai, Y., Li, J., Xie, P., Liu, Z., Wang, X., 2012. Influence of airborne particles on the acidity of rainwater during wash-out process. Atmos. Environ. 59, 192–201. https://doi.org/10.1016/j.atmosenv.2012.05.035

Jawad Al Obaidy, A.H.M., Joshi, H., 2006. Chemical composition of rainwater in a tropical urban area of northern India. Atmos. Environ. 40, 6886–6891. https://doi.org/10.1016/j.atmosenv.2005.01.031

Jiang, Y., Yan, J., 2010. Effects of land use on hydrochemistry and contamination of karst groundwater from Nandong Underground River System, China. Water. Air. Soil Pollut. 210, 123–141. https://doi.org/10.1007/s11270-009-0229-z

Jones, P.D., Hulme, M., Briffa, K.R., 1993. A comparison of Lamb circulation types with an objective classification scheme. Int. J. Climatol.

https://doi.org/10.1002/joc.3370130606
Kaneyasu, N., Yoshikado, H., Mizuno, T., Sakamoto, K., Soufuku, M., 1999. Chemical forms and sources of extremely high nitrate and chloride in winter aerosol pollution in the Kanto Plain of Japan. Atmos. Environ. 33, 1745–1756. https://doi.org/10.1016/S1352-2310(98)00396-3
Kaya, G., Tuncel, G., 1997. Trace element and major ion composition of wet and dry depositon in Ankara, Turkey. Atmos. Environ. 31, 3985–3998. https://doi.org/10.1016/S1352-2310(97)00221-5
Keene, W.C., Pszenny, A.P., Galloway, J.N., Hawley, M.E., 1986. Sea-salt corrections and interpretation of constituent ratios in marine precipitation. J. Geophys. Res. 91, 6647. https://doi.org/10.1029/JD091iD06p06647
Keresztesi, Á., Birsan, M.-V.M.-V., Nita, I.-A.I.-A., Bodor, Z., Szép, R., 2019. Assessing the neutralisation, wet deposition and source contributions of the precipitation chemistry over Europe during 2000–2017. Environ. Sci. Eur. 31, 50. https://doi.org/10.1186/s12302-019-0234-9
Keresztesi, Á., Nita, I.-A.I., Birsan, M.M.-V., Bodor, Z., Szép, R., 2020a. The risk of cross-border pollution and the influence of regional climate on the rainwater chemistry in the Southern Carpathians ,. Environ. Sci. Pollut. Res. 27. https://doi.org/https://doi.org/10.1007/s11356-019-07478-9
Keresztesi, Á., Nita, I.A., Boga, R., Birsan, M.V., Bodor, Z., Szép, R., 2020b. Spatial and long-term analysis of rainwater chemistry over the conterminous United States. Environ. Res. 188. https://doi.org/10.1016/j.envres.2020.109872
Keresztesi, Á., Nita, I.A.I.-A., Birsan, M.V.M.-V., Bodor, Z., Pernyeszi, T., Micheu, M.M.M.M., Szép, R., 2020c. Assessing the variations in the chemical composition of rainwater and air masses using the zonal and meridional index. Atmos. Res. 237, 104846. https://doi.org/10.1016/j.atmosres.2020.104846
Khare, P., Goel, A., Patel, D., Behari, J., 2004. Chemical characterization of rainwater at a developing urban habitat of Northern India. Atmos. Res. 69, 135–145. https://doi.org/10.1016/j.atmosres.2003.10.002
Khemani, L.T., Momin, G.A., Rao, P.S.P., Pillai, A.G., Safai, P.D., Mohan, K., Rao, M.G., 1994. Atmospheric pollutants and their influence on acidification of rain water at an industrial location on the West Coast OF India. Atmos. Environ. 28, 3145–3154. https://doi.org/10.1016/1352-2310(94)00148-E
Knorr, W., Dentener, F., Lamarque, J.F., Jiang, L., Arneth, A., 2017. Wildfire air pollution hazard during the 21st century. Atmos. Chem. Phys. 17, 9223–9236. https://doi.org/10.5194/acp-17-9223-2017
Kossmann, M., Sturman, A.P., Zawar-Reza, P., McGowan, H.A., Oliphant, A.J., Owens, I.F., Spronken-Smith, R.A., 2002. Analysis of the wind field and heat budget in an alpine lake basin during summertime fair weather conditions. Meteorol. Atmos. Phys. 81, 27–52. https://doi.org/10.1007/s007030200029
Krupa, S. V., 2003. Effects of atmospheric ammonia (NH3) on terrestrial vegetation: A review. Environ. Pollut. 124, 179–221. https://doi.org/10.1016/S0269-7491(02)00434-7
Kulshrestha, U.C., Kulshrestha, M.J., Sekar, R., Sastry, G.S.R., Vairamani, M., 2003. Chemical characteristics of rainwater at an urban site of south-central India. Atmos. Environ. 37, 3019–3026. https://doi.org/10.1016/S1352-2310(03)00266-8
Kumar, P., Yadav, S., Kumar, A., 2014. Sources and processes governing rainwater chemistry in New Delhi, India. Nat. Hazards 74, 2147–2162. https://doi.org/10.1007/s11069-014-1295-0

Kutiel, H., Maheras, P., Guika, S., 1996. Circulation and extreme rainfall conditions in the eastern mediterranean during the last century. Int. J. Climatol. 16, 73–92. https://doi.org/10.1002/(SICI)1097-0088(199601)16:1<73::AID-JOC997>3.0.CO;2-G

Lehmann, C.M.B., Bowersox, V.C., Larson, S.M., 2005. Spatial and temporal trends of precipitation chemistry in the United States, 1985-2002. Environ. Pollut. 135, 347–361. https://doi.org/10.1016/j.envpol.2004.11.016

Li, C., Kang, S., Zhang, Q., Kaspari, S., 2007. Major ionic composition of precipitation in the Nam Co region, Central Tibetan Plateau. Atmos. Res. 85, 351–360. https://doi.org/10.1016/j.atmosres.2007.02.006

Lu, X., Li, L.Y., Li, N., Yang, G., Luo, D., Chen, J., 2011. Chemical characteristics of spring rainwater of Xi'an city, NW China. Atmos. Environ. 45, 5058–5063. https://doi.org/10.1016/j.atmosenv.2011.06.026

Lupikasza, E., 2010. Relationships between occurrence of high precipitation and atmospheric circulation in Poland using different classifications of circulation types. Phys. Chem. Earth 35, 448–455. https://doi.org/10.1016/j.pce.2009.11.012

Lynch, J.A., Grimmf, J.W., 1995. Trends in Precipitation States : a National Chemistry in the United. Science (80-.). 29.

Maas, R., Grennfelt, R.P., 2016. Towards Cleaner Air, Scientifi c Assessment Report 2016: Summary for Policymakers. EMEP Steer. Body Work. Gr. Eff. Conv. Long-Range Transbound. Air Pollution, Oslo. 16. https://doi.org/10.1016/S0140-6736(54)91963-7

Mahato, K., Singh, K., Singh, K., Tiwari, K., 2016. Assessment of major ionic compositions and anthropogenic influences in the rainwater over a coal mining environment of Damodar River basin , India 2, 461–474. https://doi.org/10.7508/pj.2016.04.008

Migliavacca, D., Teixeira, E.C., Wiegand, F., Machado, A.C.M., Sanchez, J., 2005. Atmospheric precipitation and chemical composition of an urban site, Guaíba hydrographic basin, Brazil. Atmos. Environ. 39, 1829–1844. https://doi.org/10.1016/j.atmosenv.2004.12.005

Mouli, P.C., Mohan, S.V., Reddy, S.J., 2005. Rainwater chemistry at a regional representative urban site: Influence of terrestrial sources on ionic composition. Atmos. Environ. 39, 999–1008. https://doi.org/10.1016/j.atmosenv.2004.10.036

Niu, H., He, Y., Kang, S., Lu, X., Shi, X., Wang, S., 2016. Chemical compositions of snow from Mt. Yulong, southeastern tibetan plateau. J. Earth Syst. Sci. 125, 403–416. https://doi.org/10.1007/s12040-016-0670-5

Niu, H., He, Y., Lu, X.X., Shen, J., Du, J., Zhang, T., Pu, T., Xin, H., Chang, L., 2014. Chemical composition of rainwater in the Yulong Snow Mountain region, Southwestern China. Atmos. Res. 144, 195–206. https://doi.org/10.1016/j.atmosres.2014.03.010

Nollet, L.M.L., 2007. Handbook of Water Analysis, 2nd Editio. ed. CRC Press, Taylor and Francis Group.

Otero, N., Sillmann, J., Butler, T., 2018. Assessment of an extended version of the Jenkinson–Collison classification on CMIP5 models over Europe. Clim. Dyn. https://doi.org/10.1007/s00382-017-3705-y

Panday, A.K., Prinn, R.G., Schär, C., 2009. Diurnal cycle of air pollution in the Kathmandu Valley, Nepal: 2. Modeling results. J. Geophys. Res. Atmos. 114. https://doi.org/10.1029/2008JD009808

Panno, S., Hackley, K., Hwang, H., Greenberg, S., Krapac, I., Landsberger, S., 2005. Database for the characterization and identification of sources of sodium and chloride in natural waters of Illinois. Open File Ser. 1, 15.

Pu, W., Quan, W., Ma, Z., Shi, X., Zhao, X., Zhang, L., Wang, Z., Wang, W., 2017. Long-term trend of chemical composition of atmospheric precipitation at a regional background station in Northern China. Sci. Total Environ. 580, 1340–1350. https://doi.org/10.1016/j.scitotenv.2016.12.097

Rao, P.S.P., Tiwari, S., Matwale, J.L., Pervez, S., Tunved, P., Safai, P.D., Srivastava, A.K., Bisht, D.S., Singh, S., Hopke, P.K., 2016. Sources of chemical species in rainwater during monsoon and non-monsoonal periods over two mega cities in India and dominant source region of secondary aerosols. Atmos. Environ. 146, 90–99. https://doi.org/10.1016/j.atmosenv.2016.06.069

Rao, W., Han, G., Tan, H., Jin, K., Wang, S., Chen, T., 2017. Chemical and Sr isotopic characteristics of rainwater on the Alxa Desert Plateau, North China: Implication for air quality and ion sources. Atmos. Res. 193, 163–172. https://doi.org/10.1016/j.atmosres.2017.04.007

Ruprecht, H., Sigg, L., 1990. Interactions of Aerosols (Ammonium Sulfate , Ammonium Nitrate and Ammonium Chloride) and of Gases (Hc1 , Hno3) With Fogwater 24.

Sakihama, H., Ishiki, M., Tokuyama, A., 2008. Chemical characteristics of precipitation in Okinawa Island, Japan. Atmos. Environ. 42, 2320–2335. https://doi.org/10.1016/j.atmosenv.2007.12.026

Salve, P.R., Maurya, A., Wate, S.R., Devotta, S., 2008. Chemical composition of major ions in rainwater. Bull. Environ. Contam. Toxicol. 80, 242–246. https://doi.org/10.1007/s00128-007-9353-x

Samara, C., Tsitouridou, R., 2000. Fine and Coarse Ionic Aerosol Components in Relation. Water. Air. Soil Pollut. 120, 71–88. https://doi.org/10.1023/A:1005267021828

Seinfeld, J.H., 1986. Atmospheric Chemistry and Physics of Air Pollution.

Seinfield, J., Pandis, S., 1998. Atmospheric Chemistry and Physics. Atmos. Chem. Phys.

Shukla, S.P., Sharma, M., 2010. Neutralization of rainwater acidity at Kanpur, India. Tellus, Ser. B Chem. Phys. Meteorol. 62, 172–180. https://doi.org/10.1111/j.1600-0889.2010.00454.x

Silva, E.I.L., Manuweera, L., 2004. Surface and Rainwater Chemistry in Sri Lanka? A Risk of Acidification. Asian J. Water, Environ. Pollut. 1, 79–86.

Stein, A.F., Draxler, R.R., Rolph, G.D., Stunder, B.J.B., Cohen, M.D., Ngan, F., 2015. Noaa's hysplit atmospheric transport and dispersion modeling system. Bull. Am. Meteorol. Soc. 96, 2059–2077. https://doi.org/10.1175/BAMS-D-14-00110.1

Stoiber, R.E., Rose, W.I., 1974. Fumarole incrustations at active central american volcanoes. Geochim. Cosmochim. Acta 38, 495–516. https://doi.org/10.1016/0016-7037(74)90037-4

Szép, R., Bodor, Z., Miklóssy, I., Niţă, I.-A., Oprea, O.A., Keresztesi, Á., 2019. Influence of peat fires on the rainwater chemistry in intra-mountain basins with specific atmospheric circulations (Eastern Carpathians, Romania). Sci. Total Environ. 647. https://doi.org/10.1016/j.scitotenv.2018.07.462

Szép, Róbert, Bodor, Z., Miklóssy, I., Niţă, I.-A.I.A., Oprea, O.A.O.A., Keresztesi, Á., 2019. Influence of peat fires on the rainwater chemistry in intra-mountain basins with specific atmospheric circulations (Eastern Carpathians, Romania). Sci. Total Environ. 647, 275–289. https://doi.org/10.1016/j.scitotenv.2018.07.462

Szép, R., Mateescu, E., Nechifor, A.C., Keresztesi, Á., 2017. Chemical characteristics and source analysis on ionic composition of rainwater collected in the Carpathians "Cold Pole," Ciuc basin, Eastern Carpathians, Romania. Environ. Sci. Pollut. Res. 24, 27288–27302. https://doi.org/10.1007/s11356-017-0318-2

Szép, R., Mateescu, E., Niţă, I.A., Birsan, M.V., Bodor, Z., Keresztesi, Á., 2018. Effects of the

Eastern Carpathians on atmospheric circulations and precipitation chemistry from 2006 to 2016 at four monitoring stations (Eastern Carpathians, Romania). Atmos. Res. 214, 311–328. https://doi.org/10.1016/j.atmosres.2018.08.009

Szép, R., Mátyás, L., 2014. The role of regional atmospheric stability in high-PM 10 concentration episodes in Miercurea Ciuc (Harghita). Carpathian J. Earth Environ. Sci. 9, 241–250.

Tang, A., Zhuang, G., Wang, Y., Yuan, H., Sun, Y., 2005. The chemistry of precipitation and its relation to aerosol in Beijing. Atmos. Environ. 39, 3397–3406. https://doi.org/10.1016/j.atmosenv.2005.02.001

Thornton, J.A., Kercher, J.P., Riedel, T.P., Wagner, N.L., Cozic, J., Holloway, J.S., Dub́, W.P., Wolfe, G.M., Quinn, P.K., Middlebrook, A.M., Alexander, B., Brown, S.S., 2010. A large atomic chlorine source inferred from mid-continental reactive nitrogen chemistry. Nature 464, 271–274. https://doi.org/10.1038/nature08905

Tiwari, S., Chate, D.M., Bisht, D.S., Srivastava, M.K., Padmanabhamurty, B., 2012. Rainwater chemistry in the North Western Himalayan Region, India. Atmos. Res. 104–105, 128–138. https://doi.org/10.1016/j.atmosres.2011.09.006

Tiwari, S., Hopke, P.K., Thimmaiah, D., Dumka, U.C., Srivastava, A.K., Bisht, D.S., Rao, P.S.P., Chate, D.M., Srivastava, M.K., Tripathi, S.N., 2016. Nature and sources of ionic species in precipitation across the indo-gangetic plains, India. Aerosol Air Qual. Res. 16, 943–957. https://doi.org/10.4209/aaqr.2015.06.0423

Vet, R., Artz, R.S., Carou, S., Shaw, M., Ro, C.U., Aas, W., Baker, A., Bowersox, V.C., Dentener, F., Galy-Lacaux, C., Hou, A., Pienaar, J.J., Gillett, R., Forti, M.C., Gromov, S., Hara, H., Khodzher, T., Mahowald, N.M., Nickovic, S., Rao, P.S.P., Reid, N.W., 2014. A global assessment of precipitation chemistry and deposition of sulfur, nitrogen, sea salt, base cations, organic acids, acidity and pH, and phosphorus. Atmos. Environ. 93, 3–100. https://doi.org/10.1016/j.atmosenv.2013.10.060

Wai, K.M., Lin, N.H., Wang, S.H., Dokiya, Y., 2008. Rainwater chemistry at a high-altitude station, Mt. Lulin, Taiwan: Comparison with a background station, Mt. Fuji. J. Geophys. Res. Atmos. 113, 1–14. https://doi.org/10.1029/2006JD008248

Wang, H., Han, G., 2011. Chemical composition of rainwater and anthropogenic influences in Chengdu, Southwest China. Atmos. Res. 99, 190–196. https://doi.org/10.1016/j.atmosres.2010.10.004

Wang, R., Ye, X., Liu, Y., Li, H., Yang, X., Chen, J., Gao, W., Yin, Z., 2018. Characteristics of atmospheric ammonia and its relationship with vehicle emissions in a megacity in China. Atmos. Environ. 182, 97–104. https://doi.org/10.1016/j.atmosenv.2018.03.047

Wang, W., Xu, W., Collett, J.L., Liu, D., Zheng, A., Dore, A.J., Liu, X., 2019. Chemical compositions of fog and precipitation at Sejila Mountain in the southeast Tibetan Plateau, China. Environ. Pollut. 253, 560–568. https://doi.org/10.1016/j.envpol.2019.07.055

Wekker, S.F.J. De, Kossmann, M., 2015. Convective Boundary Layer Heights Over Mountainous Terrain — A Review of Concepts 3, 1–22. https://doi.org/10.3389/feart.2015.00077

Whelpdale, D.M., Kaiser, M.., 1996. Global Acid Deposition Assessment, World Meteorological Organisation/Global Atmosphere Watch.

Whelpdale, D.M., Summers, P.W., Sanhueza, E., 1997. A global overview of atmospheric acid deposition fluxes. Environ. Monit. Assess. https://doi.org/10.1023/A:1005708821454

Whiteman, C.D., Zhong, S., Shaw, W.J., Hubbe, J.M., Bian, X., Mittelstadt, J., 2001. Cold Pools

in the Columbia Basin. Weather Forecast. 16, 432–447. https://doi.org/10.1175/1520-0434(2001)016<0432:CPITCB>2.0.CO;2
Wilks, D.S., 2006. Statistical Methods in the Atmospheric Sciences. Int. Geophys. Ser. 102, 380–380. https://doi.org/10.1198/jasa.2007.s163
Wu, J., Li, P., Qian, H., Duan, Z., Zhang, X., 2014. Using correlation and multivariate statistical analysis to identify hydrogeochemical processes affecting the major ion chemistry of waters: a case study in Laoheba phosphorite mine in Sichuan, China. Arab. J. Geosci. 7, 3973–3982. https://doi.org/10.1007/s12517-013-1057-4
Wu, Q., Han, G., Tao, F., Tang, Y., 2012. Chemical composition of rainwater in a karstic agricultural area, Southwest China: The impact of urbanization. Atmos. Res. 111, 71–78. https://doi.org/10.1016/j.atmosres.2012.03.002
Wu, Y., Xu, Z., Liu, W., Zhao, T., Zhang, X., Jiang, H., Yu, C., Zhou, L., Zhou, X., 2016. Chemical compositions of precipitation at three non-urban sites of Hebei Province, North China: Influence of terrestrial sources on ionic composition. Atmos. Res. 181, 115–123. https://doi.org/10.1016/j.atmosres.2016.06.009
Xiao, H.-Y., Shen, C.-Y., Xiao, H.-W., Chen, L., Luo, L., Long, Z.-H., Li, D.-N., Long, A.-M., 2017. Atmospheric aerosol compositions over the South China Sea: temporal variability and source apportionment. Atmos. Chem. Phys. 17, 3199–3214. https://doi.org/10.5194/acp-17-3199-2017
Xiao, J., 2016. Chemical composition and source identification of rainwater constituents at an urban site in Xi???an. Environ. Earth Sci. 75, 1–12. https://doi.org/10.1007/s12665-015-4997-z
Xing, J., Song, J., Yuan, H., Li, X., Li, N., Duan, L., Qu, B., Wang, Q., Kang, X., 2017. Chemical characteristics, deposition fluxes and source apportionment of precipitation components in the Jiaozhou Bay, North China. Atmos. Res. 190, 10–20. https://doi.org/10.1016/j.atmosres.2017.02.001
Xu, Z., Li, Y., Tang, Y., Han, G., 2009. Chemical and strontium isotope characterization of rainwater at an urban site in Loess Plateau, Northwest China. Atmos. Res. 94, 481–490. https://doi.org/10.1016/j.atmosres.2009.07.005
Xu, Z., Wu, Y., Liu, W.J., Liang, C.S., Ji, J., Zhao, T., Zhang, X., 2015. Chemical composition of rainwater and the acid neutralizing effect at Beijing and Chizhou city, China. Atmos. Res. 164–165, 278–285. https://doi.org/10.1016/j.atmosres.2015.05.009
Yatkin, S., Adali, M., Bayram, A., 2016. A study on the precipitation in Izmir, Turkey: chemical composition and source apportionment by receptor models. J. Atmos. Chem. 73, 241–259. https://doi.org/10.1007/s10874-015-9325-1
Zhang, M., Wang, S., Wu, F., Yuan, X., Zhang, Y., 2007. Chemical compositions of wet precipitation and anthropogenic influences at a developing urban site in southeastern China. Atmos. Res. 84, 311–322. https://doi.org/10.1016/j.atmosres.2006.09.003
Zunckel, M., Saizar, C., Zarauz, J., 2003. Rainwater composition in northeast Uruguay. Atmos. Environ. 37, 1601–1611. https://doi.org/10.1016/S1352-2310(03)00007-4

7. Aknowledgements

First and foremost, I would like to express my sincere gratitude to my supervisor and friend, Dr. Szép Róbert, for his patience, guidance, and support. I am grateful that you took me on as a student and continued to have faith in me over the years, for continuously encouraging me and making it possible for me to have access to this wealth of knowledge. Thank you for making this work possible, for your meticulous editing, and for offering me the opportunity to work on such an interesting and innovative topic.

I would also like to express my gratitude to Dr. Kilár Ferenc, for his valuable advice and extended discussions, by offering a different point of view, and which have greatly contributed on the improvement of this thesis.

I owe special thanks to all my professors, colleagues, and friends from the University of Sapientia and from the University of Pécs.

Immerse debt of gratitude belongs to the reviewers of this thesis, to all specialists, colleagues and researchers who helped me throughout the years and contributed to making this thesis better.

I am deeply grateful that I have such loving parents, who always supported me, and helped me to pursue my dreams, making me believe that I can achieve everything. My appreciation also goes out to all my family and friends for their encouragement and support all through my studies.

Thank you!

8. Publications

Publications related to the thesis

ISI papers indexed in Web of Science

N°	Article	IF	AIS
1	Szép R, Mateescu E, Nechifor AC, **Keresztesi Á** (2017) Chemical characteristics and source analysis on ionic composition of rainwater collected in the Carpathians "Cold Pole," Ciuc basin, Eastern Carpathians, Romania. *Environmental Science and Pollution Research* **24**: 27288–27302. https://doi.org/10.1007/s11356-017-0318-2	4.223	0.520
2	**Keresztesi Á**, Petres S, Ghita G, Dumitru FD, Moncea MA, Ozunu A, Szép R (2018) Ammonium neutralization effect on rainwater chemistry in the basins of the Eastern Carpathians-Romania. *Revista de Chimie* **69**: 57–63.	1.755	0.064
3	Szép R, Mateescu E, Niţă IA, Birsan MV, Bodor Z, **Keresztesi Á** (2018) Effects of the Eastern Carpathians on atmospheric circulations and precipitation chemistry from 2006 to 2016 at four monitoring stations (Eastern Carpathians, Romania). *Atmospheric Research* **214**: 311–328. https://doi.org/10.1016/j.atmosres.2018.08.009	5.369	1.010
4	Szép R, Bodor Z, Miklóssy I, Niţă IA, Oprea OA, **Keresztesi Á** (2019) Influence of peat fires on the rainwater chemistry in intra-mountain basins with specific atmospheric circulations (Eastern Carpathians, Romania). *Science of the Total Environment* **647**: 275–289. https://doi.org/10.1016/j.scitotenv.2018.07.462	7.963	1.119
5	**Keresztesi Á**, Boga R, Bodor Z, Bodor K, Tonk S, Deák G, Nita IA (2019) The Analysis of the Chemical Composition of Precipitation During the Driest Year from the Last Decade. *Present Environment and Sustainable Development* **13**: 19–32. https://doi.org/10.2478/pesd-2019-0002	0	0
6	**Keresztesi Á**, Birsan MV, Nita IA, Bodor Z, Szép R (2019) Assessing the neutralisation, wet deposition and source contributions of the precipitation chemistry over Europe during 2000–2017. *Environmental Sciences Europe* **31**: 50. https://doi.org/10.1186/s12302-019-0234-9	5.893	0
7	Birsan MV, Micu DM, Niţă IA, Mateescu E, Szép R, **Keresztesi Á**, (2019) Spatio-temporal changes in annual temperature extremes over Romania (1961–2013). *Romanian Journal of Physics* **64**: 816.	1.888	0.194

N°	Article	IF	AIS
8	**Keresztesi Á**, Nita I, Birsan MV, Bodor Z, Szép R, (2020) The risk of cross-border pollution and the influence of regional climate on the rainwater chemistry in the Southern Carpathians, Romania. *Environmental Science and Pollution Research* **27**: 9382–9402. https://doi.org/10.1007/s11356-019-07478-9	4.223	0.520
9	**Keresztesi Á**, Nita IA, Birsan MV, Bodor Z, Pernyeszi T, Micheu MM, Szép R (2020) Assessing the variations in the chemical composition of rainwater and air masses using the zonal and meridional index. *Atmospheric Research* **237**: 104846. https://doi.org/10.1016/j.atmosres.2020.104846	5.369	1.010
10	Birsan MV, Nita IA, Craciun A, Sfîcă L, Radu C, Szep R, **Keresztesi Á,** Micheu MM (2020) Observed changes in mean and maximum monthly wind speed over Romania since AD 1961. *Romanian Reports in Physics* **72**: 702.	1.785	0.170
11	Nita IA, Sfica L, Apostol L, Radu C, **Keresztesi Á**, Szep R (2020) Changes in cyclone intensity over Romania according to 12 tracking methods. *Romanian Reports in Physics* **72**: 706.	1.785	0.170
12	**Keresztesi Á,** Nita IA, Boga R, Birsan MV, Bodor Z, Szép R (2020). Spatial and long-term analysis of rainwater chemistry over the conterminous United States. *Environmental Research* **188**: 109872. https://doi.org/10.1016/j.envres.2020.109872	6.498	1.218
13	Bodor Z, Bodor K, **Keresztesi Á,** Szép R (2020) Major air pollutants seasonal variation analysis and long-range transport of PM_{10} in an urban environment with specific climate condition in Transylvania (Romania). *Environmental Science and Pollution Research* **27**: 38181–38199. https://doi.org/10.1007/s11356-020-09838-2	4.223	0.520
	Total	**50.974**	**6.515**

ISI Proceedings & Publications in international databases

1. **Keresztesi Á**, Korodi A, Boga R, Ghita G, Ilie M, Petres S (2017) Chemical characteristics of wet precipitation in the Eastern Carpathians, Romania. ECOTERRA - J. Environ. Res. Prot. 14, 52–59.

Complementary publications (not related to the topic of the thesis)

ISI papers indexed in Web of Science

N°	Article	IF	AIS
1	Petres S, Lanyi S, Piriianu M, **Keresztesi Á**, Nechifor AC (2018) Evolution of Tropospheric Ozone and Relationship with Temperature and NOx for the 2007-2016 Decade in the Ciuc Depression. *Revista de Chimie* **69**: 601–608.	1.755	0.064
2	Rápó E, Szép R, **Keresztesi Á**, Suciu M, Tonk S (2018) Adsorptive removal of cationic and anionic dyes from aqueous solutions by using eggshell household waste as biosorbent. *Acta Chimica Slovenica* **65**: 709–717. https://doi.org/10.17344/acsi.2018.4401	1.735	0.151
3	Micheu MM, Birsan MV, Szép R, **Keresztesi Á**, Nita IA (2020) From air pollution to cardiovascular diseases: the emerging role of epigenetics. Molecular Biology Reports **47**: 5559–5567. https://doi.org/10.1007/s11033-020-05570-9	2.316	0.40
4	Micheu MM, Birsan MV, Nita IA, Andrei MD, Nebunu D, Acatrinei C, Sfica L, Szép R, **Keresztesi Á**, F-dez. de Arróyabe Hernáez P, Onciul S, Scafa-Udriste A, Dorobantu M (2021) Influence of meteorological variables on people with cardiovascular diseases in Bucharest, Romania (2011-2012). *Romanian Reports in Physics* 73 (707).	1.785	0.170
5	Boga R, **Keresztesi Á**, Bodor Z, et al (2021) Influence of rising air temperature and solar radiation on the tropospheric ozone in the Ciuc Basin, Romania. *Romanian Journal of Physics* 66, 805.	1.888	0.194
6	Boga R, **Keresztesi Á**, Bodor Z, Tonk S, Szép R, Micheu MM (2021) Source identification and exposure assessment to PM10 in the Eastern Carpathians, Romania. *Journal of Atmospheric Chemistry 78 (77-97).*	2.158	0.73
7	Bodor K, Micheu MM, **Keresztesi Á**, Birsan MV, Nita IA, Bodor Z, Petres S, Korodi A, Szép R (2021) Effects of PM10 and Weather on Respiratory and Cardiovascular Diseases in the Ciuc Basin (Romanian Carpathians). Atmosphere 12 (289). https://doi.org/10.3390/atmos12020289	2.686	0
8	Kósa CsA, Nagy K, Szenci O, Baska-Vincze B, Andrásofszky E, Szép R, **Keresztesi Á**, Mircean M, Taulescu M, Kutasi O (2021) The role of selenium and vitamin E in a Transylvanian enzootic equine recurrent rhabdomyolysis syndrome. Acta Veterinaria Hungarica 69 (3).	0.955	0

9	Elena HOLBAN, Gyorgy DEAK, Răzvan MATACHE, Tiberius DĂNĂLACHE, Monica MATEI, Mădălina BOBOC, Marius RAISCHI, Ionuţ GHEORGHE, Ágnes KERESZTESI , Ferenc KILÁR, IDENTIFICATION OF STURGEON BEHAVIOR IN DIFFERENT HYDROMORPHODYNAMIC CONDITIONS RESULTING FROM THE IMPLEMENTATION OF HYDROTECHNICAL ARRANGEMENTS, International Journal of Conservation Science, In press, 2022.	0	0
10	György DEÁK, Natalia ENACHE, Lucian LASLO, Anda ROTARU, Monica MATEI, Madalina BOBOC, Cristina SILAGHI, Sorina CALIN, Ágnes KERESZTESI, Ferenc KILÁR, CO2 EFFLUX MEASUREMENTS ON AQUATIC AND TERRESTRIAL ECOSYSTEMS IN THE CONTEXT OF CLIMATE CHANGE, International Journal of Conservation Science, In press, 2022.	0	0
	Total	**15.278**	**1.709**

ISI proceedings & Publications in international databases

1. Korodi A, Petres S, **Keresztesi Á**, Szép R (2017) Sustainable Developement. Theory or Practice? SGEM2017 17th Int. Multidiscip. Sci. GeoConference 54. https://doi.org/10.5593/sgem2017/54/s23.049
2. Ilie M, Deák G, Anghel AM, **Keresztesi Á**, Mărcuş IM (2017) Mathematical modelling of pollutant dispersion in atmosphere resulting from an asphalt mixture preparation plant, in: International Multidisciplinary Scientific GeoConference Surveying Geology and Mining Ecology Management, SGEM. https://doi.org/10.5593/sgem2017H/43/S19.054
3. Petres S, Boga R, **Keresztesi Á,** Ghita G, Ilie M, Deák Gy (2017) Comparative study of air temperature evolution in the Ciuc depression, *ECOTERRA – Journal of Environmental Research and Protection*, 14(2), 60-69.
4. Boga R, Korodi A, **Keresztesi Á,** Ghita G, Ilie M, Deák Gy (2017) Tropospheric ozone temporal variations and relationship to atmospheric oxidation, *ECOTERRA – Journal of Environmental Research and Protection*, 14(2), 44 – 51.
5. Dumitru FD, Panait AM, Olteanu MV, Holban E, Deák Gy, Szép R, **Keresztesi Á** (2017) Assessing the preservation state of a Romanian historic concrete icon – the Constanta Casino, *Ecoterra*, Volume: 14, Issue: 3, pp. 1-7.
6. Raischi SN, Balaceanu CN, Raischi M, Dumitru FD, Moncea A, Laslo L, Deák Gy, **Keresztesi Á** (2018) Air Pollution Analysis in Moldova Noua Waste Dump, *ECOTERRA – Journal of Environmental Research and Protection*, 14(2), 70-77.

Posters and presentations related to this thesis

1. **Keresztesi Á**, Szép R, Boga R, Korodi A, Petres S, Miklóssy I (2017) Precipitation Chemistry in The Ciuc Basin. *International Symposium, Present Environment and Sustainable Development*, Book Of Abstracts, P. 46–47, 2-4 June 2017, Iasi [presentation].
2. Szép R, **Keresztesi Á**, Korodi A, Petres S, Miklóssy I, Boga R (2017) Calitatea Aerului În Depresiunea Ciucului - Realitate Şi Percepţie. *International Symposium, Present*

Environment and Sustainable Development, Book Of Abstracts, P. 87–88, 2-4 June 2017, Iasi. [presentation]

3. Szép R, **Keresztesi Á**, Boga R, Korodi A, Petres S, Schimbări Cliatice. Realitate Şi Percepţie. *Conferinţa Internaţională, Fenomene Meteo Extreme Şi Sisteme De Avertizare Timpurie În Contextul Managementului Riscului Dezastrelor Naturale*, Bucureşti, 16-17 October 2017 - [presentation]
4. **Keresztesi Á**., Szép R., Boga R., Korodi A., Petres S., Schimbări Climatice În Depresiunea Ciucului. *Conferinţa Internaţională, Centrul Educaţional Privind Adaptarea La Efectele Schimbărilor Climatice Perspective şi Cooperare la Nivel Naţional şi European*, Târgu-Mureş, 18-19 October 2017. [presentation]
5. **Keresztesi Á**, Szép R, Boga R, Korodi A, Petres S,(2021) Climate Change effects on ecosystems in the Ciuc Basin..*International Conference on Natural Ecosystems and Climate Change Adaptation Needs*, Brasov, 20-21 October 2017. [presentation]
6. **Keresztesi Á**, Szép R, Boga R, Bodor Zs, Miklóssy I (2012) Precipitation Chemistry And The Influence Of Different Sources On The Ionic Composition Of Rainwater Collected In Harghita County, Romania. *XXIII-th International Conference Of Chemistry*, 25-28 October 2017, Deva, Romania. [presentation]
7. **Keresztesi Á**, Szép R, Bodor Zs, Péter H (2018) Variabilitate în Chimia Precipitaţiilor în Depresiunile Intra- şi Extra-Montane, *International Symposium, Present Environment and Sustainable Development*, 1 – 3 June 2018, Iasi, Romania [presentation]
8. **Keresztesi Á**, Szép R, Bodor Zs, Boga R, Tonk Sz, Nita IA (2018) The Dinaric Alps Foehn Effect on The Ionic Composition Of Rainwater Collected In Caras-Severin County, Romania. *24th International Conference On Chemistry, Sovata Bai, Romania*, 24-27 October 2018. [presentation]
9. **Keresztesi Á,** Szép R, Birsan MV, Nita IA, Bodor Zs, Assessing The Chemical Composition Of Precipitation Over The European Continent During The Last Two Decades, *21st Edition Of The Scientific Research And Education In The Air Force International Conference (AFASES 2019)*, 28 May – 02 June 2019, Brasov, Romania. [presentation]
10. Bodor Zs, Bodor K, Szep R, **Keresztesi Á** (2019) Seasonal variation and long-range transport of major air pollutants in the Ciuc Basin (Romania) with specific climate condition. *XIX International Multidisciplinary Scientific Geoconference SGEM 2019*, 28 June – 7 July, 2019, Albena, Bulgaria - International Scientific Geoconference SGEM2019 [poster]
11. **Keresztesi Á**, Szép R, Bodor Z, Bodor K, Schmutzer G, Bálint K (2020) Long-term analysis of rainwater chemistry over the European continent, 26th International Conference on Chemistry, October 30th. [presentation]
12. **Keresztesi Á**, Szép R, Bodor Z, Bodor K, Tánczos S (2021) Long-term analysis of rainwater chemistry over the conterminous United States, 27th International Conference on Chemistry, October 29th. [presentation]

Posters and presentations not related to this thesis

1. Boga R, Szép R, Korodi A, **Keresztesi Á** (2017) Tropospheric ozone temporal variations and relationship to atmospheric oxidation. International Symposium. *Present Environment and Sustainable Development*, 2-4 June 2017 Iasi. Book of Abstracts, p. 72-73. [presentation]

2. Bodor K, Bodor Z, Boga R, **Keresztesi Á** (2019) Time series analysis from 2008 to 2018 of PM10 evaluation of Bucharest region, Romania. *The 14th Edition of Present Environment and Sustainable Development International Conference*, Iaşi, 2019. [presentation]
3. Bodor K, Bodor Z, Szép R, **Keresztesi Á**, Szép A (2020) Characterization of some bottled Romanian mineral waters on the basis of the total mineral content, 26th International Conference on Chemistry, October 30th. [presentation]
4. Bodor K, Bodor Z, Szép A, Szép R, **Keresztesi Á** (2021) Human health impact assessment and time series analysis of lead content of PM10 particulate matter in Copsa Mică Romania, 27th International Conference on Chemistry, October 29th. [presentation]

Awards and merit scholarships

Awards

1. BEST PRESENTATION AWARD: Bodor Zs., Bodor K, Szep R, **Keresztesi Á** (2019) Seasonal variation and long-range transport of major air pollutants in the Ciuc Basin (Romania) with specific climate condition. *XIX International Multidisciplinary Scientific Geoconference SGEM 2019*, 28 June – 7 July 2019, Albena, Bulgaria. [poster]
2. SPECIAL AWARD: **Keresztesi Á**, Szép R, Bodor Z, Bodor K, Schmutzer G, Bálint K (2020) Long-term analysis of rainwater chemistry over the European continent, 26th International Conference on Chemistry, October 30th. [presentation]
3. 2nd PLACE: Bodor K, Bodor Z, Szép R, **Keresztesi Á**, Szép A (2020) Characterization of some bottled Romanian mineral waters on the basis of the total mineral content, 26th International Conference on Chemistry, October 30th. [presentation]

Scholarships

1. Székely Forerunner Fellowship, 2018
2. Collegium Talentum Scholarship for 2020/2021 school year.
3. New National Excellence Program (Új Nemzeti Kiválóság Program) Scholarship for 2020/2021 school year.
4. New National Excellence Program (Új Nemzeti Kiválóság Program) Scholarship for 2021/2022 school year.

Scientific impact

- Cumulative Impact Factor (IF): **66.252**
- Impact Factor / No. of authors: **50.326**
- Cumulative Article Influence Score (AIS): **8.224**
- Hirsch index (Web of Science): **10**
- Citations (Web of Science): **319 total**
- ISI indexed publications: **23 total (12 as first/corresponding author)**
- Total participation to international and national conferences: **13**